Random Matrices for Information Processing – A Democratic Vision

Cakmak, Burak

DOI (link to publication from Publisher):
10.5278/vbn.phd.engsci.00162

Publication date:
2016

Document Version
Publisher's PDF, also known as Version of record

RANDOM MATRICES FOR INFORMATION PROCESSING

– A DEMOCRATIC VISION

BY
BURAK ÇAKMAK

DISSERTATION SUBMITTED 2016

AALBORG UNIVERSITY
DENMARK

Random Matrices for Information Processing – A Democratic Vision

PhD Thesis

Burak Çakmak

Dissertation submitted October, 2016

Dissertation submitted: October, 2016

PhD supervisor: Professor Bernard Henri Fleury
Aalborg University, Demmark

PhD committee: Associate Professor Jan Østergaard (chairman)
Aalborg University, Denmark

Professor Tom Heskes
Radboud University Nijmegen, The Netherlands

Professor Antonia Tulino
Nokia Bell Labs, USA

PhD Series: Faculty of Engineering and Science, Aalborg University

ISSN (online): 2246-1248
ISBN (online): 978-87-7112-828-4

Published by:
Aalborg University Press
Skjernvej 4A, 2nd floor
DK – 9220 Aalborg Ø
Phone: +45 99407140
aauf@forlag.aau.dk
forlag.aau.dk

Printed in Denmark by Rosendahls, 2016

Summary

The thesis studies three important applications of random matrices to information processing. Our main contribution is that we consider probabilistic systems involving more general random matrix ensembles than the classical ensembles with iid entries, i.e. models that account for statistical dependence between the entries. Specifically, the involved matrices are invariant or fulfill a certain asymptotic freeness condition as their dimensions grow to infinity (large-system limit). Informally speaking, all latent variables contribute to the system model in a democratic fashion – there are no preferred latent variables in the system.

The thesis consists of one introductory chapter, a chapter providing a background on random matrices (Chapter 2), followed by three chapters addressing specific applications of random matrix theory (Chapters 3-5). The derivations of the results are collected in four appendices. Conclusions and an outlook are presented in Chapter 6.

The background on random matrices provided in Chapter 2 is meant to introduce the concepts, properties, and results that will be used in the applications addressed in the next chapters. This chapter also contains some novel results, such as fundamental integral formulas involving the R-transform and S-transform in free probability.

In Chapter 3 we investigate how the capacity of multiple-input–multiple-output (MIMO) communication systems scales when the number of transmit or receive antenna is altered. While doing this, we restrict ourself to the transmission scenario where transmit antennas of the system send equal signal powers. In particular, for a system with R receive and T transmit antennas and $T < R$, we showed the following universal capacity law: By removing as many receive antennas as to get a square system, the maximum resulting loss of capacity over all signal-to-noise-ratio (SNR)s does not depend on the singular values of the channel. It only depends only on R, T and the left singular vectors of the (initial) channel matrix. Assuming the matrix of left singular vectors to be Haar, the ergodic rate loss can be expressed in terms of the digamma function. As the system dimensions tend to infinity with the ratio $\phi = T/R$ kept fixed, the rate loss normalized by R converges to the

binary entropy function of the aspect ratio ϕ. We also unveil two integral formulas involving the S-transform that fundamentally relate the capacity to its affine approximation at high SNR.

In Chapter 4 we consider the signal recovery problem where the input signal vector is mapped via a linear transformation to a vector that is then passed through an output channel. We extend approximate message passing (AMP) techniques to a general class of random matrices by combining two frameworks: approximate inference based on expectation propagation and free probability theory of random matrices. In particular, we obtain a set of fixed point equations for solving the approximate inference problem. When the entries of the transformation matrix are drawn iid with zero mean and vanishing variance (in the large-system limit), these equations yield the fixed points of AMP (or generalized AMP – GAMP). The generalization is simple; it involves the R-transform (and/or S-transform) of the limiting eigenvalue distribution of the Gramian of the transformation matrix.

In Chapter 5 we introduce a theoretical framework – on the basis of dynamical functional analysis – for iteratively solving the TAP fixed-point equations of the Ising model with general invariant random coupling matrices. In particular, our method enables to construct a system of dynamical equations that expresses the implicit memory terms which depend on the magnetizations at previous iteration steps. We can cancel these implicit memory terms in such a way that the iterative algorithms depend only on Gaussian distributed fields. By doing so we expect to get convergent algorithms. Our framework allows to describe/analyze such iterative algorithms with a single-variable trajectory in the large-system limit.

Resumé

Afhandlingen studerer tre vigtige anvendelser af tilfældige matricer indenfor informationabehandling. Vores vigtigste bidrag er, at vi anser stokastiske systemer der involverer mere generelle ensembler af tilfældige matricer, end de klassiske ensembler med iid indgange, dvs. modeller der tager højde for den statistiske afhængighed mellem indgangene. Konkret er de involverede matricer invariante eller opfylder en bestemt asymptotisk frihedstilstand når deres dimensioner vokser til uendeligt (stor-system grænsen). Uformelt set bidrager alle latente variable i system modellen på demokratisk vis – der er ingen foretrukne latente variable i systemet.

Afhandlingen består af et indledende kapitel, et kapitel der introducerer baggrundsviden om tilfældige matricer (Kapitel 2), efterfulgt af tre kapitler der omhandler specifikke anvendelser af tilfældig matrix teori (Kapitel 3-5). Udledning af resultaterne er samlet i fire bilag. Konklusioner og videre perspektiver presenteres i Kapitel 6.

Baggrunden om tilfældige matricer, der fremføres i Kapitel 2, introducerer de begreber, egenskaber og resultater som anvendes i de følgende kapitler kapitler. Dette kapitel indeholder også nogle nye resultater, såsom grundlæggende integralformler der involverer R-transformen og S-transformen i fri sandsynlighed.

I Kapitel 3 undersøger vi, hvordan kapaciteten af multiple-input-multiple-output (MIMO) kommunikationssystemer skalerer, når antallet af sende- eller modtageantenner ændres. Vi begrænser os selv til et scenario, hvor sende antennerne har den samme sendestyrke. For et system med R modtage og T sendeantenner med $T < R$, finder vi følgende universelle kapacitets lov: Ved at fjerne modtage antenner indtil der er lige mange modtage og sende antenner, er der største resulterende tab af kapacitet over alle signal-til-støj forhold (SNR) uafhængigt af kanalens singulærværdier. Det afhænger kun af R, T og de venstre singulær vektorer af kanalmatricen. Antages matricen af vens singulær vektorer at være Haar, kan det ergodiske rate tab udtrykkes ved hjælp af digamma funktionen. Som systemets dimensioner går mod uendeligt med forholdet $\phi = T/R$ fastholdt, vil rate tabet normaliseret med R konvergere til den binære entropi funktion evalueret i forholdet ϕ. Vi fremviser også to in-

tegral formler via S-transformationen. De relaterer kapaciteten til dets affine approksimation ved højt SNR.

I Kapitel 4 betragter vi det signal genskabelses problem, hvor indgangs signal vektoren afbildedes via en lineær transformation til en vektor, som derefter føres gennem en udgangskanal. Vi udvider approximate message passing (AMP) teknikker til en generel klasse af tilfældige matricer ved at kombinere to metoder: approksimativ inferens baseret på expectation propagation og fri sandsynlighedsteori af tilfældige matricer. Herved opnås et sæt fixpunkt ligninger til løsning af det approksimative inferens problem. Når indgangene i transformations matricen trækkes iid med middelværdi nul og forsvindende varians (i stor-system grænsen), opnås fixpunkt ligningerne for AMP (eller generaliseret AMP – GAMP). Generaliseringen er simpel; den involverer R-transformationen (og/eller S-transformationen) af grænse egenværdidistributionen af Gramianen af transformations matricen.

I Kapitel 5 introducerer vi en teoretisk metode - baseret på dynamisk funktionel analyse - for iterativ løsning af TAP fastpunkt ligningerne af Ising modellen med generelle invariante tilfældige koblingsmatricer. Vores metode gør det muligt at konstruere et system af dynamiske ligninger, der udtrykker de implicitte hukommelses termer – som afhænger af forrige iterations magnetiseringer. Vi kan annullere disse implicitte hukommelses termer, således at de iterative algoritmer kun afhænger af Gaussisk distribuerede felter; vi forventer således at opnå konvergente algoritmer. Via vores metodik kan sådanne iterative algoritmer beskrives og analyseres via en enkelt-variable sporing i stor-system grænsen.

This thesis is dedicated to my family and my future wife.

Contents

Thesis Details

Thesis Title:	Random Matrices for Information Processing – A Democratic Vision
PhD Student:	Burak Çakmak
Supervisor:	Prof. Bernard H. Fleury, Aalborg University

The thesis is based on the following five papers.

A Burak Çakmak, Ralf Müller and Bernard H. Fleury, "Capacity scaling for MIMO systems with general unitarily invariant random matrices," (**arXiv: 1306.2595**), *submitted to IEEE Transactions on Information Theory*, December 2015.

B Burak Çakmak, Ole Winther and Bernard H. Fleury "S-AMP: Approximate message passing for general matrix ensembles," *In Proceeding IEEE Information Theory Workshop (ITW)*, Hobart, Tasmania, Australia, pp. 2807–2811, November 2014.

C Burak Çakmak, Ole Winther and Bernard H. Fleury "S-AMP for nonlinear observations," *In Proceeding IEEE International Symposium on Information Theory (ISIT)*, Hong-Kong, China, pp. 2807–2811, June 2015.

D Burak Çakmak, Manfred Opper, Bernard H. Fleury and Ole Winther "Self-averaging expectation propagation," (**arXiv: 1608.06602**) *In Preparation to be submitted to Journal of Machine Learning Research.*

E Manfred Opper, Burak Çakmak and Ole Winther, "A theory of solving TAP equations for Ising model with general invariant random matrices," *Journal of Physics A: Mathematical and Theoretical*, vol. 49, no. 11, February 2016.

In addition, Paper F below was published during my PhD study but it is not part of the thesis.

F Burak Çakmak, Daniel N. Urup, Florian Meyer, Troels Pedersen, Bernard H. Fleury and Franz Hlawatsch, "Cooperative localization for mobile

networks: A distributed belief propagation-mean field message passing algorithm," *IEEE Signal Processing Letters*, vol. 23, no. 6, pp. 828–832, April 2016.

The material in Section II of Paper D is directly or indirectly reproduced in Section 1 of Chapter 1. The proofs of Theorem 2.6 and Theorem 2.7 in Chapter 2 indirectly appeared in Paper E and Paper A, respectively. Part of the material of Chapter 4 appeared in Paper B and Paper C. Apart from some editorial modifications, the materials of Chapter 3, Chapter 4 and Chapter 5 appeared in their entirety as Paper A, Paper D and Paper E, respectively.

This thesis has been submitted for assessment in partial fulfillment of the PhD degree. The thesis is based on the submitted or published scientific papers which are listed above. As part of the assessment, co-author statements have been made available to the assessment committee and are also available at the faculty. The thesis is not in its present form acceptable for open publication but only in limited and closed circulation as copyright may not be ensured.

Preface

This thesis is submitted to the International Doctoral School of Engineering and Science at Aalborg University, Denmark, in partial fulfillment of the PhD degree. The thesis is written in the format of monograph and it is based on four published or submitted papers and one paper under preparation.

The PhD study has been carried out during the period spanning from October 2012 to June 2016 at Aalborg University. The study has been co-funded by the project ICT-216715 FP7 Network of Excellence in Wireless COMmunication (NEWCOM++) and the VIRTUOSO cooperative research project funded by Intel Mobile Communications, Keysight, Telenor, Aalborg University and Innovation Fund Denmark.

Acknowledgment

First and foremost, let me start by thanking God – the Infinitely Good and the All-Merciful. Indeed, this PhD study helped me recognize Him more clearly. In my opinion, if one thinks sufficiently deep (s)he would realize that all His divine attributes tend to infinity.

I would like to express my sincere gratitude for the guidance provided by my supervisor Professor Bernard Fleury. He created very good research atmosphere and showed a high tolerance to me. He helped me improve my scientific method. My particular gratitude goes to Professor Ole Winther for his "unofficial" guidance during my PhD study.

I owe a great appreciation to Professor Manfred Opper for hosting me 5 months at Technical University of Berlin and for all inspiring and fruitful daily discussions we had. My deep expression of appreciation also goes to Professor Ralf Müller and Professor Tuncay Ertaş for their continued supports.

I would like to thank the members of my PhD assessment committee Professor Tom Heskes, Professor Antonia Tulino and Associate Professor Jan Østergaard for reading and assessing of thesis.

Very special thanks go to Associate Professor Carles Navarro Manchon and Dr. Gerhard Steinboeck for their insightful discussions on the introduction of the thesis.

Last but not least, I would like to extend my sincere gratitude to my family for giving me continuous support and encouragement during my PhD study.

Burak Çakmak
Aalborg University
October 25, 2016

Acronyms

AMP	approximate message passing
AT	Almedia-Thouless
BP	belief propagation
CDMA	code-division multiple access
DCT	discrete cosine transform
DFT	discrete Fourier transform
EP	expectation propagation
iid	independent identically distributed
LED	limiting eigenvalue distribution
MIMO	multiple-input–multiple-output
MMSE	minimum-mean-square-error
pdf	probability density function
SNR	signal-to-noise ratio
TAP	Thoules-Andersen-Palmer

Notations

Analysis

$\mathbb{C}, \mathbb{R}, \mathbb{N}$	complex, real, and natural numbers.
$\Re x$, $\Re\{x\}$	real part of x
$\Im x$, $\Im\{x\}$	imaginary part of x
$\lvert x \rvert$	for $x \in \mathbb{R}$, absolute value of x
$(x)^+$	for $x \in \mathbb{R}$, $\max(x, 0)$
i	if $\sqrt{-1}$
z^*	complex conjugate of z
$f'(x)$	first derivative of function $f(x)$
$u(x)$	unit step function
$\delta(x)$	Dirac delta function, i.e. $u'(x)$
δ_{ij}	Kronecker delta function, i.e. $\delta_{ij} = 0$ if $i \neq j$ and $\delta_{ii} = 1$.
$a_n \simeq b_n$	for sequences a_n and b_n, $n \in \mathbb{N}$, $(a_n - b_n) \to 0$ as $n \to \infty$

Linear Algebra

$\boldsymbol{x}$	vector (column by default)
x_i	entry i of vector $\boldsymbol{x}$
$\boldsymbol{x}_{\setminus i}$	the vector $\boldsymbol{x}$ whose i entry is removed
$\langle \boldsymbol{x} \rangle$	for a vector $\boldsymbol{x}$ of size N, $\frac{1}{N}\sum_i x_i$ (by default)
$(\cdot)^\dagger$	conjugate transposition
$(\boldsymbol{x}, \boldsymbol{y})$	$(\boldsymbol{x}^\dagger, \boldsymbol{y}^\dagger)^\dagger$
$\boldsymbol{X}$	matrix
$\mathbf{I}$	identity matrix
$\mathbf{0}$	all zero matrix
X_{ij}, $[\boldsymbol{X}]_{ij}$, $(\boldsymbol{X})_{ij}$	entry (i, j) of $\boldsymbol{X}$
$\mathrm{tr}(\boldsymbol{X})$	trace of $\boldsymbol{X}$
$\mathrm{Tr}(\boldsymbol{X})$	for a matrix $\boldsymbol{X}$ of size $N \times N$, $\mathrm{tr}(\boldsymbol{X})/N$
$\phi(\boldsymbol{X})$	for a matrix $\boldsymbol{X}$ of size $N \times N$, $\lim_{N\to\infty} \mathrm{Tr}(\boldsymbol{X})$
$\lvert \boldsymbol{X} \rvert$	determinant of $\boldsymbol{X}$

Probability Theory

F_X	probability distribution function of random variable X
f_X	probability density function of random variable X
$\langle X \rangle$, $\langle X \rangle_{\mathrm{f}_X}$, $\langle X \rangle_{\mathrm{F}_X}$	expectation of random variable X, i.e. $\int x \, \mathrm{dF}_X(x)$
$\mathrm{Var}(X)$	variance of random variable X, i.e. $\langle X^2 \rangle$- $\langle X \rangle^2$
$X \sim \mathrm{F}$	X is a random variable with distribution F
$X \sim Y$	X and Y are identically distributed.
$N(\boldsymbol{x}; \boldsymbol{\mu}, \boldsymbol{\Sigma})$	real or complex Gaussian probability density function with mean $\boldsymbol{\mu}$ and covariance $\boldsymbol{\Sigma}$
$\mathcal{N}(\boldsymbol{x}; \boldsymbol{\mu}, \boldsymbol{\Sigma})$	real or complex Gaussian probability distribution with mean $\boldsymbol{\mu}$ and covariance $\boldsymbol{\Sigma}$

For a random matrix $\boldsymbol{X} = \boldsymbol{X}^\dagger$ of size $N \times N$

$\mathrm{F}_{\boldsymbol{X}}^N$	empirical eigenvalue distribution function of $\boldsymbol{X}$
$\mathrm{F}_{\boldsymbol{X}}$	limiting eigenvalue distribution function of $\boldsymbol{X}$
$\mathrm{G}_{\boldsymbol{X}}^N$	Stieltjes transform of $\mathrm{F}_{\boldsymbol{X}}^N$
$\mathrm{G}_{\boldsymbol{X}}$	Stieltjes transform of $\mathrm{F}_{\boldsymbol{X}}$
$\mathrm{R}_{\boldsymbol{X}}^N$	R-transform of $\mathrm{F}_{\boldsymbol{X}}^N$
$\mathrm{R}_{\boldsymbol{X}}$	R-transform of $\mathrm{F}_{\boldsymbol{X}}$
$\mathrm{S}_{\boldsymbol{X}}^N$	S-transform of $\mathrm{F}_{\boldsymbol{X}}^N$
$\mathrm{S}_{\boldsymbol{X}}$	S-transform of $\mathrm{F}_{\boldsymbol{X}}$

Chapter 1

Introduction

Section 1 of this chapter directly, or indirectly, uses the material in Section II of Burak Çakmak, Manfred Opper, Bernard H. Fleury and Ole Winther, "Self-averaging expectation propagation," arXiv preprint arXiv: 1608.06602, August 2016.

Due to the recent technological advances, the demand for techniques capable of processing large amount of information data has dramatically grown. Within this context, large systems – which operate with large dimensional input and output information – are becoming increasingly important research subjects in the information processing community. In particular, accurately performing analysis and inference of such systems is often challenging because a large number of (latent, typically) variables are coupled to each other.

Statistical mechanics precisely studies large systems consisting of many constituents, e.g. electrons, molecules, etc., which interact with one another [1], [2]. While the theory starts with the microscopic laws of physics – that explain the behavior of the constituents of the system – it eventually brings answers to macroscopic quantities, such as temperature and pressure. The theory does not care about the impact of a particular constituent of the system; it rather provides an understanding as a whole. Statistical mechanics typically uses the Hamiltonian formalism. A so-called Hamiltonian function describes the total energy of the system as a function of the state of all its constituents. Vaguely speaking, it is implicitly assumed that there is no preferred constituent in the Hamiltonian, i.e. all constituents contribute to the total energy of the system in a "democratic fashion" – a phrase suggested by A. D. Jackson [3] to explain the so-called invariance property of a certain class of random matrices.

Our conceptual view to deal with large information processing systems is similar to that adopted in statistical mechanics. In a word, we require the system to obey a *democratic order*. The system does not include preferred latent variables. We consider that this restriction is important if one needs to accu-

rately describe the system via some macroscopic quantities without making reference to some specific variables. For systems that involve an asymmetry, i.e. some variables have more (or less) impact than others, the description should reflect the impact of each variable individually. But, deriving such a description is typically infeasible when the system is large. We next present a mathematical argumentation for a general probabilistic system model that clarifies our intuitive rationale presented above.

1 Systems Obeying a Democratic Order

By design or through the physical description of the system, the input vector is often coupled via a matrix. This is the case when the input vector $\boldsymbol{x}$ is first linearly transformed as $\boldsymbol{z} = \boldsymbol{H}\boldsymbol{x}$ and then the vector $\boldsymbol{z}$ is mapped to the output vector $\boldsymbol{y}$. For the sake of simplicity, we assume that all variables are real-valued. The extension of our discussion to the complex-valued case is straightforward. Here we consider a probabilistic system and describe the mapping $\boldsymbol{z} \to \boldsymbol{y}$ with the conditional probability density function (pdf) $f(\boldsymbol{y}|\boldsymbol{z})$. Furthermore, we adopt the Bayesian philosophy and assign a prior pdf $f(\boldsymbol{x})$ to the input vector. Moreover, we consider the typical assumption that the prior pdf and the conditional pdf are both separable, i.e. $f(\boldsymbol{x}) = \prod_k f_k(x_k)$ and $f(\boldsymbol{y}|\boldsymbol{z}) = \prod_n f_n(y_n|z_n)$. The joint posterior pdf of the latent variables $(\boldsymbol{x}, \boldsymbol{z})$ is given by

$$f(\boldsymbol{x}, \boldsymbol{z}|\boldsymbol{y}, \boldsymbol{H}) = \frac{1}{Z} f(\boldsymbol{x}) \delta(\boldsymbol{z} - \boldsymbol{H}\boldsymbol{x}) f(\boldsymbol{y}|\boldsymbol{z}) \tag{1.1}$$

where Z denotes a normalization constant. We now borrow the conceptual view of statistical mechanics: We define a Hamiltonian function of the system and restrict it in such a way that the latent variables equally contribute to the Hamiltonian in a statistical sense. For mathematical convenience, we will work on a slightly amended form of the pdf (1.1):

$$f_\tau(\boldsymbol{x}, \boldsymbol{z}|\boldsymbol{y}, \boldsymbol{H}) = \frac{1}{Z} f(\boldsymbol{x}) N(\boldsymbol{z}|\boldsymbol{H}\boldsymbol{x}, \tau\mathbf{I}) f(\boldsymbol{y}|\boldsymbol{z}) \tag{1.2}$$

$$= \frac{1}{Z} e^{\mathcal{H}_\tau(\boldsymbol{x}, \boldsymbol{z}|\boldsymbol{y})}. \tag{1.3}$$

We obtain the pdf (1.1) by taking the limit $\tau \to 0$. Here $\mathcal{H}_\tau$ is the Hamiltonian function of the system. It is given by

$$\mathcal{H}_\tau(\boldsymbol{x}, \boldsymbol{z}|\boldsymbol{y}) \triangleq \sum_k \ln f_k(x_k) + \sum_n \ln f_n(y_n|z_n) - \frac{1}{\tau} (\boldsymbol{x}, \boldsymbol{z})^\dagger \boldsymbol{J} (\boldsymbol{x}, \boldsymbol{z}) - \frac{N}{2} \ln 2\pi\tau \tag{1.4}$$

where N is the dimension of $\boldsymbol{z}$ and we define

$$\boldsymbol{J} \triangleq \begin{pmatrix} \boldsymbol{H}^\dagger \boldsymbol{H} & \boldsymbol{H}^\dagger \\ \boldsymbol{H} & \mathbf{I} \end{pmatrix}. \tag{1.5}$$

Thereby, with (1.4) we have obtained a probabilistic representation of the system whose form is typical in statistical mechanics. For example, we can associate the Hamiltonian $\mathcal{H}_\tau$ in (1.4) with the total energy of the electrons and nuclei in a molecule in quantum chemistry [4]. Specifically, we interpret $\ln f_k(x_k)$ as the kinetic energy of the position of nucleus x_k, $\ln f_n(y_n|z_n)$ as the kinetic energy of the position of electron z_n and $(\boldsymbol{x}, \boldsymbol{z})^\dagger \boldsymbol{J}(\boldsymbol{x}, \boldsymbol{z})$ as the potential energy of the electrons and nuclei.

We now restrict the probabilistic system to obey a *democratic order*. Basically, we constrain the Hamiltonian function to reflect the fact that the system does not contain preferred latent entries in $\boldsymbol{x}$ and $\boldsymbol{z}$ in a statistical sense. Mathematically speaking, let $\boldsymbol{U}$ and $\boldsymbol{V}$ be (uniformly distributed) independent random permutation matrices. Then we say that the system obeys a democratic order when its Hamiltonian fulfills the symmetry property

$$\mathcal{H}_\tau(\boldsymbol{x}, \boldsymbol{z}|\boldsymbol{y}) \sim \mathcal{H}_\tau(\boldsymbol{U}\boldsymbol{x}, \boldsymbol{V}\boldsymbol{z}|\boldsymbol{V}\boldsymbol{y}) \tag{1.6}$$

where $X \sim Y$ implies that random variables X and Y are identically distributed. Note that by writing (1.6) we treat $\boldsymbol{H}$ as a random matrix. Property (1.6) is fulfilled if the following conditions hold:

(i) $f_k(x) = f_l(x)$ for all $k \neq l$;

(ii) $f_n(y|z) = f_m(y|z)$ for all $n \neq m$;

(iii) $\boldsymbol{H} \sim \boldsymbol{U}\boldsymbol{H}\boldsymbol{V}$, i.e. the probability distribution of $\boldsymbol{H}$ is invariant under multiplications from left and right with an independent random permutation matrix.

Conditions (i) and (ii) are commonly made assumptions in practice. As regards condition (iii) two points are worth stressing: In case $\boldsymbol{H}$ arises as the result of a description of a physical system and gives similar weights to the interactions between the variables, then (iii) is a reasonable assumption. In case $\boldsymbol{H}$ is specified by design, it is reasonable to restrict the system model such that condition (iii) holds. Moreover, depending on the particular application some of the restrictions above may not apply. For example, it might be the case that we only need

$$\mathcal{H}_\tau(\boldsymbol{x}, \boldsymbol{z}|\boldsymbol{y}) \sim \mathcal{H}_\tau(\boldsymbol{U}\boldsymbol{x}, \boldsymbol{z}|\boldsymbol{y}) \tag{1.7}$$

which is fulfilled if condition (i) holds and $\boldsymbol{H} \sim \boldsymbol{U}\boldsymbol{H}$.

1.1 Haar-type bases

Condition (iii) is still mathematically not convenient to work with in general. In the sequel, we present a convenient random matrix model for $\boldsymbol{H}$ that fulfills (iii). We start with the singular value decomposition

$$\boldsymbol{H} = \boldsymbol{L}\boldsymbol{S}\boldsymbol{R} \tag{1.8}$$

where $\boldsymbol{L}$ is an orthogonal matrix whose columns are the left singular vectors of $\boldsymbol{H}$, $\boldsymbol{R}$ is an orthogonal matrix whose columns are the right singular vectors of $\boldsymbol{H}$ and the non-negative diagonal entries of $\boldsymbol{S}$ are the singular values of $\boldsymbol{H}$. Condition (iii) holds if (presumably, if, and only if) $\boldsymbol{L}$, $\boldsymbol{S}$ and $\boldsymbol{R}$ are independent and $\boldsymbol{L}$ and $\boldsymbol{R}$ are invariant under multiplication with independent random permutation matrices, e.g. $\boldsymbol{L} \sim \boldsymbol{U}\boldsymbol{L}$. This implies that "*There are no preferred left or right singular vectors.*" Put simply "*There is no preferred basis of the left and right singular vectors.*" Specifically, the orthogonal matrices $\boldsymbol{L}$ and $\boldsymbol{R}$ are invariant under multiplication with any independent orthogonal matrix. A random matrix whose distribution is invariant under multiplication of the matrix with any orthogonal matrix is called a Haar matrix [5][1]. In summary, we assume that $\boldsymbol{L}$, $\boldsymbol{S}$ and $\boldsymbol{R}$ are independent of each other and $\boldsymbol{L}$ and $\boldsymbol{R}$ are Haar matrices. Equivalently, for orthogonal matrices $\boldsymbol{U}$ and $\boldsymbol{V}$ independent of $\boldsymbol{H}$ we have $\boldsymbol{H} \sim \boldsymbol{U}\boldsymbol{H}\boldsymbol{V}$. For short we will say that $\boldsymbol{H}$ is invariant from left and right.

It is common to assume that the entries of $\boldsymbol{H}$ are independent identically distributed (iid) Gaussian random variables with zero mean. The pdf of Gaussian random matrix can be written in the form

$$f_{\boldsymbol{H}}(\boldsymbol{H}) \propto \exp\left(-\frac{1}{2\sigma^2}\sum_{n,k} H_{n,k}^2\right) \tag{1.9}$$

$$= \exp\left(-\frac{1}{2\sigma^2}\mathrm{tr}(\boldsymbol{H}^{\dagger}\boldsymbol{H})\right) \tag{1.10}$$

with σ^2 denoting the components' variance. Notice that for any orthogonal matrices $\boldsymbol{U}$ and $\boldsymbol{V}$ we have $f_{\boldsymbol{H}}(\boldsymbol{U}\boldsymbol{H}\boldsymbol{V}) = f_{\boldsymbol{H}}(\boldsymbol{H})$. Moreover, the Jacobian of mapping $\boldsymbol{X} \to \boldsymbol{U}\boldsymbol{X}$ is one if $\boldsymbol{U}$ is orthogonal [11]. Thereby, the Gaussian random matrix $\boldsymbol{H}$ is invariant from left and right [12].

Without a clear physical or mathematical motivation, the iid assumption on the entries of $\boldsymbol{H}$ can be artificial. For example, it can be more suitable to design $\boldsymbol{H}$ to be a so-called random row-orthogonal matrix [9], [10] in which case $\boldsymbol{H}$ has statistically dependent entries but is invariant from left and right. It is the goal of this thesis to investigate systems that involve matrices that are drawn from some invariant ensemble under multiplication with independent orthogonal, or unitary, matrix from left (and/or right). Basically, we do not assume a specific distribution for the singular values of $\boldsymbol{H}$ but for the matrix of left singular vectors. This specific distribution is Haar. In the large-system limit, this assumption can also be relaxed to certain Haar-like matrices such as "fake Haar" matrices [13]. In general, we expect that the

[1]Haar matrices were already addressed in the mean-field theory of spin glasses [6], the receiver design for code-division multiple access communication channels [7] and the information theoretical analysis of vector precoding for Gaussian channels [8] and compressed sensing [9], [10].

analysis of Haar-type bases may provide good approximations for systems obeying the democratic order (1.6), i.e. the contributions of individual latent variables to the observation model are statistically identical.

2 Contributions of the Thesis

The random matrix framework underlined in the previous section applies to a broad class of research problems. We consider three applications that have drawn significant attention in the information processing community. In the sequel, we shortly introduce these problems and describe our contributions to them.

2.1 Capacity scaling in MIMO systems

Channel capacity – introduced by Shannon [14] – quantifies the maximum data rate which can be transmitted reliably over the channel. To warm up let us first consider a basic communication system with a single transmit and receive antenna and the input-output relationship described by

$$y = hx + n \tag{1.11}$$

where x is a zero mean random input signal with variance σ_x^2, h is the gain of the channel, y is the output signal and n is zero-mean circularly-symmetric complex Gaussian noise with variance σ_n^2. When the receiver (transmitter) is aware of the realization of the channel gain h, we say that perfect channel state information is available at the receiver (transmitter). Available perfect channel state information means full knowledge about the channel gain h. Under the assumption of perfect channel state information at the receiver the (ergodic) capacity (in bits per second per channel use) of channel (1.11) is given by

$$\left\langle \log_2(1 + \mathrm{SNR}|h|^2) \right\rangle_h . \tag{1.12}$$

Here, the expectation is taken over the probability distribution of the channel gain h and SNR denotes the signal-to-noise ratio, i.e.

$$\mathrm{SNR} = \frac{\sigma_x^2}{\sigma_n^2}.$$

We now extend the scalar-valued communication system (1.11) to a vector valued communication system with T transmit antennas, R receive antennas and the input-output relationship described by

$$\boldsymbol{y} = \boldsymbol{H}\boldsymbol{x} + \boldsymbol{n} \tag{1.13}$$

where $\boldsymbol{x}$ is the T-dimensional input signal vector, $\boldsymbol{y}$ the R-dimensional output signal vector and $\boldsymbol{n}$ is an R-dimensional noise vector with circularly-symmetric complex Gaussian entries. Moreover, $\boldsymbol{H}$ is the multiple-input multiple-output (MIMO) channel matrix with entries $H_{r,t}$ representing the channel gain from transmit antenna r to receive antenna t. All quantities in (1.13) are complex-valued. The entries of $\boldsymbol{x}$ and $\boldsymbol{n}$ are assumed to be iid with zero mean and variances σ_x^2 and σ_n^2, respectively. In the thesis, we primarily consider the capacity of (1.13) when the transmit antennas are restricted to send equal signal power [15]:

$$\left\langle \log_2 \left| \mathbf{I} + \mathrm{SNR} \boldsymbol{H}^\dagger \boldsymbol{H} \right| \right\rangle_{\boldsymbol{H}}. \tag{1.14}$$

As a matter of fact (1.14) is the mutual information of the communication link (1.13) when the input signal is Gaussian distributed.

When $\boldsymbol{H}$ has full-rank, the capacity (1.14) can be written in the form [16]

$$\min(T, R) \log_2 \mathrm{SNR} + O(1) \tag{1.15}$$

where $O(1)$ is a bounded function of the SNR *that does depend on T and R, in general*. Since the term $O(1)$ is a bounded function of the SNR, the expression (1.15) has frequently led to the two following misinterpretations:

(i) for any variation of T or R with $\min(T, R)$ being fixed the capacity would not vary at high SNR;

(ii) the capacity would grow linearly with $\min(T, R)$ at high SNR.

Misinterpretation (i) is studied by [17] when $\boldsymbol{H}$ is the classical matrix ensemble with zero-mean iid Gaussian entries. We elucidate both misinterpretations (i) and (ii) for *arbitrary invariant matrices*. As for (i), we obtain an expression for the variation of the capacity that is not a function of the singular values of $\boldsymbol{H}$. It only depends on the number of transmit and receive antennas before and after the variation. As for (ii), we quantify how the capacity as a function of the system dimensions deviates from the assumed linear growth. We derive remarkable properties of this deviation. Our results on the variation of the capacity are valid in the asymptotic SNR limit. However, they also provide least upper bounds on the variation of the capacity over all SNRs. This property gives these bounds a universal character.

2.2 Self-averaging expectation propagation

We consider the problem of Bayesian inference for a general class of observation models. A K-dimensional real, or complex, input vector $\boldsymbol{x}$ – generated according to a prior pdf $f(\boldsymbol{x})$ – is transformed with an $N \times K$ real, or complex, matrix as $\boldsymbol{z} \triangleq \boldsymbol{H}\boldsymbol{x}$. Then, the vector $\boldsymbol{z}$ is operated according to a conditional

pdf $f(\boldsymbol{y}|\boldsymbol{z})$ to produce the output vector $\boldsymbol{y}$ of the system. We assume that the prior and the conditional pdfs are both separable i.e.

$$f(\boldsymbol{x}) = \prod_{k=1}^{K} f_k(x_k) \tag{1.16}$$

$$f(\boldsymbol{y}|\boldsymbol{z}) = \prod_{n=1}^{N} f_n(y_n|z_n). \tag{1.17}$$

As a first example, we consider a direct-sequence binary phase shift-keying code-division multiple access (CDMA) communication system with K users where each user sends a sequence of independently, uniformly distributed bits $x_k = \mp 1$ over a single communication channel to a base station. The input bits are linearly coded as $\boldsymbol{Hx}$ where $\boldsymbol{H}$ is designed in an efficient way to mitigate the effect of interference between the users' signals. For details we refer the reader to e.g. [18], [19]. At the base station, we have the observation

$$\boldsymbol{y} = \boldsymbol{Hx} + \boldsymbol{n} \tag{1.18}$$

where $\boldsymbol{n}$ is classical additive white Gaussian noise. From the above, the prior and the conditional pdfs are given by

$$f_k(x_k) = 0.5\ \delta(x_k + 1) + 0.5\ \delta(x_k - 1) \tag{1.19}$$

$$f_n(y_n|z_n) = N\left(y_n; z_n, 1/\beta\right). \tag{1.20}$$

The second example is classical in compressed sensing. The linear observation model is the same as (1.18) with the prior distribution of x_k being Bernoulli-Gaussian. The last example is borrowed from classification [20] with a nonlinear observation model of the form

$$\boldsymbol{y} = \text{sign}(\boldsymbol{Hs}) \tag{1.21}$$

where $\text{sign}(\cdot)$ is the sign function: $\text{sign}(x) = x/|x|$ if $x \neq 0$ and $\text{sign}(0) = 0$. In this case, we have $f_n(y_n|z_n) = u(y_n z_n)$ where $u(\cdot)$ is the unit step function.

Message passing techniques for dense graphs with Thoules-Andersen-Palmer (TAP) like fixed-point equations have gained widespread use to design accurate algorithms for signal recovery in machine learning. The so-called expectation propagation (EP) algorithm [20], [21] has cubic complexity in the system size but makes no assumptions on the matrix ensemble. The approximate message passing (AMP) algorithm [22–25] – derived from applying the heuristic belief propagation (BP) on dense graphs – has quadratic complexity but assumes zero–mean iid elements of the transformation matrix.

In this contribution, we investigate the problem of applying EP for approximate Bayesian inference on large systems. Our method – that we call

self-averaging EP – attempts to overcome the computational complexity of EP due to the inversion of large matrices. When the transformation matrices are asymptotically free – a concept defined in random matrix theory – the EP cavity variances exhibit an asymptotic self-averaging property as the system dimensions grow large. They can be approximated by using the R- and S-transforms in free probability, which do not require matrix inversions. Our approach extends the framework of AMP to a general class of random matrix ensembles. The generalization is via a simple formulation of the R-transform or S-transform of the limiting eigenvalue distribution of the Gramian matrix of transformation matrix. We demonstrate the self-averaging effect and compare the performance of self-averaging EP with that of standard EP for two ensembles of transformation matrices in a nonlinear signal recovery problem from compressed sensing.

2.3 Dynamical aspects of the TAP equations

The TAP fixed-point equations for a general class of system models can be obtained in a systematic way by combining the frameworks of EP and free probability theory (Chapter 4). However, it is not necessarily clear how the resulting system of nonlinear equations can be solved efficiently. This is precisely the third contribution of the thesis, namely to introduce a method for solving TAP fixed-point equations iteratively. While doing this, we will consider the standard Ising model of spin glass theory [26, 27] for which the original TAP fixed-point equations were introduced.

For the sake of clarity of our argumentations, we next base our discussion on a specific example. We recall the CDMA system described in (1.18) with the prior and the conditional pdfs given in (1.19) and (1.20), respectively. Moreover, let the entries of $\boldsymbol{H}$ be iid with zero mean and variance $1/N$. For convenience, we define $\boldsymbol{h} \triangleq \beta \boldsymbol{H}^{\mathsf{T}} \boldsymbol{y}$ and the coupling matrix $\boldsymbol{J} = \boldsymbol{J}^{\mathsf{T}}$ such as

$$J_{ij} \triangleq \begin{cases} -\beta [\boldsymbol{H}^{\mathsf{T}} \boldsymbol{H}]_{ij} & i \neq j \\ 0 & i = j \end{cases} . \tag{1.22}$$

The TAP fixed-point equations of the CDMA model (1.18) can be written in the form

$$\boldsymbol{m} = \tanh \left(\boldsymbol{h} + \boldsymbol{J}\boldsymbol{m} - \frac{\beta^2 \alpha (1-q)}{1 + \beta \alpha (1-q)} \boldsymbol{m} \right) \tag{1.23}$$

with $q \triangleq \boldsymbol{m}^{\mathsf{T}} \boldsymbol{m}/K$ and $\alpha \triangleq N/K$. Above the so-called Almedia-Thouless (AT) [28] line of the stability condition it is generally assumed that

$$\boldsymbol{m} \simeq \langle \boldsymbol{x} \rangle_{f(\boldsymbol{x}|\boldsymbol{y})}. \tag{1.24}$$

Thereby, a nearly optimum detector simply needs to solve (1.23). A promi-

nent way of doing this is via the AMP algorithm [22]

$$\boldsymbol{m}(t+1) = \tanh(\boldsymbol{z}(t) + R(t)\boldsymbol{m}(t)) \tag{1.25}$$

$$\boldsymbol{z}(t) = \frac{R(t)}{\beta}\left(\boldsymbol{h} + (\boldsymbol{J} - \beta\mathbf{I})\boldsymbol{m}(t)\right) + \alpha(1 - q(t))R(t)\boldsymbol{z}(t-1) \tag{1.26}$$

$$R(t) \triangleq \frac{1}{1/\beta + (1-q(t))\alpha}, \quad q(t) \triangleq \frac{1}{K}\boldsymbol{m}(t)^{\dagger}\boldsymbol{m}(t). \tag{1.27}$$

The fixed points of the AMP algorithm (1.25)-(1.27) solve (1.23). AMP is derived as an asymptotic limit (when the system dimensions grow large) of heuristic loopy BP on dense graphs. It only yields the correct TAP equations for two random coupling matrix models of $\boldsymbol{J}$ [29]: (i) $\boldsymbol{J}$ is given as in (1.22) with the entries of $\boldsymbol{H}$ iid with zero mean and asymptotically vanishing variance; (ii) $\boldsymbol{J} = \boldsymbol{J}^{\dagger}$ has vanishing diagonal entries and iid off-diagonal entries with zero mean and asymptotically vanishing variance. The first and second models are variants of respectively the Hopfield model and the SK model in statistical physics [26, 27]. Even the simplest case where $\boldsymbol{J}$ is an orthogonal matrix invalidates the AMP technique because this case leads to incorrect TAP fixed-point equations in this case. This strongly indicates that there is a need for a well-defined framework to solve the TAP equations.

In this contribution, we introduce a theory on the basis of dynamical functional analysis [30–32] for solving the TAP equations with arbitrary invariant random matrices. We consider the standard Ising model introduced in spin glass theory [26, 27] where the external field is $h_i = h \; \forall i$ and h does not depend on coupling matrix $\boldsymbol{J}$. For example, the CDMA system model is an Ising model, but the external field $\boldsymbol{h}$ is random via $\boldsymbol{J}$. We show that our method reproduces previous "convergent" algorithms (i.e. the AMP algorithm) for the Hopfield model [22] and the SK model [33]. While we only consider a deterministic external field in this contribution, our theory can be extended to a random external field and also to more general probabilistic models.

3 Outline of the Thesis

The thesis is organized as follows. In Chapter 2 we provide some background on random matrices and introduce the tools that will be used in the three application chapters that follow. In Chapter 3 we present the contribution on the capacity scaling of MIMO systems as briefly introduced in Subsection 2.1. In Chapter 4 we introduce the method of self-averaging EP that is briefly mentioned in Subsection 2.2. Chapter 5 addresses the dynamical functional analysis for solving TAP equations of which a brief account is given in Subsection 2.3. Conclusions and outlook are presented in Chapter 6. Technical derivations are deferred to the Appendix.

Chapter 2

Elements of Random Matrices

Random matrices have appeared in a notable variety of areas such as mathematical statistics [34], nuclear physics [35], spin glasses [26], communication theory [36] and computational biology [37]. This chapter provides an overview of random matrices and prepares the reader to the random matrix methods used in the application chapters thereafter. We will not go into the details of the exciting mathematics of random matrices for which we refer to [5], [12]. During our discussions, we assume that the reader is familiar with the standard elements of probability theory and linear algebra.

1 Eigenvalue Distribution Functions

The most studied symmetric, or Hermitian, random matrices have a matrix of eigenvectors that is uniformly distributed in the space of orthogonal, or unitary, matrices, i.e. they are Haar. Informally, this implies that there is no preferred basis of eigenvectors. The matrix of eigenvectors does not involve relevant information and therefore, the primary interest in such random matrices lies in studying their eigenvalues.

Notation 1. *Given an $N \times N$ random matrix $\boldsymbol{X} = \boldsymbol{X}^{\dagger}$, we denote by $\mathrm{F}_{\boldsymbol{X}}^{N}$ the empirical eigenvalue distribution function of $\boldsymbol{X}$, i.e. [38]*

$$\mathrm{F}_{\boldsymbol{X}}^{N}(x) = \frac{1}{N} |\, \{x_i \in \mathcal{L} : x_i \leq x\} \,| \tag{2.1}$$

with $\mathcal{L}$ and $|\cdot|$ denoting the set of eigenvalues of $\boldsymbol{X}$ and the cardinality of a set, respectively. Moreover, if for $N \to \infty$ $\boldsymbol{X}$ has a limiting eigenvalue distribution

(LED) almost surely, its distribution function is denoted by $\mathrm{F}_{\boldsymbol{X}}$[1].

We are often interested in a mathematical quantity that depends on a matrix via an integral over its eigenvalue distribution. As an example, let us consider the (differential) entropy

$$h(\mathrm{F}) \triangleq -\int_{\mathbb{R}^N} \ln \mathrm{F}'(\boldsymbol{x})\, \mathrm{dF}(\boldsymbol{x}) \tag{2.2}$$

where $\mathrm{F}'(\boldsymbol{x}) \triangleq \mathrm{dF}(\boldsymbol{x})/\mathrm{d}\boldsymbol{x}$ is the pdf associated with F for an N-variate Gaussian probability distribution with mean $\boldsymbol{\mu}$ and positive covariance matrix $\boldsymbol{X}$. We have [15]

$$h(\mathrm{F}) = \frac{N}{2}\ln(2\pi e) + \frac{1}{2}\ln|\boldsymbol{X}|. \tag{2.3}$$

Thus, we merely need to calculate $\ln|\boldsymbol{X}|$, which can be reformulated as

$$\ln|\boldsymbol{X}| = \ln\prod_{x_i\in\mathcal{L}} x_i \tag{2.4}$$

$$= \sum_{x_i\in\mathcal{L}} \ln(x_i) \tag{2.5}$$

$$= N\int \ln(x)\, \mathrm{dF}_{\boldsymbol{X}}^N(x). \tag{2.6}$$

We may also encounter a so-called degenerate Gaussian distribution where $\boldsymbol{X}$ has rank $K < N$. In this case, the pdf is of the form [39]

$$\mathrm{F}'(\boldsymbol{x}) = \frac{1}{\sqrt{|2\pi\boldsymbol{X}|^+}} \exp\left(-\frac{1}{2}(\boldsymbol{x}-\boldsymbol{\mu})^\dagger \boldsymbol{X}^+ (\boldsymbol{x}-\boldsymbol{\mu})\right) \tag{2.7}$$

where $\boldsymbol{X}^+$ denotes the pseudo inverse of $\boldsymbol{X}$ and $|\boldsymbol{X}|^+$ denotes the pseudo determinant. The pseudo determinant can be expressed as

$$|\boldsymbol{X}|^+ = \lim_{\epsilon\to 0} |\epsilon^{\frac{K}{N}}(\mathbf{I} + \epsilon\boldsymbol{X})|. \tag{2.8}$$

One can easily show that

$$h(\mathrm{F}) = \frac{K}{2}\ln(2\pi e) + \frac{K}{2}\int \ln(x)\, \mathrm{d}\tilde{\mathrm{F}}_{\boldsymbol{X}}^N(x) \tag{2.9}$$

where $\tilde{\mathrm{F}}_{\boldsymbol{X}}^N$ represents the distribution function of the non-zero eigenvalues of $\boldsymbol{X}$. The explicit definition of this distribution function is given as follows.

[1] Eigenvalue distribution functions are uniquely associated with a distribution (or measure) on $\mathbb{R}$ with total mass one. In the text, we will use both terms "distribution functions" and "distributions" interchangeably. Which other one is meant when one term is used will be clear from the context. Integrals over any distribution associated with an eigenvalue distribution function will, however, always be expressed in terms of the distribution function.

Definition 2.1. *For an $N \times N$ non-negative definite matrix $\boldsymbol{X} \neq \mathbf{0}$, we define the normalized rank of $\boldsymbol{X}$ as*

$$\alpha_{\boldsymbol{X}}^N \triangleq 1 - \mathrm{F}_{\boldsymbol{X}}^N(0) \tag{2.10}$$

and the distribution function of non-zero eigenvalues of $\boldsymbol{X}$ as

$$\tilde{\mathrm{F}}_{\boldsymbol{X}}^N(x) \triangleq \frac{1}{\alpha_{\boldsymbol{X}}^N} \left\{ \left(\alpha_{\boldsymbol{X}}^N - 1 \right) u(x) + \mathrm{F}_{\boldsymbol{X}}^N(x) \right\}. \tag{2.11}$$

2 Random Matrices

In this section, we shortly introduce the classical random matrices studied in the literature. These are the Haar, Wishart, Wigner and Jacobi matrices. Then, we examine in detail general invariant matrix ensembles.

2.1 Haar matrices

An orthogonal, or unitary, matrix that is uniformly distributed over the space $\{\boldsymbol{X} : \boldsymbol{X}^\dagger \boldsymbol{X} = \mathbf{I}\}$ is called a Haar matrix. Haar matrices play a fundamental role in random matrix theory because the matrices of singular vectors of the classical random matrices are often Haar.

To better understand Haar matrices we first provide an implicit but insightful definition of them: An orthogonal, or unitary, random matrix $\boldsymbol{U}$ is Haar if, and only if, $\boldsymbol{U} \sim \boldsymbol{V}\boldsymbol{U}\boldsymbol{W}$ for any orthogonal, or unitary, matrices $\boldsymbol{V}$, $\boldsymbol{W}$ independent of $\boldsymbol{U}$. In other words, the matrix is Haar if, and only if, it is orthogonal, or unitary, and rotationally invariant.

Definition 2.2. *[40] Let the entries of an $N \times N$ random matrix $\boldsymbol{X}$ be independent and real, or circularly-symmetric complex, Gaussian with zero mean and unit variance. Then, the $N \times N$ Haar matrix can be defined as*

$$\boldsymbol{U} = \boldsymbol{X}(\boldsymbol{X}^\dagger \boldsymbol{X})^{-\frac{1}{2}} . \tag{2.12}$$

Calculation of the moments of the entries of Haar matrices has attracted substantial interest in the literature. For example, from Definition 2.2 one can show that $\langle U_{ij} \rangle = 0$ and $\langle |U_{ij}|^2 \rangle = 1/N$, $\forall i, j$. However, the moments of higher orders are difficult to calculate by using standard probability calculus. The so-called Weingarten calculus [41] provides a systematic way for calculating these moments. The interested reader is referred to [41], [42]. In particular, we have the following result on the fourth-order moments.

Lemma 2.1. *Let $\boldsymbol{U}$ be an $N \times N$ Haar matrix. Then we have*

$$\left\langle |U_{in}|^2 |U_{ik}|^2 \right\rangle = \begin{cases} \frac{N+1}{N(N+\beta)(N+3-2\beta)} & n \neq k \\ \frac{1+\beta}{N(N+\beta)} & n = k \end{cases} \tag{2.13}$$

where $\beta = 2$ and $\beta = 1$ when $\boldsymbol{U}$ is real and complex, respectively.

For $\boldsymbol{U}$ being unitary, this result is presented in [12]. For $\boldsymbol{U}$ being orthogonal, the result can be easily inferred from [42, Theorem 2.1, Example 3.1].

2.2 Wishart matrices

Random matrices were first introduced in the context of statistics by Wishart who investigated the behavior of sample covariance matrices of independent Gaussian random vectors [34]. Such sample covariance matrices are called Wishart matrices.

Definition 2.3. *[34] Consider an $N \times K$ random matrix $\boldsymbol{H}$ whose rows are independently drawn from a K-variate Gaussian distribution with zero mean and covariance $\boldsymbol{\Sigma}$. The $K \times K$ random matrix $\boldsymbol{X} = \boldsymbol{H}^{\dagger}\boldsymbol{H}$ is called a (central) Wishart matrix.*

A particularly important case is that where $\boldsymbol{\Sigma} = \mathbf{I}/K$, i.e. the entries of $\boldsymbol{H}$ are iid. In this case, the Gram matrix $\boldsymbol{X}$ is often called a null-Wishart matrix.

The LED of a null-Wishart matrix is the Marčenko-Pastur distribution. Specifically, let the entries of an $N \times K$ matrix $\boldsymbol{H}$ be iid with zero mean and variance $1/N$. Moreover, let $\boldsymbol{X} = \boldsymbol{H}^{\dagger}\boldsymbol{H}$. Then, as $K \to \infty$ with the aspect ratio $\phi = K/N$ fixed, the empirical distribution of the eigenvalues of $\boldsymbol{X}$ converges almost surely to a non-random distribution whose density is

$$\mathrm{F}'_{\boldsymbol{X}}(x) = \left(1 - \frac{1}{\phi}\right)^{+} \delta(x) + \frac{\sqrt{(x-\lambda_-)^+(\lambda_+ - x)^+}}{2\pi\phi x} \tag{2.14}$$

where $\lambda_{\mp} = (1 \mp \sqrt{\phi})^2$.

2.3 Wigner matrices

Wigner matrices are the first random matrices that appeared in the physics literature [35]. They are still popular because they are mathematically simple and convenient to work with.

Definition 2.4. *[35] Let the entries of an $N \times N$ matrix $\boldsymbol{H}$ be iid with zero mean and variance $1/N$. The matrix $\boldsymbol{X} \triangleq (\boldsymbol{H} + \boldsymbol{H}^{\dagger})/\sqrt{2}$ is called a Wigner matrix. Moreover, $\boldsymbol{X}$ is called a Gaussian Wigner matrix if the entries of $\boldsymbol{H}$ are real, or circularly-symmetric complex, Gaussian.*

As $N \to \infty$, the empirical eigenvalue distribution of a Wigner matrix converges almost surely to a non-random distribution with density [35]

$$\mathrm{F}'_{\boldsymbol{X}}(x) = \frac{1}{2\pi}\sqrt{(4 - x^2)^+}. \tag{2.15}$$

This distribution is usually referred to as the semi-circle law.

2.4 Jacobi matrices

Jacobi matrices are relatively less known. Nonetheless, they play an important role in random matrix theory, see e.g. [5], [43]. Worth noting is their relevant application in information theory [44], [45]. A Jacobi matrix can be defined via two independent Wishart matrices or a Haar matrix. The former approach is rather complicated; therefore, we adopt the latter. We first introduce a convenient projection operator.

Definition 2.5. *An N-dimensional projector $\boldsymbol{P}_\beta$ with $\beta \leq 1$ is a $\beta N \times N$ matrix with entries $(\boldsymbol{P}_\beta)_{ij} = \delta_{ij}, \forall i, j$, where δ_{ij} denotes the Kronecker delta.*

A Jacobi matrix can be constructed from a matrix obtained by removing certain fractions of rows and columns of a Haar matrix [43]. The removal of rows and columns of a matrix can be conveniently defined via the multiplication of the matrix with rectangular projector matrices from left and right.

Definition 2.6. *[43] Let $\boldsymbol{U}$ be an $N \times N$ Haar matrix. Furthermore, let $\boldsymbol{P}_\beta$ and $\boldsymbol{P}_\phi$ be N-dimensional projectors. Let $\boldsymbol{V} \triangleq \boldsymbol{P}_\beta \boldsymbol{U} \boldsymbol{P}_\phi^\dagger$, i.e. $\boldsymbol{V}$ is the $\beta N \times \phi N$ upper-left corner of $\boldsymbol{U}$. The Gramian $\boldsymbol{X} = \boldsymbol{V}^\dagger \boldsymbol{V}$ is called a Jacobi matrix.*

The empirical eigenvalue distribution of a Jacobi matrix converges almost surely to a non-random distribution whose density reads

$$\mathrm{F}'_{\boldsymbol{X}}(x) = \frac{\phi - \min(\phi, \beta)}{\phi} \delta(x) + \frac{(\phi + \beta - 1)^+}{\phi} \delta(x-1) + \frac{\sqrt{(x-\lambda_-)^+ (\lambda_+ - x)^+}}{2\pi\phi x(1-x)}$$

where $\lambda_\mp = \phi + \beta - 2\phi\beta \mp \sqrt{4\phi\beta(1-\phi)(1-\beta)}$ [46], [47].

Here, we draw the attention of the reader to the following striking point: Let the random matrix $\tilde{\boldsymbol{V}}$ be obtained by *randomly* and *independently* removing certain fractions of rows and columns of a discrete Fourier transform (DFT) matrix. Then, the LED of $\tilde{\boldsymbol{V}}^\dagger \tilde{\boldsymbol{V}}$ is the same as that of the Jacobi matrix [48].

2.5 Invariant random matrices

Classical random matrices, such as Haar, null-Wishart, Gaussian Wigner, and Jacobi matrices are invariant under multiplications with an independent unitary (orthogonal) matrix and its conjugate from right and left, respectively. A random matrix that exhibits this property is called invariant.

Definition 2.7. *[12] A square random matrix $\boldsymbol{X}$ is invariant if $\boldsymbol{X} \sim \boldsymbol{V}^\dagger \boldsymbol{X} \boldsymbol{V}$ for any orthogonal, or unitary, matrix $\boldsymbol{V}$ independent of $\boldsymbol{X}$.*

Equivalently, invariant random matrices admit the decomposition

$$\boldsymbol{X} = \boldsymbol{U}^\dagger \boldsymbol{\Lambda} \boldsymbol{U} \tag{2.16}$$

where $\boldsymbol{U}$ is a Haar matrix independent of the diagonal matrix $\boldsymbol{\Lambda}$ [12].

Dyson's Coulomb-gas analogy

Dyson's Coulomb gas analogy [49] provides a beautiful view of the statistics of the eigenvalues of the classical invariant ensembles. We briefly present this analogy; for more details we refer the reader to [5], [49].

Consider a gas of N point charges (or particles) with positions $x_1, \cdots, x_N$. The charges are free to move on the straight line $-\infty < x < \infty$ under the influence of forces emanating from the energy $\mathcal{H}$ which is given by

$$\mathcal{H}(\boldsymbol{x}) \triangleq \frac{1}{2}\sum_{k=1}^{N} V(x_i^2) - \frac{1}{N}\sum_{i=1}^{N}\sum_{j<i} \ln|x_i - x_j|. \tag{2.17}$$

The term V is referred to as the harmonic potential which attracts each charge independently towards the point $x = 0$. Moreover, $-\ln|x_i - x_j|$ represents an electronic repulsion. Thus, the charges repel each other with a logarithmic potential depending on the distance $|x_i - x_j|$. Let these charges be in thermodynamical equilibrium at a fixed temperature T. In this equilibrium, the probability distribution of their positions admits a Boltzmann distribution as

$$\mathrm{dF}^N(\boldsymbol{x}) = \frac{1}{Z_V^N} e^{-\tilde{\beta} N \mathcal{H}(\boldsymbol{x})} \mathrm{d}\boldsymbol{x}$$

where $\tilde{\beta} = 1/kT$ and k is the Boltzmann constant. The term Z_V^N which ensures $\int \mathrm{dF}(\boldsymbol{x}) = 1$ is referred to as the partition function.

The probability distribution of an $N \times N$ symmetric, or Hermitian, invariant matrix is typically of the form [5]

$$\mathrm{dF}_{\boldsymbol{X}}(\boldsymbol{X}) \propto e^{-\frac{\beta}{2} N \mathrm{tr} V(\boldsymbol{X})} \mathrm{d}\boldsymbol{X} \tag{2.18}$$

where the function $V(x)$ is a power series in x. Moreover, $\beta = 1$ and $\beta = 2$ when $\boldsymbol{X}$ is Hermitian and symmetric, respectively. The expression (2.18) implies that the probability distribution of the classical invariant matrices are determined via a single-valued polynomial function V. For example, if $\boldsymbol{X}$ is Gaussian Wigner, then we have $V(x) = x^2$. Note also that we have the decomposition $\boldsymbol{X} = \boldsymbol{U}^\dagger \boldsymbol{\Lambda} \boldsymbol{U}$, where $\boldsymbol{U}$ is a Haar matrix independent of the diagonal matrix $\boldsymbol{\Lambda}$. Integrating over $\boldsymbol{U}$ in (2.18) yields the probability distribution of the eigenvalues collected in vector $\boldsymbol{x} = (x_1, \cdots, x_N)$ [5], [49]

$$\mathrm{dF}_{\boldsymbol{X}}^N(\boldsymbol{x}) = \frac{1}{Z_V^N} e^{-\beta N \mathcal{H}(\boldsymbol{x})} \mathrm{d}\boldsymbol{x} \tag{2.19}$$

where $\mathcal{H}$ is as in (2.17). In a word, the probability distribution of the eigenvalues of a classical invariant matrix is identical to the thermodynamical equilibrium probability distribution of the positions of N point particles that are

free to move on the real line under the influence of forces emanating from the energy $\mathcal{H}$ in (2.17) [49].

The statistical properties of the eigenvalues can be obtained from the log-partition function $\ln Z_V^N$. We next summarize a significant large deviation result in this regard [12], [50]. First, for a probability distribution function F, we introduce the energy functional

$$\mathrm{H}(\mathrm{F}) \triangleq \int V(x)\ \mathrm{dF}(x) + \iint \ln|x-y|\ \mathrm{dF}(x)\mathrm{dF}(y). \tag{2.20}$$

Moreover, let us define the distribution function

$$\mathrm{F}_{\boldsymbol{x}}^N(x) \triangleq \frac{1}{N}|\ \{x_i \in \mathcal{L} : x_i \leq x\}\ | \tag{2.21}$$

with $\mathcal{L} = \{x_1, \cdots, x_N\}$. Thereby, we can write $\mathcal{H}(\boldsymbol{x}) = N\mathrm{H}(\mathrm{F}_{\boldsymbol{x}}^{\mathrm{N}})$. In particular, the log-partition function can be written in the form

$$\ln Z_V^N = \ln \int e^{-\beta N^2 \mathrm{H}(\mathrm{F}_{\boldsymbol{x}}^N)} \mathrm{d}\boldsymbol{x}. \tag{2.22}$$

Under a certain technical assumption on V (see [12, Eq. 5.4.5]), we have the limit [12, Theorem 5.4.3]

$$\lim_{N\to\infty} \frac{1}{\beta N^2} \ln Z_V^N = \inf \mathrm{H}(\mathrm{F}). \tag{2.23}$$

The equilibrium distribution, namely the distribution that minimizes the functional H(F), coincides with the LED of $\boldsymbol{X}$. Besides, assuming that the LED is known and has a compact support $[a, b]$, we can obtain the potential function V from the formula [12]

$$\frac{1}{\beta} V'(\omega) = \mathrm{PV} \int_a^b \frac{\mathrm{dF}_{\boldsymbol{X}}(x)}{\omega - x} \quad a < \omega < b \tag{2.24}$$

where PV stands for the Cauchy principal value.

Diagonal elements of invariant matrices

Diagonal elements of symmetric, or Hermitian, invariant matrices have a fundamental property: under some weak assumptions they converge almost surely to the same deterministic limit as the matrix dimensions tend to infinity.

Theorem 2.1. *Let an $N \times N$ random matrix $\boldsymbol{X} = \boldsymbol{X}^\dagger$ be invariant. Moreover, as $N \to \infty$ let the quantities $\langle \mathrm{Tr}(\boldsymbol{X})^2 \rangle_{\boldsymbol{X}}$ and $\langle \mathrm{Tr}(\boldsymbol{X}^2) \rangle_{\boldsymbol{X}}$ converge to some (finite) limits and $\langle \mathrm{Tr}(\boldsymbol{X}) \rangle_{\boldsymbol{X}} - \mathrm{Tr}(\boldsymbol{X}) \to 0$ almost surely. Then, we have almost surely $X_{ii} \to \phi(\boldsymbol{X})$, $\forall i$ as $N \to \infty$.*

Proof. See Appendix A.1 □

3 Stieltjes Transform

So far, we have provided a presentation of the classical random matrix ensembles in the literature. Yet, we have not referred to a specific method (or a theory) on how to deal with the operations on random matrices such as sum and product. Indeed, a direct analysis of the sum and/or the product of random matrices through their eigenvalue distributions is typically intractable. We need a sophisticated method to resolve such difficulties. In this regards, the Stieltjes transform plays a key role.

The Stieltjes transform of a probability distribution function F on the real line is the analytic function

$$\mathrm{G}(s) \triangleq \int \frac{\mathrm{dF}(x)}{s-x}, \quad s \in \mathbb{C} \backslash \mathrm{supp}(\mathrm{F}) \tag{2.25}$$

where $\mathrm{supp}(\mathrm{F})$ denotes the support of F defined as [51, pp. 10][2]

$$\mathrm{supp}(\mathrm{F}) \triangleq \{x : \mathrm{F}(x+\epsilon) - \mathrm{F}(x-\epsilon) > 0, \forall \epsilon > 0\}. \tag{2.26}$$

The probability distribution function can be retrieved from its Stieltjes transform via the so-called Stieltjes inversion formula. In particular, if F has a continuous derivative $\mathrm{F}' = \mathrm{dF}/\mathrm{d}x$ we have [12]

$$\mathrm{F}'(x) = -\lim_{y \to 0^+} \frac{1}{\pi} \Im \mathrm{G}(x+iy). \tag{2.27}$$

Thereby, the Stieltjes transform "packs" the distribution function in a way that can be conveniently manipulated with the tools of complex analysis [52]. Extensive mathematical methods developed in this direction can be found in [53], [54]. These methods have also proved fruitful in practice [55].

When the support of the distribution is in $[0, \infty)$, it is enough to consider the restriction of the Stieltjes transform to $(-\infty, 0)$ as this restriction uniquely specified (2.25) by analytic continuation. The restriction is a decreasing function with range $(-\chi, 0)$. Here χ is the inverse mean of F:

$$\chi = \int \frac{\mathrm{dF}(x)}{x} \tag{2.28}$$

where by convention $\chi = \infty$ if $\mathrm{F}(0) \neq 0$. The restriction of the Stieltjes transform to $(-\infty, 0)$ is related to practical quantities and functions, e.g. the so-called η-transform and Shannon transform introduced in communication theory [36].

[2]Note that $\mathrm{supp}(\mathrm{F})$ is also the support of the underlying probability distribution. In the sequel, we will interchangeably refer of the support of a probability measure or of the associated distribution function.

Often, we deal with compactly supported distributions. It is well-known that a probability distribution with compact support is uniquely determined by its moments. Therefore, the moment–based analysis turns out to be a generic and fruitful approach for the characterization of compactly supported eigenvalue distribution of random matrices. If the distribution has its support in $[a, b]$, its Stieltjes transform can be described by a Laurent series of its moments on the disk $\{s : |s| > \max(|a|, |b|)\}$

$$\mathrm{G}(s) = \frac{1}{s} \int \sum_{n=0}^{\infty} \frac{x^n}{s^n} \mathrm{dF}(x) \tag{2.29}$$

$$= \frac{1}{s} \sum_{n=0}^{\infty} \frac{1}{s^n} \int x^n \mathrm{dF}(x) \tag{2.30}$$

$$= \frac{1}{s} \sum_{n=0}^{\infty} \frac{m_n}{s^n}. \tag{2.31}$$

In (2.31) $m_n = \int x^n \mathrm{dF}(x)$ is the nth-order moment of F. In this case one can obtain the Stieltjes transform without the need to perform the integration in (2.25), by merely calculating the moments of the distribution and using (2.31). This property has been instrumental in the method of moments [56, 57].

The Marčenko-Pastur theorem

Obtaining the Stieltjes transform in closed-form is often intractable. In fact, there are many important random matrix models considered in the literature for which no closed-form expression of their eigenvalue distribution functions is known yet. Instead, implicit equations that involve the sought Stieltjes transforms and uniquely determine them can be found. The Marčenko-Pastur theorem is the most famous result in this respect.

Theorem 2.2. *[58] Let the entries of $\boldsymbol{H} \in \mathbb{C}^{N \times K}$ be iid with zero mean and variance $1/N$. Let the aspect ratio $\phi = K/N$ be fixed as $K \to \infty$. Furthermore, let the $K \times K$ matrix $\boldsymbol{X} = \boldsymbol{X}^\dagger$ and the $N \times N$ real diagonal matrix $\boldsymbol{\Lambda}$ have almost surely LED functions $\mathrm{F}_{\boldsymbol{X}}$ and $\mathrm{F}_{\boldsymbol{\Lambda}}$, respectively as $K \to \infty$. Moreover, let $\boldsymbol{X}$, $\boldsymbol{H}$ and $\boldsymbol{\Lambda}$ be independent. Define*

$$\boldsymbol{Y} = \boldsymbol{X} + \boldsymbol{H}^\dagger \boldsymbol{\Lambda} \boldsymbol{H}. \tag{2.32}$$

Then, as $K \to \infty$ $\mathrm{F}_{\boldsymbol{Y}}^K$ converges almost surely to a LED function $\mathrm{F}_{\boldsymbol{Y}}$ whose Stieltjes transform $\mathrm{G}_{\boldsymbol{Y}}(s)$ satisfies

$$\mathrm{G}_{\boldsymbol{Y}}(s) = \mathrm{G}_{\boldsymbol{X}} \left(s - \int \frac{x \, \mathrm{dF}_{\boldsymbol{\Lambda}}(x)}{1 - x\phi \mathrm{G}_{\boldsymbol{Y}}(s)} \right) \tag{2.33}$$

with $\mathrm{G}_{\boldsymbol{X}}$ denoting the Stieltjes transform of the LED function $\mathrm{F}_{\boldsymbol{X}}$.

If the entries of $\boldsymbol{H}$ are restricted to Gaussian, $\boldsymbol{H}$ becomes invariant from left (and right), i.e. for the unitary matrix $\boldsymbol{V}$ independent of $\boldsymbol{H}$, $\boldsymbol{H} \sim \boldsymbol{V}\boldsymbol{H}$. Thus, when $\boldsymbol{H}$ is Gaussian, the theorem is still valid for $\boldsymbol{\Lambda} = \boldsymbol{\Lambda}^\dagger$ being non-diagonal with its eigenvectors independent of its eigenvalues.

4 R-transform

The R-transform was originally introduced by Voiculescu [59] in the context of free probability – a theory that deals with non-commutative random variables such as random matrices.

Let F be a probability distribution function on the real line and G its Stieltjes transform (2.25). Then, the R-transform of F is obtained from the inverse (with respect to the composition of functions) of the Stieltjes transform as [60]

$$\mathrm{R}(\omega) \triangleq \mathrm{G}^{-1}(\omega) - \omega^{-1}. \tag{2.34}$$

When we write G^{-1} we implicitly assume that G is restricted to a domain, say $\mathcal{D}$, in which it is univalent, to ensure that G^{-1} is well-defined. The domain of R is then $\mathrm{G}(\mathcal{D})/\{0\}$. We refer the reader to [60] where the authors introduce a suitable restriction of G and the corresponding domain of R for an arbitrary distribution. If the distribution has a compact support its Stieltjes transform is invertible in a neighborhood of ∞ and R is analytical in a neighborhood of 0.

Before providing a discussion on the role of the R-transform in random matrix theory we would like first to mention some important properties of it.

4.1 R-transform of distributions with non-negative support

We now investigate the R-transform of probability distributions with support on $[0, \infty)$. In this case, the definition domain of the Stieltjes transform of F can be restricted to $(-\infty, 0)$, and thereby its range becomes $(-\chi, 0)$ with $\chi \triangleq \int x^{-1}\, \mathrm{dF}(x)$. Thus, it is enough to restrict (2.34) to $(-\chi, 0)$.

We have the following characterization of the R-transform of distributions with non-negative support.

Lemma 2.2. *Let* F *be a distribution function supported on* $[0, \infty)$ *and* R *be its R-transform and let* $\chi \triangleq \int x^{-1}\, \mathrm{dF}(x)$. *Then, unless the distribution is a Dirac measure,* R *is strictly increasing on* $(-\chi, 0)$. *We have* $\lim_{\omega \to -\chi^+} \mathrm{R}(\omega) = \chi^{-1}$.

Lemma 2.2 can be easily proved by following the arguments in [61, pp. 446]. Notice that we also have $\lim_{\omega \to 0^-} \mathrm{R}(\omega) = \int x\, \mathrm{dF}(x)$ [38].

Moreover, this study can be extended to any probability distribution function F with support in $[-a, \infty)$, $a > 0$. It suffices to first investigate the R-transform of the "shifted" distribution function $\mathrm{F}_a(x) = \mathrm{F}(x - a)$ and then

apply the simple transformation

$$\mathrm{R}(\omega) = \mathrm{R}_a(\omega) - a \tag{2.35}$$

with R and R_a denoting the R-transform of F and F_a, respectively.

4.2 Free cumulants

When F has a compact support on the real line its R-transform admits the power expansion

$$\mathrm{R}(\omega) = \sum_{n=1}^{\infty} c_n \omega^{n-1} \tag{2.36}$$

where c_n is called the nth *free cumulant* of distribution function F. By inserting (2.31) and (2.36) to (2.34) one can show the following explicit relationship between the free cumulants and the moments of F.

Theorem 2.3. *[62] Consider a probability distribution function* F *defined on the real line with its moments* $\{m_n\}$ *and free cumulants* $\{c_n\}$ *for* $n \geq 1$*. The moments can be expressed in terms of the free cumulants as*

$$m_n = c_n + \sum_{k=2}^{n} \frac{1}{k} \binom{n}{k-1} \sum_{Q_n(k)} c_{q_1} \cdots c_{q_k} \tag{2.37}$$

where $q_1, \cdots, q_k$ *are positive integers and* $Q_n(k) \triangleq \{(q_1, \cdots, q_k) : \sum_{j=1}^{k} q_j = n\}$*. Conversely, the free cumulants can be expressed in terms of the moments as*

$$c_n = m_n + \sum_{k=2}^{n} \frac{(-1)^{k-1}}{k} \binom{n+k-2}{k-1} \sum_{Q_n(k)} m_{q_1} \cdots m_{q_k}. \tag{2.38}$$

The first two free cumulants are the mean and variance of the underlying distribution, respectively, i.e. $c_1 = m_1$ and $c_2 = m_2 - m_1^2$. Free cumulants of higher order are more involved expressions of the moments, see [63]:

$$c_3 = m_3 - 3m_2m_1 + 2m_1^3 \tag{2.39}$$

$$c_4 = m_4 - 4m_3m_1 - 2m_2 + 10m_2m_1^2 - 5m_1^4 \tag{2.40}$$

$$c_5 = m_5 - 5m_4m_1 + 15m_3m_1^2 + 15m_2^2m_1 - 35m_2m_1^3 - 5m_3m_2 + 14m_1^5. \tag{2.41}$$

Calculating the free cumulants via the moments can be important in practice. In particular, we may encounter the case where no closed-form expression of the R-transform of the underlying eigenvalue distribution function is known. In fact, the distribution function itself might be even unknown. In such a case, provided the underlying matrix is known, we can calculate the moments directly and thus the free cumulants as well. Thereby, we obtain a method to approximate the R-transform via the free cumulants of the distribution function up to a certain order.

4.3 Revisiting the Marčenko-Pastur theorem

To better understand the role of the R-transform in random matrices, we revisit the famous Marčenko-Pastur theorem, i.e. Theorem 2.2. Let us consider the random matrix model $\boldsymbol{Y} = \boldsymbol{X} + \boldsymbol{H}^\dagger \boldsymbol{\Lambda} \boldsymbol{H}$ in (2.32). Recall the expression of the Stieltjes transform of the LED of $\boldsymbol{Y}$, i.e. (2.33) and let insert $s = \mathrm{G}_{\boldsymbol{Y}}^{-1}(\omega)$ in this equation. Then, by the definition of the R-transform we easily obtain

$$\mathrm{R}_{\boldsymbol{Y}}(\omega) = \mathrm{R}_{\boldsymbol{X}}(\omega) + \int \frac{x \, \mathrm{dF}_{\boldsymbol{\Lambda}}(x)}{1 - x\phi\omega}. \tag{2.42}$$

This trivial reformulation of the Marčenko-Pastur theorem yields the following important results: Firstly, for $\boldsymbol{X} = \boldsymbol{0}$ (2.42) yields

$$\mathrm{R}_{\boldsymbol{H}^\dagger \boldsymbol{\Lambda} \boldsymbol{H}}(\omega) = \int \frac{x \, \mathrm{dF}_{\boldsymbol{\Lambda}}(x)}{1 - x\phi\omega}. \tag{2.43}$$

Secondly, we have

$$\mathrm{R}_{\boldsymbol{Y}}(\omega) = \mathrm{R}_{\boldsymbol{X}}(\omega) + \mathrm{R}_{\boldsymbol{H}^\dagger \boldsymbol{\Lambda} \boldsymbol{H}}(\omega). \tag{2.44}$$

Thus, the Marčenko-Pastur theorem essentially states nothing but the additivity of the R-transforms of the LED of the summands in $\boldsymbol{Y} = \boldsymbol{X} + \boldsymbol{H}^\dagger \boldsymbol{\Lambda} \boldsymbol{H}$. This may give the impression that the R-transform of the LED of a sum of arbitrary independent symmetric, or Hermitian, random matrices is the sum of the R-transforms of the respective LEDs of these matrices. This is correct in general if the "independence" property in the statement is replaced by the so-called "asymptotic freeness" property.

4.4 Asymptotic freeness

The matrices $\boldsymbol{X} = \boldsymbol{X}^\dagger$ and $\boldsymbol{Y} = \boldsymbol{Y}^\dagger$ are asymptotically free if for all $k \geq 1$ and for all integers $n_1, m_1, \cdots n_k, m_k \geq 1$ we have [64]

$$\phi\left(\prod_{i=1}^{k} (\boldsymbol{X}^{n_i} - \phi(\boldsymbol{X}^{n_i})\mathbf{I})(\boldsymbol{Y}^{m_i} - \phi(\boldsymbol{Y}^{m_i})\mathbf{I})\right) = 0. \tag{2.45}$$

In other words, the normalized trace of any product of powers of $\boldsymbol{X}$ and $\boldsymbol{Y}$ centered around their normalized trace vanishes asymptotically[3]. We give a well-known example: Let $\boldsymbol{U}$ be an $N \times N$ Haar matrix and $\boldsymbol{\Lambda}_1$ and $\boldsymbol{\Lambda}_2$ be two real diagonal matrices of dimensions $N \times N$. Moreover, let $\boldsymbol{\Lambda}_1$ and $\boldsymbol{\Lambda}_2$ have uniformly bounded spectral norms or compactly supported LEDs in the limit $N \to \infty$. In the latter case additionally assume that $\boldsymbol{U}$, $\boldsymbol{\Lambda}_1$ and $\boldsymbol{\Lambda}_2$ are independent. Then, $\boldsymbol{\Lambda}_1$ and $\boldsymbol{U}^\dagger \boldsymbol{\Lambda}_2 \boldsymbol{U}$ are asymptotically free [12, 41, 61].

[3]By replacing operation $\phi(\cdot)$ in (2.45) with operation $\mathrm{Tr}(\cdot)$, we get the definition of freeness in finite dimensions. Notice that any matrix and the identity matrix are free. However, this is presumably the only case of free matrices.

4.5 Additive free convolution

In classical probability theory, for independent random variables, say X and Y, the cumulant generating function of the distribution of $X + Y$ is given by

$$\ln\langle e^{\mathrm{i}t(X+Y)}\rangle_{X,Y} = \ln\langle e^{\mathrm{i}tX}\rangle_X + \ln\langle e^{\mathrm{i}tY}\rangle_Y. \tag{2.46}$$

Conceptually, the R-transform is the counterpart in random matrix theory to the cumulant generating function in classical probability theory.

Theorem 2.4. *[60] If $\boldsymbol{X} = \boldsymbol{X}^\dagger$ and $\boldsymbol{Y} = \boldsymbol{Y}^\dagger$ are asymptotically free, then*

$$\mathrm{R}_{\boldsymbol{X}+\boldsymbol{Y}}(\omega) = \mathrm{R}_{\boldsymbol{X}}(\omega) + \mathrm{R}_{\boldsymbol{Y}}(\omega) \tag{2.47}$$

where $\mathrm{R}_{(\cdot)}$ denotes the R-transform of the LED of the matrix given in the subscript.

This result is usually referred to as the additive free convolution.

4.6 A Fourier view of the R-transform

Since the R-transform is the conceptual counterpart in random matrix theory of the cumulant generating function in classical probability theory, for a given symmetric, or Hermitian, random matrix $\boldsymbol{X}$ independent of a matrix $\boldsymbol{Q} = \boldsymbol{U}\boldsymbol{\Lambda}\boldsymbol{U}^\dagger$ with $\boldsymbol{U}$ and $\boldsymbol{\Lambda}$ being an orthogonal, or unitary, matrix and a diagonal matrix, respectively, it is natural to ask how the so-called asymptotic Itzykson-Zuber integral [65]

$$\mathrm{I}_{\boldsymbol{X}}(\boldsymbol{Q}) \triangleq \lim_{N\to\infty} \frac{1}{N} \ln\langle e^{\frac{\beta}{2}N\mathrm{tr}(\boldsymbol{Q}\boldsymbol{X})}\rangle_{\boldsymbol{X}} \tag{2.48}$$

is related to the R-transform of the LED of $\boldsymbol{X}$. Here, and in the following $\beta = 2$ ($\beta = 1$) for $\boldsymbol{X}$ complex-(real-)valued.

Theorem 2.5. *[65], [66], [61], [67] Let an $N \times N$ symmetric, or Hermitian matrix $\boldsymbol{X}$ be invariant and independent of the $N \times N$ matrix $\boldsymbol{Q} = \boldsymbol{U}\boldsymbol{\Lambda}\boldsymbol{U}^\dagger$ with $\boldsymbol{U}$ and $\boldsymbol{\Lambda}$ being an orthogonal, or unitary, matrix and a diagonal matrix, respectively. Assume that as $N \to \infty$ $\boldsymbol{Q}$ has bounded spectral norm and rank and $\boldsymbol{X}$ has a bounded spectral norm and a LED almost surely. Then, we have*

$$\mathrm{I}_{\boldsymbol{X}}(\boldsymbol{Q}) = \frac{\beta}{2} \sum_{n=1}^{\infty} \frac{c_n}{n} \mathrm{tr}(\boldsymbol{Q}^n) \tag{2.49}$$

whenever the right-hand side of (2.49) *exists. In* (2.49)*, c_n denotes the nth order free cumulant of the LED $\boldsymbol{X}$.*

It is worth mentioning some sufficient condition for the existence of the right-hand side of (2.49). To this end, we first recall that the R-transform of the LED function $\mathrm{F}_{\boldsymbol{X}}$ (with a compact support) can be written as the formal power series (2.36). Let r be the radius of convergence of (2.36). Since $\mathrm{d}\mathrm{I}_{\boldsymbol{X}}(\omega) = \frac{\beta}{2}\mathrm{R}_{\boldsymbol{X}}(\omega)\mathrm{d}\omega$, the radius of convergence of $\mathrm{I}_{\boldsymbol{X}}$ is r as well, see [68, pp. 39]. This implies that the power series in (2.49) converges if $\|\boldsymbol{Q}\|_2 < r$.

4.7 The log det relationship

Though we have not yet studied a particular application of random matrices, the reader should have the impression so far that the R-transform is an important tool in random matrix theory as is the Fourier transform in probability theory. However, the computation of the R-transform is cumbersome, and it is sometimes difficult to obtain it in an analytical form. In this section, we show a fundamental relationship between the log det operation for a symmetric, or Hermitian, matrix and the R-transform of its eigenvalue distribution.

Theorem 2.6. *Consider the distribution function* F *with support in* $[0, \infty)$ *and let* R *be its R-transform. Moreover, let* $\chi \triangleq \int x^{-1} \, \mathrm{dF}(x)$. *Let* $a \in (0, \chi)$ *and define the positive quantity* $\epsilon \triangleq a^{-1} - \mathrm{R}(-a)$. *Then, we have*

$$\int_0^a \mathrm{R}(-\omega) \, \mathrm{d}\omega = 1 + \ln a - \epsilon a + \int \ln(\epsilon + x) \, \mathrm{dF}(x). \tag{2.50}$$

Proof. See Appendix A.2. □

The variable ϵ in Theorem 2.6 can be uniquely defined through the identity $a = -\mathrm{G}(-\epsilon)$. This implies that for any $\epsilon \in (0, \infty)$ Theorem 2.6 can be equivalently represented as

$$\int \ln(\epsilon + x) \, \mathrm{dF}(x) = -(1 + \ln a) + \epsilon a + \int_0^a \mathrm{R}(-\omega) \, \mathrm{d}\omega \tag{2.51}$$

where the range of $a = -\mathrm{G}(-\epsilon)$ is $(0, \chi)$. In particular, recall that $-\mathrm{G}(-\epsilon) \to \chi$ as $\epsilon \to 0$. Thereby, we obtain the following compact corollary.

Corollary 2.1. *Let the distribution function* F *have its support in* $[0, \infty)$ *and* R *be its R-transform. Moreover, let* $\chi \triangleq \int x^{-1} \, \mathrm{dF}(x)$. *Then, for* $\chi < \infty$ *we have*

$$\int \ln(x) \, \mathrm{dF}(x) = -(1 + \ln \chi) + \int_0^\chi \mathrm{R}(-\omega) \, \mathrm{d}\omega. \tag{2.52}$$

We can substitute F with the eigenvalue distribution function of an $N \times N$ positive definite matrix, say $\boldsymbol{X}$. Then, we can write

$$\frac{1}{N} \ln |\boldsymbol{X}| = -(1 + \ln \chi_{\boldsymbol{X}}^N) + \int_0^{\chi_{\boldsymbol{X}}^N} \mathrm{R}_{\boldsymbol{X}}^N(-\omega) \, \mathrm{d}\omega \tag{2.53}$$

where we introduce $\chi_{\boldsymbol{X}}^N \triangleq \mathrm{Tr}(\boldsymbol{X}^{-1})$.

4.8 Compression of random matrices

This subsection introduces a stunning property of the R-transform in connection to "compression" of random matrices. To be more specific let us consider an $N \times N$ matrix $\boldsymbol{X}$, e.g. with $N = 4$:

$$\boldsymbol{X} = \begin{pmatrix} X_{11} & X_{12} & X_{13} & X_{14} \\ X_{21} & X_{22} & X_{23} & X_{24} \\ X_{31} & X_{32} & X_{33} & X_{34} \\ X_{41} & X_{42} & X_{43} & X_{44} \end{pmatrix}. \tag{2.54}$$

Let $\boldsymbol{P}_\beta$ be an N-dimensional projector, see Definition 2.5. For example, for $N = 4$ and $\beta = 1/2$ we obtain the 2×2 upper-left corner of $\boldsymbol{X}$ as

$$\boldsymbol{P}_{\frac{1}{2}} \boldsymbol{X} \boldsymbol{P}_{\frac{1}{2}}^\dagger = \begin{pmatrix} X_{11} & X_{12} \\ X_{21} & X_{22} \end{pmatrix}. \tag{2.55}$$

The question is how to relate the eigenvalue distribution of $\boldsymbol{X}$ to the eigenvalue distribution of its corner $\boldsymbol{P}_\beta \boldsymbol{X} \boldsymbol{P}_\beta^\dagger$. For random matrices that are asymptotically free of the projector, the answer is simple in terms of the R-transforms of their LEDs.

Lemma 2.3. *[69] Let $\boldsymbol{X} = \boldsymbol{X}^\dagger$ have dimension $N \times N$ and $\boldsymbol{P}_\beta$ be an N-dimensional projector. Let $\boldsymbol{X}$ have a LED (i.e. as $N \to \infty$). Assume that $\boldsymbol{X}$ and $\boldsymbol{P}_\beta^\dagger \boldsymbol{P}_\beta$ are asymptotically free. Then, we have almost surely*

$$\mathrm{R}_{\boldsymbol{P}_\beta \boldsymbol{X} \boldsymbol{P}_\beta^\dagger}(\omega) = \mathrm{R}_{\boldsymbol{X}}(\beta\omega). \tag{2.56}$$

As a quick application of Lemma 2.3, we next calculate the R-transform of the LED of a Jacobi random matrix, see Definition 2.6.

Example 2.1. *Let $\boldsymbol{X} \triangleq \boldsymbol{V}^\dagger \boldsymbol{V}$ where $\boldsymbol{V} \triangleq \boldsymbol{P}_\beta \boldsymbol{U} \boldsymbol{P}_\phi^\dagger$ with $\boldsymbol{U}$ being a Haar matrix and $\boldsymbol{P}_\beta$, $\boldsymbol{P}_\phi$ projectors of appropriate dimensions. Note that*

$$\mathrm{F}_{\boldsymbol{P}_\phi^\dagger \boldsymbol{P}_\phi}(x) = (1 - \phi) u(x) + \phi u(x - 1). \tag{2.57}$$

Then, one can easily show that [9]

$$\mathrm{R}_{\boldsymbol{P}_\phi^\dagger \boldsymbol{P}_\phi}(\omega) = \frac{\omega - 1 + \sqrt{(\omega - 1)^2 + 4\phi\omega}}{2\omega}. \tag{2.58}$$

Thus, from Lemma 2.3 the R-transform of the LED of the Jacobi matrix $\boldsymbol{X}$ reads

$$\mathrm{R}_{\boldsymbol{X}}(\omega) = \frac{\beta\omega - 1 + \sqrt{(\beta\omega - 1)^2 + 4\beta\phi\omega}}{2\beta\omega}. \tag{2.59}$$

5 S-transform

Voiculescu introduced the S-transform in free probability to handle the product of free random matrices [70] . Specifically, consider the product $\boldsymbol{XY}$ where $\boldsymbol{X} = \boldsymbol{X}^\dagger$ and $\boldsymbol{Y}^\dagger = \boldsymbol{Y}$. Furthermore, let these matrices have non-vanishing asymptotic normalized traces, i.e. $\phi(\boldsymbol{X}) \neq 0 \neq \phi(\boldsymbol{Y})$. Moreover, let $\boldsymbol{X}$ and $\boldsymbol{Y}$ be asymptotically free, see Definition 2.45. Then, we have

$$\mathrm{S}_{\boldsymbol{XY}}(z) = \mathrm{S}_{\boldsymbol{X}}(z)\mathrm{S}_{\boldsymbol{Y}}(z) \tag{2.60}$$

where $\mathrm{S}_{(.)}$ denotes the S-transform of the LED of the matrix given in the subscript.

Let G be the Stieltjes transform of a probability distribution function F, see (2.25). Define

$$\Psi(s) \triangleq s^{-1}\mathrm{G}(s^{-1}) - 1 \tag{2.61}$$

$$= \int \frac{sx \, \mathrm{dF}(x)}{1 - sx}. \tag{2.62}$$

Clearly the function Ψ is well defined and analytic on a domain in $\mathbb{C}$ that includes $\{s : \Im s > 0\}$. Let assume that the restriction of Ψ to a sub-domain, say $\mathcal{D}$, is univalent. For any element in the two classes of probability distributions that we consider such a domain exists. For any distribution with non-negative expectation and compact support, $\mathcal{D}$ is a neighborhood of 0. For any distribution with non-vanishing expectation and non-negative support, $\mathcal{D}$ is a neighborhood of $(-\infty, 0)$. The S-transform of F is obtained from the inverse function Ψ^{-1} as [71]

$$\mathrm{S}(z) \triangleq \frac{z+1}{z}\Psi^{-1}(z). \tag{2.63}$$

5.1 The relationship between the S- and R- transforms

From the definition (2.61) one can observe that

$$\Psi^{-1}(z) = \frac{1}{\mathrm{G}^{-1}(z\Psi^{-1}(z))}. \tag{2.64}$$

Hence, by the definitions of the S- and R-transforms, (2.64) implies that [71]

$$\mathrm{R}(z\mathrm{S}(z))\mathrm{S}(z) = 1 = \mathrm{S}(\omega\mathrm{R}(\omega))\mathrm{R}(\omega). \tag{2.65}$$

This straightforward observation is important as it allows us to bypass the Stieltjes transform for finding the R-transform of the underlying distribution function via the S-transform and vice-versa. We next examine this identity for two specific random matrix models.

Example 2.2. *Consider the random matrix $\boldsymbol{A} = \boldsymbol{A}_2\boldsymbol{A}_1$ where the entries of $N \times L$ matrix $\boldsymbol{A}_2$ and $L \times K$ matrix $\boldsymbol{A}_1$ are iid with zero mean and variances $1/N$ and $1/L$, respectively. For convenience, define $\boldsymbol{X} \triangleq \boldsymbol{A}^\dagger\boldsymbol{A}$, $\alpha \triangleq N/K$ and $\beta \triangleq L/K$. As $K \to \infty$ with the ratios α and β fixed, the S-transform of the LED of $\boldsymbol{X}$ is given (in the almost sure sense) as [72]*

$$\mathrm{S}_{\boldsymbol{X}}(z) = \frac{1}{(z/\alpha + 1)(z/\beta + 1)}. \tag{2.66}$$

Then, by invoking (2.65) *we obtain the R-transform of the LED of $\boldsymbol{X}$:*

$$\mathrm{R}_{\boldsymbol{X}}(\omega) = \frac{\alpha(\beta - \omega) - \beta\omega - \sqrt{\alpha^2\beta^2 - 2\alpha\beta\omega(\alpha + \beta) + \omega^2(\alpha - \beta)^2}}{2\omega^2}. \tag{2.67}$$

In the second example, we show how to transform a result involving the R-transform into a result involving the S-transform. Specifically, we compute the S-transform of the LED of the Jacobi matrix from its R-transform.

Example 2.3. *Let $\boldsymbol{X} \triangleq \boldsymbol{P}_\beta\boldsymbol{U}\boldsymbol{P}_\phi^\dagger\boldsymbol{P}_\phi\boldsymbol{U}^\dagger\boldsymbol{P}_\beta^\dagger$ where $\boldsymbol{U}$ is a Haar matrix, and $\boldsymbol{P}_\beta$, $\boldsymbol{P}_\phi$ are projectors of appropriate dimensions. Then, by invoking* (2.66) *and* (2.59) *we obtain that*

$$\mathrm{S}_{\boldsymbol{X}}(z) = \frac{1 + \phi z}{\beta + \phi z}. \tag{2.68}$$

5.2 S-transform of distributions with non-negative support

In practice, we often encounter Gramians, which have their eigenvalue distribution functions confined on $[0, \infty)$. In the rest the section, we present some recent technical results for the S-transform of such distributions. Let F be a probability distribution function with support in $[0, \infty)$. Moreover, let $\alpha \triangleq 1 - \mathrm{F}(0) \neq 0$. In this case it is enough to restrict the definition domain of the Stieltjes transform in (2.25) to $(-\infty, 0)$. Then, one can show that $\Psi(s)$ is a strictly increasing function of $s \in (-\infty, 0)$ with range $(\alpha - 1, 0)$. So the S-transform of F is well defined on $(-\alpha, 0)$ [73].

Lemma 2.4. *[73, Lemma 2 & Lemma 4] Let* F *be a probability distribution function with support in $[0, \infty)$ and* S *its S-transform. Furthermore, let $\alpha \triangleq 1 - \mathrm{F}(0) \neq 0$. Moreover, let* F *be not a Dirac distribution. Then,* S *is strictly decreasing on $(-\alpha, 0)$. In particular, we have*

$$\lim_{z \to 0^-} \mathrm{S}(z) = \left(\int x \, \mathrm{dF}(x) \right)^{-1} \tag{2.69}$$

$$\lim_{z \to -\alpha^+} \mathrm{S}(z) = \int \frac{1}{x} \, \mathrm{dF}(x) \tag{2.70}$$

where by convention $1/0 = \infty$ in (2.70) *when $\mathrm{F}(0) > 0$.*

In particular, the inverse-mean characterization (2.70) provides an interesting flavor to the S-transform in the large-system limit: Let $\boldsymbol{X}$ and $\boldsymbol{P}_{\beta}$ be an $N \times N$ positive definite matrix and an N-dimensional projector, respectively. Moreover, let $\boldsymbol{X}$ and $\boldsymbol{P}_{\beta}^{\dagger}\boldsymbol{P}_{\beta}$ be asymptotically free. Then, by invoking (2.56) to (2.65), we have

$$\mathrm{S}_{\boldsymbol{P}_{\beta}\boldsymbol{X}\boldsymbol{P}_{\beta}^{\dagger}}(\omega) = \mathrm{S}_{\boldsymbol{X}}(\beta\omega). \tag{2.71}$$

Then, combining (2.70) with (2.71) we get

$$\mathrm{S}_{\boldsymbol{X}}(-\beta) = \int \frac{1}{x}\, \mathrm{dF}_{\boldsymbol{P}_{\beta}\boldsymbol{X}\boldsymbol{P}_{\beta}^{\dagger}}(x), \quad 0 < \beta < 1. \tag{2.72}$$

5.3 The log det relationship

In analogy to the log det relationship involving the R-transform in Subsection 4.7 we provide a similar relationship that involves the S-transform. Since the S-transform of the LED of product of asymptotically free matrices is the products of the respective S-transforms of the LEDs of these matrices, we investigate the logarithm of the S-transform.

Theorem 2.7. *Let* F *be a probability distribution function with support in* $[0, \infty)$ *and* S *its S-transform. Furthermore, let* $\alpha \triangleq 1 - \mathrm{F}(0) \neq 0$*. Moreover, let* $0 < a < \alpha$ *and*

$$\epsilon \triangleq \frac{1-a}{a\mathrm{S}(-a)} \in (0, \infty). \tag{2.73}$$

Then, we have

$$\int_0^a \ln \mathrm{S}(-z)\, \mathrm{d}z = \tilde{H}(a) + (1-a)\ln\epsilon - \int \ln(\epsilon + x)\, \mathrm{dF}(x) \tag{2.74}$$

where $\tilde{H}(x) \triangleq (x-1)\ln(1-x) - x\ln(x)$ *for* $x \in [0,1]$ *with convention* $0 \ln 0 = 0$*. Moreover,* $\int |\ln x|\, \mathrm{d}\tilde{\mathrm{F}}(x)$ *is finite if, and only if,* $\int_0^{\tilde{\alpha}} |\ln \mathrm{S}(-z)| \mathrm{d}z$ *is finite. If either of these integrals is finite, we have*

$$\int_0^{\alpha} \ln \mathrm{S}(-z)\, \mathrm{d}z = \tilde{H}(\alpha) - \alpha \int \ln(x)\, \mathrm{d}\tilde{\mathrm{F}}(x). \tag{2.75}$$

Here $\tilde{\mathrm{F}}$ *is defined by substituting* $\tilde{\mathrm{F}}_{\boldsymbol{X}}^{N}$ *and* $\alpha_{\boldsymbol{X}}^{N}$ *for* F *and* α *respectively in* (2.11)*.*

Proof. See Appendix A.3. □

By the definition of the S-transform, the variable ϵ in Theorem 2.7 is uniquely defined by the equation $a = -\Psi(-1/\epsilon)$ where the function Ψ is given in (2.61). Thus, for a given $\gamma \in (0, \infty)$, we can recast (2.74) as

$$\int \ln(\gamma + x)\, \mathrm{dF}(x) = \tilde{H}(a) + (1-a)\ln\epsilon - \int_0^a \ln \mathrm{S}(-z)\, \mathrm{d}z \tag{2.76}$$

where for short we wrote $a = -\Psi(-1/\epsilon)$.

For $\mathrm{F}(0) = 0$, the result (2.75) was proven in [73]. More specifically, Haagerup and Möller in [73] showed that in this case the integral $\int |\ln x| \mathrm{dF}(x)$ is finite if, and only if, $\int_0^1 |\ln \mathrm{S}(-z)| \mathrm{d}z$ is finite and if either of these integrals is finite, then

$$\int_0^1 \ln \mathrm{S}(-z)\, \mathrm{d}z = \int \ln(x)\, \mathrm{dF}(x). \tag{2.77}$$

The proof of Theorem 2.7 follows by using an approach similar to that used in [73].

6 Discussion

We have focused our attentions on the essential tools of free probability that we will use in the subsequent chapters. For the sake of keeping the discussion simple and compact, we intentionally did not drown the reader with the details. Some of these details, such as the scaling property of R- and S-transforms, are well known, see e.g. [38], [36] and [55]. However, we chose deliberately not to introduce this kind of standard aspects of random matrices in this chapter.

In practice, there are some important non-invariant random matrices for which the asymptotic freeness holds. In particular, one can define a random matrix whose eigenvectors are determined via a uniformly randomized DFT matrix instead of a Haar matrix. This type of random matrices plays a fundamental role in compressed sensing [74]. In [13], the authors showed the following interesting results: Let $\boldsymbol{\Lambda}_1$ and $\boldsymbol{\Lambda}_2$ be an $N \times N$ real matrices and $\boldsymbol{U}$ be the $N \times N$ DFT matrix. Assume that the entries of $\boldsymbol{\Lambda}_1$ and $\boldsymbol{\Lambda}_2$ are asymptotically bounded when $N \to \infty$. Moreover, let π be a uniformly distributed random permutation of the sequence $(1, \cdots N)$ and $\boldsymbol{P}_\pi$ be the $N \times N$ random permutation matrix corresponding to the random permutation π. Define the so-called "fake Haar" matrix:

$$\boldsymbol{U}_\pi \triangleq \boldsymbol{P}_\pi \boldsymbol{U} \boldsymbol{P}_\pi^\dagger. \tag{2.78}$$

Then, $\boldsymbol{\Lambda}_1$ and $\boldsymbol{U}_\pi \boldsymbol{\Lambda}_2 \boldsymbol{U}_\pi^\dagger$ are asymptotically free [13].

Chapter 3

Capacity Scaling in MIMO Systems

This chapter is based directly on

Burak Çakmak, Ralf Müller and Bernard H. Fleury, "Capacity scaling for MIMO systems with general unitarily invariant random matrices," arXiv preprint arXiv: 1306.2595, December 2015.

1 Introduction

In this chapter, we investigate how the capacity of a MIMO communication system scales as a function of the system dimensions as briefly described in Subsection 2.1 of Chapter 1. We start with recalling the general ergodic capacity expression of a MIMO system with perfect channel state information at the receiver [16]:

$$\min(T, R) \log_2 \mathrm{SNR} + O(1). \tag{3.1}$$

Here T and R denote the number of receive and transmit antennas, respectively, and $O(1)$ is a bounded function of the SNR that does depend on T and R in general. The scaling term $\min(T, R)$ is often referred to as the multiplexing gain. The explicit expression for the capacity scaling when T or R varies is difficult to calculate. Closed-form expressions can be obtained only in few particular cases, e.g. for a channel matrix of asymptotically large size with iid zero-mean entries [75].

In order to better understand capacity scaling in MIMO channels with more complicated structures, such as correlation at transmit and/or receive antennas, related works use either implicit solutions, e.g. [76], or consider asymptotically high SNR and express the capacity in terms of the multiplexing gain, e.g. [18]. However, implicit solutions do not provide intuitive in-

sight into the capacity scaling and the multiplexing gain is a crude measure of capacity.

We study the capacity of MIMO systems when the transmit antennas are restricted to send equal signal power, i.e. the mutual information. This transmission scenario is typical when the channel state information is available at the receiver only. In particular, we consider an affine approximation to the mutual information at high SNR. We investigate how mutual information varies when the numbers of antennas (at either receiver or transmitter side) is altered. Our affine approximation to the mutual information is a generalization of the multiplexing gain which we call the *multiplexing rate*. Such an approximation was formerly addressed in [16], which was the baseline of many published works, e.g. [17, 77, 78].

We investigate the variation of the multiplexing rate when the number of antennas either at the transmit or receive side varies. The variation of the number of antennas is formulated by utilizing a convenient (linear) projection operator. This formulation allows us to assess the mutual information at high SNR in insightful and explicit closed form. Specifically, our sole restriction is that the matrix of left, or right, singular vectors of the channel matrix of the reference system from which antennas are removed is Haar distributed when the number of receive, or transmit, antennas is varied. Informally speaking, this implies that the channel matrices involve symmetry (or invariance) with respect to the antennas. An individual antenna contributes in a "democratic fashion" to the mutual information. There are no preferred antennas in the system. In fact, such an invariance assumption is rather essential for the mutual information to depend on T and R only, but not on the specific antennas in the system.

Since the term $O(1)$ in (3.1) is a bounded function of SNR, the expression (3.1) has more than once led to misinterpretations in the wireless communications community: (i) for any variation of T or R with $\min(T, R)$ being fixed the ergodic mutual information would not vary at high SNR; (ii) the ergodic mutual information would grow linearly with $\min(T, R)$ at high SNR. In [17], the authors addressed misinterpretation (i) for the zero-mean iid Gaussian matrix ensemble. In this contribution, we debunk both misinterpretations (i) and (ii) by considering arbitrary invariant matrix ensembles. As regards (i), we derive a universal expression for the variation of the ergodic multiplexing rate that results when the number of antennas is altered in a controlled way such that $\min(R, T)$ is kept fixed. This expression is not a function of the singular values of the channel matrix. It solely depends on the number of transmit and receive antennas before and after the variation and can be expressed in terms of the digamma function. Moreover, in the large-system limit, the expression only involves the binary entropy functions evaluated at the aspect ratios of the channel matrices before and after the alteration of the system. As regards (ii), we quantify how the multiplexing rate as a

function of the number of antennas deviates from the approximately linear growth versus the minimum of the system dimensions. We derive remarkable properties of this quantity. The aforementioned results on the variation of the multiplexing rate provide least upper bounds on the variation of the mutual information over all SNRs. These bounds are exact in the high SNR limit. Finally, we derive new formulas for the mutual information and the multiplexing rate, which fundamentally relate these two quantities via the S-transform.

The chapter is structured as follows. In Section 2, we present the details of the system model. In Section 3, we introduce new integral formulations of the mutual information and the multiplexing rate in terms of the S-transform. Sections 4 and 5 are dedicated to lift misinterpretations (i) and (ii), respectively. Conclusions are outlined in Section 6. The technical lemmas and the proofs are located in Appendix B.

2 System Model

Consider the MIMO system

$$\boldsymbol{y} = \boldsymbol{H}\boldsymbol{x} + \boldsymbol{n} \tag{3.2}$$

where $\boldsymbol{H} \in \mathbb{C}^{R\times T}$, $\boldsymbol{x} \in \mathbb{C}^{T\times 1}$, $\boldsymbol{y} \in \mathbb{C}^{R\times 1}$, $\boldsymbol{n} \in \mathbb{C}^{R\times 1}$ are respectively the channel matrix, the input vector, the output vector, and the noise vector. The entries of $\boldsymbol{x}$ and $\boldsymbol{n}$ are assumed to be independent circularly-symmetric complex Gaussian with zero mean and variances σ_x^2 and σ_n^2, respectively. The transmit SNR is defined as

$$\gamma \triangleq \frac{\sigma_x^2}{\sigma_n^2}\,, \quad 0 < \gamma < \infty. \tag{3.3}$$

For notational convenience, we define the two possible Gramians of the channel matrix as

$$\boldsymbol{J} \triangleq \boldsymbol{H}^\dagger\boldsymbol{H} \text{ and } \tilde{\boldsymbol{J}} \triangleq \boldsymbol{H}\boldsymbol{H}^\dagger. \tag{3.4}$$

The mutual information per transmit antenna of the communication link (3.2) is given by [15]

$$\mathcal{I}(\gamma; \mathrm{F}_{\boldsymbol{J}}^T) \triangleq \int \log_2(1+\gamma x)\, \mathrm{dF}_{\boldsymbol{J}}^T(x). \tag{3.5}$$

Similarly, $\mathcal{I}(\gamma; \mathrm{F}_{\tilde{\boldsymbol{J}}}^R)$ is the mutual information per receive antenna of (3.2).

2.1 Antenna removal via projector

In the sequel, we formulate the variation of mutual information when the number of antennas either at the transmit or receive side of reference system (3.2) changes. This variation is achieved by removing a certain fraction of antennas at the corresponding side of the system. We formulate this removal

process via a multiplication of the channel matrix with a rectangular projector matrix, see Definition 2.5.

We distinguish between two cases: the removal of receive antennas and the removal of transmit antennas. In the first case, the system model resulting after removing a fraction $1-\beta$ of receive antennas in (3.2) reads

$$\boldsymbol{y}_\beta = \boldsymbol{P}_\beta(\boldsymbol{H}\boldsymbol{x}+\boldsymbol{n}) \tag{3.6}$$

$$= \boldsymbol{P}_\beta\boldsymbol{H}\boldsymbol{x}+\boldsymbol{n}_\beta. \tag{3.7}$$

The $\beta R \times R$ matrix $\boldsymbol{P}_\beta$ is an R-dimensional projector which removes a fraction $1-\beta$ of receive antennas in reference system (3.2) and $\boldsymbol{n}_\beta = \boldsymbol{P}_\beta\boldsymbol{n}$. For the sake of notational compactness, we introduce

$$\boldsymbol{J}_\beta \triangleq \boldsymbol{H}^\dagger\boldsymbol{P}_\beta^\dagger\boldsymbol{P}_\beta\boldsymbol{H}. \tag{3.8}$$

The mutual information of MIMO system (3.7) is equal to

$$T\mathcal{I}(\gamma;\mathrm{F}_{\boldsymbol{J}_\beta}^T). \tag{3.9}$$

Similarly, removing a fraction $1-\beta$ of transmit antennas in (3.2) yields the $R \times \beta T$ system

$$\tilde{\boldsymbol{y}} = \boldsymbol{H}\boldsymbol{P}_\beta^\dagger\boldsymbol{x}_\beta+\boldsymbol{n}. \tag{3.10}$$

Here, $\boldsymbol{x}_\beta$ is the vector obtained by removing from $\boldsymbol{x}$ the $(1-\beta)T$ entries fed to the removed transmit antennas, i.e. $\boldsymbol{x}_\beta = \boldsymbol{P}_\beta\boldsymbol{x}$ with $\boldsymbol{P}_\beta$ being a T-dimensional projector. Similarly to (3.8), let us introduce

$$\tilde{\boldsymbol{J}}_\beta \triangleq \boldsymbol{H}\boldsymbol{P}_\beta^\dagger\boldsymbol{P}_\beta\boldsymbol{H}^\dagger. \tag{3.11}$$

The mutual information of system (3.10) reads

$$R\mathcal{I}(\gamma;\mathrm{F}_{\tilde{\boldsymbol{J}}_\beta}^R). \tag{3.12}$$

2.2 Unitary invariance

For channel matrices that are invariant from left, i.e. $\boldsymbol{H} \sim \boldsymbol{U}\boldsymbol{H}$ for any unitary matrix $\boldsymbol{U}$ independent of $\boldsymbol{H}$, it does not matter which receive antennas are removed. Only their number counts. The same applies to channel matrices that are invariant from right for the removal of transmit antennas. For channel matrices that involve an asymmetry with respect to the antennas, i.e. some antennas contribute more to the mutual information than others, it must be specified which antennas are to be removed and the mutual information will depend (typically in a complicated manner) on the choice of the removed antennas. We restrict the considerations to cases where only the

number of removed antennas matters since this leads to explicit closed-form expressions.

For asymmetric channel matrices, one could obtain antenna-independent scaling laws if all antennas with equal contributions to mutual information are grouped together and all those groups were decimated proportionally. Doing so would heavily complicate the formulation of the antenna removal by means of multiplication with projector matrices. However, we can utilize the fact that for the channel in (3.2), mutual information is invariant to right- and left-multiplication with any unitary matrices $\boldsymbol{U}$ and $\boldsymbol{V}$. Since the channel matrix $\boldsymbol{UHV}$ is bi-invariant for all random unitary matrices $\boldsymbol{U}$ and $\boldsymbol{V}$ independent of $\boldsymbol{H}$, and thus has the same mutual information as $\boldsymbol{H}$, we can assume without loss of generality that $\boldsymbol{H}$ is invariant from left for receive and from right for transmit antenna removal, respectively, and keep the projector formulation of Subsection 2.1 as it is.

The multiplication with a random unitary matrix followed by a fixed selection of antennas has statistically the same effect as a random selection of antennas. It provides the symmetry required to make performance (e.g. mutual information) only depend on the number of removed antennas and not on which antennas are removed.

3 Mutual Information and Multiplexing Rate

The normalized mutual information in (3.5) can be decomposed as

$$\mathcal{I}(\gamma;\mathrm{F}_{\boldsymbol{J}}^{T}) = \underbrace{\alpha_{\boldsymbol{J}}^{T}\int \log_2(\gamma x)\,\mathrm{d}\tilde{\mathrm{F}}_{\boldsymbol{J}}^{T}(x)}_{\mathcal{I}_0(\gamma;\mathrm{F}_{\boldsymbol{J}}^{T})} + \underbrace{\alpha_{\boldsymbol{J}}^{T}\int \log_2\left(1+\frac{1}{x\gamma}\right)\,\mathrm{d}\tilde{\mathrm{F}}_{\boldsymbol{J}}^{T}(x)}_{\Delta\mathcal{I}(\gamma;\mathrm{F}_{\boldsymbol{J}}^{T})}. \tag{3.13}$$

Here, $\tilde{\mathrm{F}}_{\boldsymbol{J}}^{T}$ represents the distribution function of the non-zero egienvalues of $\boldsymbol{J}$, see Definition 2.1. We refer to the first term $\mathcal{I}_0(\gamma;\mathrm{F}_{\boldsymbol{J}}^{T})$ as the *multiplexing rate* per transmit antenna. Note that the factor $\alpha_{\boldsymbol{J}}^{T}$ is the multiplexing gain normalized by the number of transmit antennas. The second term $\Delta\mathcal{I}(\gamma;\mathrm{F}_{\boldsymbol{J}}^{T})$ is the difference between the mutual information per transmit antenna and the multiplexing rate per transmit antenna. To alleviate the terminology, in the sequel we skip the explicit reference to the normalization by the number of transmit antennas when we refer to the three functions defined in (3.13) and $\alpha_{\boldsymbol{J}}^{T}$. Whether the quantities considered are absolute or normalized will be clear from the context. The same convention applies when we later normalize

by the number of receive antennas. We have

$$\lim_{\gamma\to\infty} \Delta\mathcal{I}(\gamma; \mathrm{F}_{\boldsymbol{J}}^{T}) = 0. \tag{3.14}$$

For example, if $\boldsymbol{J}$ is invertible we have

$$\mathcal{I}_0(\gamma; \mathrm{F}_{\boldsymbol{J}}^{T}) = \frac{1}{T} \log_2 |\gamma \boldsymbol{J}| \tag{3.15}$$

$$\Delta\mathcal{I}(\gamma; \mathrm{F}_{\boldsymbol{J}}^{T}) = \frac{1}{T} \log_2 \left| \mathbf{I} + (\gamma \boldsymbol{J})^{-1} \right| \tag{3.16}$$

with $\mathbf{I}$ denoting the identity matrix.

The multiplexing rate corresponds to the affine approximation of the mutual information at high SNR introduced in [16], see also [17, Eq. (9)] for a compact formulation of it.

We show now that both the mutual information and the multiplexing rate can be formulated conveniently in terms of the S-transform of $\mathrm{F}_{\boldsymbol{J}}^{T}$. This result makes use of the minimum-mean-square-error (MMSE) achieved by the optimal receiver for (3.2) normalized by the number of transmit antennas:

$$\eta_{\boldsymbol{J}}^{T}(\gamma) \triangleq \int \frac{\mathrm{dF}_{\boldsymbol{J}}^{T}(x)}{1+\gamma x}. \tag{3.17}$$

The MMSE is a strictly decreasing function of the SNR with range $(1-\alpha_{\boldsymbol{J}}^{T}, 1)$ [36]. Reformulating, Theorem 2.7 in Chapter 2 in terms of mutual information, MMSE and multiplexing rate, we obtain the following fundamental result in our context.

Theorem 3.1. *We introduce*

$$f_{\boldsymbol{J}}(x) \triangleq H(x) - \int_0^x \log_2 \mathrm{S}_{\boldsymbol{J}}^{T}(-z)\, \mathrm{d}z, \quad 0 \le x \le \alpha_{\boldsymbol{J}}^{T}. \tag{3.18}$$

Here H denotes the binary entropy function, i.e.

$$H(x) \triangleq (x-1)\log_2(1-x) - x\log_2 x, \quad x \in [0,1] \tag{3.19}$$

where by convention $0\log_2 0 = 0$. Then, we have

$$\mathcal{I}(\gamma; \mathrm{F}_{\boldsymbol{J}}^{T}) = f_{\boldsymbol{J}}(1-\eta_{\boldsymbol{J}}^{T}) + (1-\eta_{\boldsymbol{J}}^{T})\log_2\gamma \tag{3.20}$$

$$\mathcal{I}_0(\gamma; \mathrm{F}_{\boldsymbol{J}}^{T}) = f_{\boldsymbol{J}}(\alpha_{\boldsymbol{J}}^{T}) + \alpha_{\boldsymbol{J}}^{T}\log_2\gamma. \tag{3.21}$$

For short we wrote $\eta_{\boldsymbol{J}}^{T}$ for $\eta_{\boldsymbol{J}}^{T}(\gamma)$ in (3.20)*.*

Note that by definition the function $f_{\boldsymbol{J}}$ in (3.18) may involve $\alpha_{\boldsymbol{J}}^{T}$ via the S-transform $\mathrm{S}_{\boldsymbol{J}}^{T}$. We have the following implications of Theorem 3.1: (i) the

mutual information can be directly expressed as a function of the (normalized) MMSE; ii) for any expression of the mutual information as a function of the MMSE $\eta_{\boldsymbol{J}}^T$ the multiplexing rate results by direct substitution of $\eta_{\boldsymbol{J}}^T$ for $1-\alpha_{\boldsymbol{J}}^T$; iii) the converse of ii) is not always true: given an expression of the multiplexing rate as a function of $\alpha_{\boldsymbol{J}}^T$, substituting $\alpha_{\boldsymbol{J}}^T$ for $1-\eta_{\boldsymbol{J}}^T$ does not always yield the mutual information. This is precisely the case when the expression for $\mathrm{S}_{\boldsymbol{J}}^T$ involves $\alpha_{\boldsymbol{J}}^T$. An intermediate step is required here to guarantee that the converse holds: the expression needs first to be recast as a function of $f_{\boldsymbol{J}}$. Then substituting $\alpha_{\boldsymbol{J}}^T$ for $1-\eta_{\boldsymbol{J}}^T$ in the latter function yields the mutual information.

Note that, if any probability distribution function with support in $[0,\infty)$, say F, is substituted for $\mathrm{F}_{\boldsymbol{J}}^T$ in (3.13) the formulas (3.20) and (3.21) remain valid provided $\mathcal{I}(\gamma;\mathrm{F})$ is finite and $\log(x)$ is absolutely integrable over $\tilde{\mathrm{F}}$, respectively[1]. The absolute integrability condition holds if, and only if, $\mathcal{I}(\gamma;\mathrm{F})$ and $\Delta\mathcal{I}(\gamma;\mathrm{F})$ are finite. In the sequel, we substitute $\mathrm{F}_{\boldsymbol{J}}$ for $\mathrm{F}_{\boldsymbol{J}}^T$ to calculate the integrals $\mathcal{I}(\gamma;\mathrm{F}_{\boldsymbol{J}})$ and $\mathcal{I}_0(\gamma;\mathrm{F}_{\boldsymbol{H}})$. In particular, in Appendix B.1 we provide some sufficient conditions that guarantee the almost sure convergence of $\mathcal{I}(\gamma;\mathrm{F}_{\boldsymbol{J}}^T)$ and $\mathcal{I}_0(\gamma;\mathrm{F}_{\boldsymbol{J}}^T)$ to $\mathcal{I}(\gamma;\mathrm{F}_{\boldsymbol{J}})$ and $\mathcal{I}_0(\gamma;\mathrm{F}_{\boldsymbol{J}})$, respectively, in the large-system limit. We conclude by assuming that this asymptotic convergence is reasonable in practice. For the details, we refer the reader to Appendix B.1.

Recall that the S-transform of the LED of the product of asymptotically free matrices is the product of the respective S-transforms of the LEDs of these matrices. Therefore, Theorem 4.1 provides a means to calculate the large-system limit of the mutual information and the multiplexing rate for MIMO channel matrices that involve a compound structure. We next address two relevant random matrix ensembles that exhibit this structure.

Example 3.1. *We consider the concatenation of the vector-valued fading channel described in [79]. Specifically we assume that the channel matrix $\boldsymbol{H}$ factorizes according to*

$$\boldsymbol{H} = \boldsymbol{X}_N \boldsymbol{X}_{N-1} \cdots \boldsymbol{X}_2 \boldsymbol{X}_1 \tag{3.22}$$

where the entries of $K_n \times K_{n-1}$ matrix $\boldsymbol{X}_n$ are iid with zero mean and variance $1/K_n$ for $n \in [1,N]$. Moreover let $K_n \to \infty$ with the ratios $\rho_n \triangleq K_n/K_0$ fixed for $n \in [1,N]$. By invoking Theorem 4.1 we obtain the following expression for the large-system limit of the mutual information:

$$\begin{aligned}\mathcal{I}(\gamma;\mathrm{F}_{\boldsymbol{J}}) &= H(\eta_{\boldsymbol{J}}) + (1-\eta_{\boldsymbol{J}})(\log_2\gamma - N\log_2 e) + \\ &(1-\eta_{\boldsymbol{J}})\left[\sum_{n=1}^{N}\frac{\rho_n}{1-\eta_{\boldsymbol{J}}} H\left(\frac{1-\eta_{\boldsymbol{J}}}{\rho_n}\right) + \log_2\frac{1-\eta_{\boldsymbol{J}}}{\rho_n}\right].\end{aligned} \tag{3.23}$$

[1]Here $\tilde{\mathrm{F}}$ is defined by substituting $\tilde{\mathrm{F}}_{\boldsymbol{J}}^T$ for F in (2.11).

In this expression, $\eta_{\boldsymbol{J}}$ denotes the large-system limit of MMSE $\eta_{\boldsymbol{J}}^T$. This result provides an explicit expression for $\mathcal{I}(\gamma;\mathrm{F}_{\boldsymbol{J}})$ in terms of the (asymptotic) MMSE. An explicit expression of the MMSE as a function of SNR is difficult to obtain in general. However, for a given value of the SNR, one can solve the MMSE from the fixed-point equation (see [79, Eq. (21)])

$$\frac{\eta_{\boldsymbol{J}}}{1-\eta_{\boldsymbol{J}}}\prod_{n=1}^{N}\frac{\eta_{\boldsymbol{J}}+\rho_n-1}{\rho_n}=\gamma. \tag{3.24}$$

As regards the multiplexing rate, we have the following explicit expression

$$\begin{aligned}\mathcal{I}_0(\gamma;\mathrm{F}_{\boldsymbol{J}}) =& H(\alpha_{\boldsymbol{J}})+\alpha_{\boldsymbol{J}}(\log_2\gamma - N\log_2 e)+\\ &\alpha_{\boldsymbol{H}}\left[\sum_{n=1}^{N}\frac{\rho_n}{\alpha_{\boldsymbol{J}}}H\left(\frac{\alpha_{\boldsymbol{J}}}{\rho_n}\right)+\log_2\frac{\alpha_{\boldsymbol{J}}}{\rho_n}\right]\end{aligned} \tag{3.25}$$

with $\alpha_{\boldsymbol{J}}=\min(1,\rho_1,\cdots,\rho_N)$.

Example 3.2. *We consider a Jacobi matrix ensemble, see e.g. [46], [43], which has recently found an application in the context of optical MIMO communications [44], [45]. Accordingly, the channel matrix $\boldsymbol{H}$ factorizes as*

$$\boldsymbol{H}=\boldsymbol{P}_{\beta_2}\boldsymbol{U}\boldsymbol{P}_{\beta_1}^{\dagger} \tag{3.26}$$

where $\boldsymbol{U}$ is an $N\times N$ Haar matrix. From Theorem 4.1 we obtain

$$\begin{aligned}\mathcal{I}(\gamma;\mathrm{F}_{\boldsymbol{J}}) =& H(\eta_{\boldsymbol{J}})+(1-\eta_{\boldsymbol{J}})\log_2\gamma-\\ &\frac{H(\beta_1(1-\eta_{\boldsymbol{J}}))}{\beta_1}+\frac{\beta_2}{\beta_1}H\left(\frac{\beta_1}{\beta_2}(1-\eta_{\boldsymbol{J}})\right)\end{aligned} \tag{3.27}$$

where $\eta_{\boldsymbol{J}}=\eta_{\boldsymbol{J}}(\gamma)$ is given by

$$\eta_{\boldsymbol{J}}(\gamma)=1+\frac{-(1+\kappa\gamma)+\sqrt{(1+\kappa\gamma)^2-4\beta_1\beta_2\gamma(1+\gamma)}}{2\beta_1(1+\gamma)} \tag{3.28}$$

with $\kappa\triangleq\beta_1+\beta_2$. Moreover we have

$$\begin{aligned}\mathcal{I}_0(\gamma;\mathrm{F}_{\boldsymbol{J}}) =& H(\alpha_{\boldsymbol{J}})+\alpha_{\boldsymbol{J}}\log_2\gamma-\\ &\frac{H(\beta_1\alpha_{\boldsymbol{J}})}{\beta_1}+\frac{\beta_2}{\beta_1}H\left(\frac{\beta_1}{\beta_2}\alpha_{\boldsymbol{J}}\right)\end{aligned} \tag{3.29}$$

with $\alpha_{\boldsymbol{J}}=\min(1,\beta_2/\beta_1)$.

The proofs of (3.23)-(3.25) and (3.27)-(3.29) are given in Appendix B.2.

4 The Universal Rate Loss

In Section 1 we underlined the following misinterpretation of (3.1): when the number of antennas (at either the transmit or receive side) varies, while the minimum of the system dimensions is kept fixed, the ergodic mutual information does not vary at high SNR. In this section, we provide an analysis of the variation of multiplexing rate versus such variation of the system dimensions that lifts this misinterpretation[2]. To do so, we need to distinguish between two cases as to system (3.2): (i) $T \leq R$; (ii) $T \geq R$. In the former, or latter, case we consider the removal of receive, or transmit, antennas. In both cases, the reduction of antennas is constrained in a way that keeps the minimum of the numbers of antennas at both sides fixed.

4.1 Case (i) – Removing receive antennas

We remove a fraction $(1-\beta)$ of receive antennas in system (3.2) to obtain system (3.7). We constrain the reduction such that $\beta \geq \phi \triangleq T/R$ to ensure that $\min(T, \beta R) = T$. This reduction of the number of receive antennas causes a loss in mutual information given by $T\mathcal{I}(\gamma; \mathrm{F}_{\boldsymbol{J}}^T) - T\mathcal{I}(\gamma; \mathrm{F}_{\boldsymbol{J}_\beta}^T)$, see (3.8). Normalizing this loss to the number of transmit antennas yields

$$\mathcal{I}(\gamma; \mathrm{F}_{\boldsymbol{J}}^T) - \mathcal{I}(\gamma; \mathrm{F}_{\boldsymbol{J}_\beta}^T). \tag{3.30}$$

Assuming $\boldsymbol{J}_\beta$ is almost surely full rank, (3.30) converges to

$$\chi_{\boldsymbol{J}}^T(R, \beta R) \triangleq \mathcal{I}_0(\gamma; \mathrm{F}_{\boldsymbol{J}}^T) - \mathcal{I}_0(\gamma; \mathrm{F}_{\boldsymbol{J}_\beta}^T), \quad \beta \geq \phi \tag{3.31}$$

as the SNR tends to infinity, see (3.14). Here the full-rank assumption is essential. Otherwise (3.31) may depend on the SNR and diverge as the SNR tends to infinity.

Lemma 3.1. *Assume that $\boldsymbol{J}_\beta$ has almost surely full rank. Let the $R \times R$ unitary matrix $\boldsymbol{U}$ be the eigenvector matrix of $\boldsymbol{J}$. Then, we have*

$$\chi_{\boldsymbol{J}}^T(R, \beta R) = -\frac{1}{T} \log_2 |\boldsymbol{P}_\phi \boldsymbol{U}^\dagger \boldsymbol{P}_\beta^\dagger \boldsymbol{P}_\beta \boldsymbol{U} \boldsymbol{P}_\phi^\dagger|. \tag{3.32}$$

Proof. See Appendix B.3. □

Thus, the rate loss $\chi_{\boldsymbol{J}}^T(R, \beta R)$ solely depends on the matrix of left singular vectors of the channel matrix $\boldsymbol{H}$, i.e. $\boldsymbol{U}$, and the number of antennas before and after the removal of antennas. We now assume that $\boldsymbol{U}$ to be Haar distributed. Doing so allows us to calculate both the ergodic rate loss, i.e. $\langle \chi_{\boldsymbol{J}}^T(R, \beta R) \rangle_{\boldsymbol{J}}$, and the large-system limit of the rate loss.

[2] In [17] the authors unraveled this misinterpretation for the iid Rayleigh fading channel.

Theorem 3.2 (Universal Rate Loss). *Assume that $\boldsymbol{J}$ has almost surely full rank and $\boldsymbol{J}$ is unitarily invariant. Then, we have*

$$\langle \chi_{\boldsymbol{J}}^{T}(R,\beta R)\rangle_{\boldsymbol{J}} = \frac{\log_2 e}{T}\sum_{l=0}^{T-1}\psi(R-l)-\psi(\beta R-l) \tag{3.33}$$

with $\psi(\cdot)$ denoting the digamma function. Moreover, we have almost surely

$$\chi_{\boldsymbol{J}}^{T}(R,\beta R) \to \frac{H(\phi)}{\phi}-\frac{\beta}{\phi}H\left(\frac{\phi}{\beta}\right) \tag{3.34}$$

as $R,T\to\infty$ with the ratio $\phi = T/R$ fixed.

Proof. See Appendix B.3. □

The name Universal Loss Theorem refers to the fact that neither the premises nor the results stated in the theorem refer explicitly to the singular values of the channel matrix. Moreover, interestingly, the large-system limit of $\chi_{\boldsymbol{J}}^{T}$, i.e. (3.34), involves only the binary entropy function evaluated at the two aspect ratios ϕ and β/ϕ of the channel matrices (the one before and the one after the removal of the antennas). This motivates us to coin this limit the *binary entropy loss*. Later in the section, we show by simulation that the binary entropy loss provides a good approximation already for systems with moderate dimensions.

If we remove as many antennas as needed to obtain a square system, i.e. $\beta R = T$, and we normalize the mutual information to the number of receive antennas before the removal instead of the number of transmit antennas, we have the following particularly striking case of (3.34).

Remark 3.1. *Assume that $\boldsymbol{J}$ has almost surely full rank and is invariant. Let $T < R$. Then, for sufficiently large T and R, removing as many receive antennas in* (3.2) *to obtain a square system results in a mutual information loss normalized by R that is arbitrarily close to $H(\phi)$ in the high SNR limit.*

Next, we show that Theorem 3.2 holds for the supremum of the mutual information loss (3.30) over the SNR range. Note that both quantities in (3.30) increase with SNR. It is shown in Appendix B.3 that their difference, i.e. (3.30), increases with the SNR too. Hence, the Universal Rate Loss Theorem also provides the least upper bound on the mutual information loss (over the SNR range).

Corollary 3.1. *Let the random matrix $\boldsymbol{J}$ be defined as in Theorem 3.2. Furthermore, let $\boldsymbol{P}_\beta$ be the R-dimensional projector with $\beta \geq \phi$. Then by removing a fraction $(1-\beta)$ of the receive antennas in system* (3.7) *the maximum amount of mutual information loss in the ergodic sense per receive antenna over all SNRs, i.e.*

$$\sup_{\gamma}\left\langle \mathcal{I}(\gamma;\mathrm{F}_{\boldsymbol{J}}^{T}) - \mathcal{I}(\gamma;\mathrm{F}_{\boldsymbol{J}_\beta}^{T})\right\rangle_{\boldsymbol{J}}, \tag{3.35}$$

is equal to the right-hand side of (3.33)*. Moreover,* (3.35) *converges to the binary entropy loss* (3.34) *as* $R, T \to \infty$ *with the ratio* ϕ *fixed.*

It turns out that Theorem 3.2 also holds when the multiplexing rates in (3.31) are replaced by the respective capacities in the high SNR limit. Let us consider the class of T-dimensional positive definite Hermitian matrices. Let the trace of any element, say $\boldsymbol{Q}$, of this class be equal to T. Then we denote the ergodic capacity of (3.7) as

$$\mathcal{C}(\gamma; \mathrm{F}_{\boldsymbol{J}_\beta}^T) \triangleq \max_{\boldsymbol{Q}:\mathrm{tr}(\boldsymbol{Q})=T} \left\langle \mathcal{I}(\gamma; \mathrm{F}_{\boldsymbol{Q}\boldsymbol{J}_\beta}^T) \right\rangle_{\boldsymbol{J}} \tag{3.36}$$

with $\mathrm{tr}(\cdot)$ denoting the trace operator.

Corollary 3.2. *Let the random matrix* $\boldsymbol{J}$ *be defined as in Theorem 3.2. Furthermore, let* $\boldsymbol{P}_\beta$ *be the* R*-dimensional projector with* $\beta \geq \phi$*. Then by removing a fraction* $(1-\beta)$ *of the receive antennas in system* (3.7) *the amount of capacity loss per receive antenna in the high SNR limit, i.e.*

$$\lim_{\gamma\to\infty} \left\{ \mathcal{C}(\gamma; \mathrm{F}_{\boldsymbol{J}}^T) - \mathcal{C}(\gamma; \mathrm{F}_{\boldsymbol{J}_\beta}^T) \right\}, \tag{3.37}$$

is equal to the right-hand side of (3.33)*. Moreover,* (3.37) *converges to the binary entropy loss* (3.34) *as* $R, T \to \infty$ *with the ratio* ϕ *fixed.*

Proof. See Appendix B.3. □

4.2 Case (ii) – Removing transmit antennas

We remove a fraction $(1-\beta)$ of transmit antennas in (3.2) to obtain system (3.10). We limit the reduction of receive antennas by $\beta \geq 1/\phi = T/R$ to ensure $\min(\beta T, R) = R$. Reducing the number of transmit antennas results in a loss of mutual information equal to $R\mathcal{I}(\gamma; \mathrm{F}_{\tilde{\boldsymbol{J}}}^R) - R\mathcal{I}(\gamma; \mathrm{F}_{\tilde{\boldsymbol{J}}_\beta}^R)$. Normalizing this loss with the number of receive antennas gives

$$\mathcal{I}(\gamma; \mathrm{F}_{\tilde{\boldsymbol{J}}}^R) - \mathcal{I}(\gamma; \mathrm{F}_{\tilde{\boldsymbol{J}}_\beta}^R). \tag{3.38}$$

Assuming that $\tilde{\boldsymbol{J}}_\beta$ has almost surely full rank, (3.38) converges to

$$\tilde{\chi}_{\tilde{\boldsymbol{J}}}^R(T, \beta T) \triangleq \mathcal{I}_0(\gamma; \mathrm{F}_{\tilde{\boldsymbol{J}}}^R) - \mathcal{I}_0(\gamma; \mathrm{F}_{\tilde{\boldsymbol{J}}_\beta}^R), \quad \beta \geq 1/\phi \tag{3.39}$$

as the SNR tends to infinity. Again the full rank assumption is essential here. Otherwise (3.39) may depend on the SNR and diverge when the SNR tends to infinity.

Corollary 3.3. *Assume that $\tilde{\boldsymbol{J}}$ is almost surely full rank and is invariant. Then, we have*

$$\langle \tilde{\chi}^R_{\tilde{\boldsymbol{J}}}(T, \beta T) \rangle_{\tilde{\boldsymbol{J}}} = \frac{\log_2 e}{T} \sum_{l=0}^{R-1} \psi(T-l) - \psi(\beta T - l). \tag{3.40}$$

Moreover, we have almost surely

$$\tilde{\chi}^R_{\tilde{\boldsymbol{J}}_\beta}(T, \beta T) \to H\left(\frac{1}{\phi}\right) - \beta H\left(\frac{1}{\phi\beta}\right) \tag{3.41}$$

as $R, T \to \infty$ with the ratio $\phi = T/R$ fixed.

Note that the right-hand side in (3.41) is obtained by formally replacing ϕ with ϕ^{-1} in the right-hand side of (3.34). This substitution is valid for any result that refers to mutual information, e.g. as in Corollary 1. However, it does not apply in general to capacity related results, such as in Corollary 2, due to the placement of the projection operator on the transmitter side.

4.3 Discussions of the universal rate loss

In the sequel, we discuss the property and behavior of the universal rate loss. For the sake of keeping the discussion simple, we only consider the antenna removal process specified in Remark 3.1. For convenience we define

$$\chi(R, T) \triangleq \frac{\log_2 e}{T} \sum_{l=0}^{T-1} \psi(R-l) - \psi(T-l). \tag{3.42}$$

This quantity is equal to the right-hand side of (3.33) for $\beta = \phi$.

Discussion 1: We consider first a 4×2 MIMO system that is stripped off two of its four receive antennas. For full-rank channel matrices that are invariant from left Theorem 3.2 gives the exact ergodic loss in the high SNR limit equal to $4\chi(4,2) = 3.37$ bit. This is depicted in Figure 3.1 for a Gaussian channel. The asymptotic loss (3.34) is $4H(2/4) = 4$ bit.

Note also that (3.42) is the supremum of the mutual information loss over all SNRs. From Figure 3.1 we may conclude that (3.42) yields an accurate approximation of mutual information loss when the SNR is around 20dB and above.

Discussion 2: We illustrate the universality of the rate loss and the tightness of the approximation provided by the binary entropy loss, i.e. $RH(T/R)$, already for small system dimensions. To this end, we study the ergodic rate loss in the high SNR limit for three different channel models that are invariant from the left: (i) the channel matrix $\boldsymbol{H} = \boldsymbol{U}\boldsymbol{\Lambda}$ where $\boldsymbol{U} \in \mathbb{C}^{R \times T}$ is uniformly distributed over the manifold of complex $R \times T$ matrices such that $\boldsymbol{U}^\dagger \boldsymbol{U} = \boldsymbol{I}$ and $\boldsymbol{\Lambda} \in \mathbb{R}^{T \times T}$ is a positive diagonal matrix that represents the power profile at the transmitter. This is a typical channel model in the context of massive

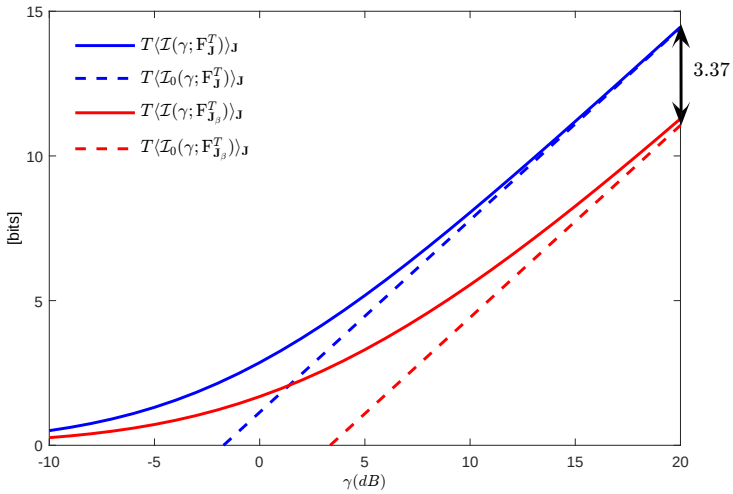

Fig. 3.1: Ergodic mutual information (continuous lines) and ergodic multiplexing rate (dashed lines) versus SNR of a zero-mean iid circularly-symmetric complex Gaussian MIMO channel with $T = 2$ transmit antennas and a number of receive antennas decreased from $R = 4$ (blue curves) to $R = 2$ (red curves).

MIMO, i.e. $T \ll R$. Here we point out that $\mathbf{\Lambda}$ does not impact the rate loss due to the identity

$$\det \mathbf{\Lambda}^2 \boldsymbol{U}^\dagger \boldsymbol{P}_\beta^\dagger \boldsymbol{P}_\beta \boldsymbol{U} = \det \mathbf{\Lambda}^2 \det \boldsymbol{U}^\dagger \boldsymbol{P}_\beta^\dagger \boldsymbol{P}_\beta \boldsymbol{U}. \tag{3.43}$$

Therefore for convenience, we set $\mathbf{\Lambda} = \mathbf{I}$. (ii) the channel matrix $\boldsymbol{H} = \boldsymbol{X}$ with the entries of $\boldsymbol{X}$ being zero-mean iid complex-valued Gaussian with finite variance; (iii) the channel matrix $\boldsymbol{H} = \boldsymbol{X}_2 \boldsymbol{D} \boldsymbol{X}_1$. Here $\boldsymbol{X}_1 \in \mathbb{C}^{S \times T}$ represents the propagation channel from the transmit antennas to scatterers with the corresponding power profile represented by the $S \times S$ positive diagonal matrix $\boldsymbol{D}$. The matrix $\boldsymbol{X}_2 \in \mathbb{C}^{R \times S}$ represents the propagation channels from the scatterers to the receive antennas. The entries of $\boldsymbol{X}_1$ and $\boldsymbol{X}_2$ are assumed to be zero-mean iid circularly-symmetric complex Gaussian with finite variance. This random matrix ensemble models the channel under the assumption of propagation via one-bounce scattering only [72]. In order to fulfill the full-rank condition, we restrict to the case $S \geq T$. The amounts of ergodic mutual information loss in the high SNR limit is depicted in Figure 3.2 for the three channel matrix ensembles. From this figure we conclude that the binary entropy loss yields an accurate approximation even for small system dimensions.

Discussion 3: We show a symmetry property of the universal rate loss. First let us consider two separate MIMO systems, one of dimensions 3×2 and one of dimensions 3×1. Let the antenna removal processes be $3 \times 1 \to 1 \times 1$

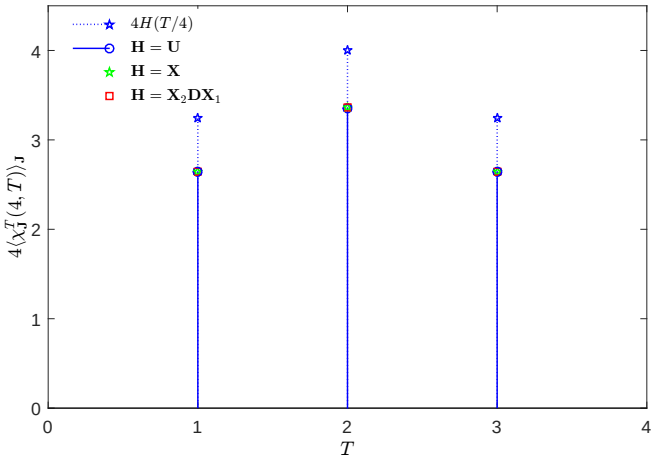

Fig. 3.2: The maximal ergodic mutual information loss over the SNR range: The entries of $\boldsymbol{X} \in \mathbb{C}^{4\times T}$, $\boldsymbol{X}_1 \in \mathbb{C}^{S=4\times T}$ and $\boldsymbol{X}_2 \in \mathbb{C}^{4\times S=4}$ are zero mean iid circularly-symmetric complex Gaussian. The matrix $\boldsymbol{U} \in \mathbb{C}^{4\times T}$ is uniformly distributed over the manifold of complex $4 \times T$ matrices fulfilling $\boldsymbol{U}^\dagger\boldsymbol{U} = \boldsymbol{I}$. The $S \times S$ matrix $\boldsymbol{D}$ is positive diagonal. Its diagonal entries are iid and uniformly distributed.

for the former system and $3 \times 2 \to 2 \times 2$ for the latter. Thus, in both cases two communication links are removed from the reference systems. Furthermore, let the channel matrices of the reference systems fulfill the conditions stated in Theorem 3.2 (i.e. full-rank and unitary invariance). The binary entropy loss amounts to $3H(1/3) = 3H(2/3) = 2.75$ bit. We have the symmetric behavior for the exact (ergodic) losses as well: $3\chi(3,1) = 3\chi(3,2) = 2.17$ bit. Indeed, it is shown in Appendix B.4 that

$$\chi(R, \phi R) = \chi(R, (1-\phi)R), \quad \phi \leq 1. \tag{3.44}$$

Identity (3.44) has the following interpretation: let the channel matrix be invariant from left (or right for the antenna removal process at the transmitter) and have almost surely full-rank. Then (3.44) implies that the ergodic rate loss in the high SNR limit does not actually depend on the number of transmit (or receive) antennas of the reference system. Only the total number of communication links removed from the reference system matters.

5 Deviation from Linear Growth

In this section, we clarify the second misinterpretation underlined in Section 1. Specifically, we analyze the variation of the multiplexing rate when either the number of receive or the number transmit antennas varies while their maximum is kept fixed.

For a channel matrix having *orthogonal* columns when the number of transmit or receive antennas varies, the linear growth of mutual information is obvious. However, for a channel matrix with e.g. iid entries, a crosstalk arises due to the lack of orthogonality of its columns. The effect of this crosstalk onto mutual information is non-linear in the number of antennas.

The mutual information scales approximately linearly in the minimum of the numbers of transmit and receive antennas. For a tall rectangular channel matrix that becomes wider and wider, the mutual information can only grow approximately linearly until the matrix becomes square. The same holds for a wide rectangular channel matrix growing taller and taller. Therefore, we have to distinguish between two cases: (i) the number of receive antennas is smaller than the number of transmit antennas, i.e. a wide channel matrix, and (ii) the converse of (i), i.e. a tall channel matrix. Since case (ii) can be easily treated by replacing the channel matrix with its conjugate-transpose, we restrict our investigations to case (i).

The linear growth cannot continue once the channel matrix has grown square. Thus, it makes sense to constrain the matrix of reference system (3.2) to be square; i.e. *we assume that the channel matrix* $\boldsymbol{H}$ *in* (3.2) *is* $N \times N$ *i.e.* $N = R = T$.

The exact mutual information of (rectangular) system (3.10) of size $\beta N \times N$, $\beta \leq 1$ is

$$N\mathcal{I}(\gamma; \mathrm{F}^N_{\boldsymbol{J}_\beta}). \tag{3.45}$$

The mutual information (3.45) scales approximately linearly with the number of receive antennas if it is close to

$$\beta N\mathcal{I}(\gamma; \mathrm{F}^N_{\boldsymbol{J}}). \tag{3.46}$$

Thus, in the high SNR limit, the deviation from the linear growth normalized by N (the deviation from linear growth for short) is given by

$$\Delta\mathcal{L}(\beta; \mathrm{F}^N_{\boldsymbol{J}}) \triangleq \mathcal{I}_0(\gamma; \mathrm{F}^N_{\boldsymbol{J}_\beta}) - \beta\mathcal{I}_0(\gamma; \mathrm{F}^N_{\boldsymbol{J}}) \tag{3.47}$$

where $\boldsymbol{J}$ is assumed to be full-rank almost surely, so that $\alpha^N_{\boldsymbol{J}_\beta} = \beta\alpha^N_{\boldsymbol{J}}$. Note that the full-rank assumption is necessary, otherwise (3.47) depends on the SNR and diverges as the SNR tends to infinity.

Example 3.3. *Let* $\boldsymbol{H}$ *be unitary. Then, we have*

$$\Delta\mathcal{L}(\beta; \mathrm{F}^N_{\boldsymbol{J}}) = 0. \tag{3.48}$$

The large-system limit consideration

The deviation from linear growth (3.47) differs from the quantity $\chi^T_{\boldsymbol{J}}$ defined in (3.31) only by the factor β scaling the second term. Unlike $\chi^T_{\boldsymbol{J}}$, $\Delta\mathcal{L}$ does

depend on the singular values of the channel matrix. This makes the analysis somehow intractable. However, it is well-known that results obtained for asymptotically large systems provide a good approximation already for systems of moderate dimensions, i.e. typically consisting of a dozen on antennas. This motivates us to conduct a large-system analysis of the deviation from linear growth. In doing so we employ the following assumption:

Assumption 3.1. *The Gramian matrix $\boldsymbol{J}$ has full rank almost surely. Furthermore, $\boldsymbol{J}$ is unitarily invariant and has a compactly supported LED almost surely, as $N \to \infty$. Moreover, the integral $\Delta\mathcal{I}(1;\mathrm{F}_{\boldsymbol{J}})$ is finite.*

We carry out the analysis on the basis of the LED function $\mathrm{F}_{\boldsymbol{J}_\beta}$. Specifically, we consider

$$\Delta\mathcal{L}(\beta;\mathrm{F}_{\boldsymbol{J}}) = \mathcal{I}_0(\gamma;\mathrm{F}_{\boldsymbol{J}_\beta}) - \beta\mathcal{I}_0(\gamma;\mathrm{F}_{\boldsymbol{J}}). \tag{3.49}$$

However, in the numerical investigations with considering the ergodic counterparts of these quantities. To still be able to relate the theoretical results with the numerical results we assume that the ergodic multiplexing rate converges for any $\beta \leq 1$:

$$\lim_{N\to\infty} \langle \mathcal{I}_0(\gamma;\mathrm{F}^N_{\boldsymbol{J}_\beta})\rangle_{\boldsymbol{J}} = \mathcal{I}_0(\gamma;\mathrm{F}_{\boldsymbol{J}_\beta}). \tag{3.50}$$

It is easy to show that the convergence (3.50) is a mild assumption for $\beta < 1$: Since the LED of $\boldsymbol{J}$ is assumed to have a compact support, the LED of $\boldsymbol{J}_\beta$ has a compact support too, see [69, Corollary 1.14]. Note also that a compactly supported probability distribution can be uniquely characterized by its moments. We now relax the compactly supported LED property of $\boldsymbol{J}_\beta$ by assuming that the maximum eigenvalue of $\boldsymbol{J}_\beta$ converges to a finite limit. Thus, $\boldsymbol{J}_\beta$ has uniformly bounded spectral norm. This fact allows us to use the machinery provided in Proposition B.1. Specifically, $\sup_N \langle \int x^{-1} \mathrm{d}\tilde{\mathrm{F}}^N_{\boldsymbol{J}_\beta}(x)\rangle_{\boldsymbol{J}} < \infty$ is sufficient for (3.50) to hold since

$$\int \frac{1}{x}\, \mathrm{d}\tilde{\mathrm{F}}_{\boldsymbol{P}_\beta \boldsymbol{H}}(x), \quad 0 < \beta < 1 \tag{3.51}$$

is strictly increasing with β, see (2.72).

Example 3.4. *Let the entries of the random matrix $\boldsymbol{H}$ be iid with zero mean and variance σ^2/N. Then, as $N \to \infty$ we have almost surely*

$$\Delta\mathcal{L}(\beta;\mathrm{F}_{\boldsymbol{J}}) = (\beta - 1)\log_2(1-\beta), \quad 0 < \beta \leq 1 \tag{3.52}$$

where by convention $0 \log_2 0 = 0$.

Proof. See Appendix B.5. □

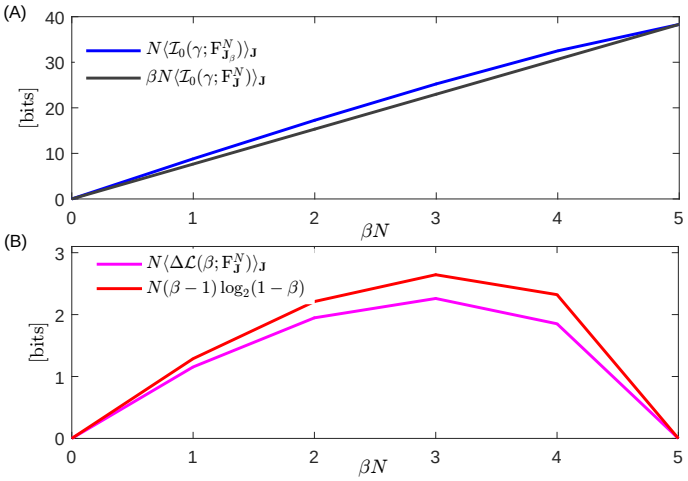

Fig. 3.3: Ergodic multiplexing rate and corresponding linear growth (A) and (ergodic) deviation from linear growth (B) versus number of receive antennas βN. The entries of $\boldsymbol{H} \in \mathbb{C}^{5\times 5}$ are iid circularly-symmetric complex Gaussian with zero mean and variance $1/5$. The SNR is $\gamma = 20\ dB$.

In other words, at high SNR the normalized mutual information of a MIMO system with zero-mean iid channel entries grows approximately linearly with the minimum of the numbers of transmit and receive antennas up to 1st order and the deviation from the linear growth is close to $(\beta-1)\log_2(1-\beta)$ as illustrated in Figure 3.3. This result can be obtained from previous capacity results, e.g. [17, Proposition 2]. We obtained it as a special case of the following lemma.

Lemma 3.2. *Let $\boldsymbol{H}$ fulfill Assumption 3.1. Then, as $N \to \infty$ we have almost surely*

$$\Delta\mathcal{L}(\beta;\mathrm{F}_{\boldsymbol{J}}) = -\beta\int_0^1 \log_2\frac{\mathrm{S}_{\boldsymbol{J}}(-\beta z)}{\mathrm{S}_{\boldsymbol{J}}(-z)}\,\mathrm{d}z. \tag{3.53}$$

Proof. See Appendix B.6. □

Alternatively, we may bypass the need for using the S-transform by invoking (2.72), i.e.

$$\mathrm{S}_{\boldsymbol{H}}(-t) = \int\frac{1}{x}\,\mathrm{d}\tilde{\mathrm{F}}_{J_t}(x), \quad 0 < t < 1. \tag{3.54}$$

The result in (2.72) also provides a convenient means to calculate the deviation from linear growth in the large-system limit. The right-hand side of (2.72) is nothing but the asymptotic inverse spectral mean of the channel matrix $\boldsymbol{P}_t\boldsymbol{H}$.

From Figure 3.3 we conclude that for the zero-mean iid matrix ensemble the deviation from linear growth is notable but not significant. In fact we have the following general property:

Remark 3.2. *Let $\boldsymbol{H}$ fulfill Assumption 3.1. Furthermore let $\mathrm{F}_{\boldsymbol{J}}$ be not a Dirac distribution function. Then, the quantity*

$$\mathcal{I}(\gamma;\mathrm{F}_{\boldsymbol{J}_\beta}) - \beta\mathcal{I}(\gamma;\mathrm{F}_{\boldsymbol{J}}) \tag{3.55}$$

increases with the SNR. Thus, we have

$$\Delta\mathcal{L}(\beta,\mathrm{F}_{\boldsymbol{J}}) = \sup_{\gamma}\left\{\mathcal{I}(\gamma;\mathrm{F}_{\boldsymbol{J}_\beta}) - \beta\mathcal{I}(\gamma;\mathrm{F}_{\boldsymbol{J}})\right\}. \tag{3.56}$$

Proof. See Appendix B.7. □

The result (3.56) leads us to expect that the linear growth may provide a reasonable approximation of the mutual information at moderate SNR region in practice. We also draw the attention to another remarkable property of the deviation from linear growth:

Remark 3.3. *Let $\boldsymbol{X} = \boldsymbol{X}^\dagger$ and $\boldsymbol{Y} = \boldsymbol{Y}^\dagger$ be independent random matrices in $\mathbb{C}^{N\times N}$. Moreover let $\boldsymbol{X}$ and $\boldsymbol{Y}$ fulfill Assumption 1. Then, we have*

$$\Delta\mathcal{L}(\beta;\mathrm{F}_{\boldsymbol{XY}}) = \Delta\mathcal{L}(\beta;\mathrm{F}_{\boldsymbol{X}}) + \Delta\mathcal{L}(\beta;\mathrm{F}_{\boldsymbol{Y}}). \tag{3.57}$$

Proof. See Appendix B.8. □

We can exploit this result to show that the deviation from linear growth increases with the amount of correlation between the entries of a channel matrix in a particular setting.

Example 3.5. *Consider a random matrix defined as*

$$\boldsymbol{H} = \prod_{m=1}^{M} \boldsymbol{A}_m \tag{3.58}$$

where the $N \times N$ matrices $\boldsymbol{A}_m$, $m = 1,\ldots,M$, are independent, have iid entries with zero mean and variance σ^2/N. Then, we have

$$\Delta\mathcal{L}(\beta;\mathrm{F}_{\boldsymbol{J}}) = M\Delta\mathcal{L}(\beta;\mathrm{F}_{\boldsymbol{A}_1^\dagger\boldsymbol{A}_1}) \tag{3.59}$$

$$= M(\beta-1)\log_2(1-\beta). \tag{3.60}$$

where by convention $0\log_2 0 = 0$.

The entries of the product of two matrices with iid entries are not iid anymore, but correlated. As M in (3.58) increases, so does the correlation between the entries of $\boldsymbol{H}$, and therefore the deviation from the linear growth.

6 Conclusions

We have addressed the problem of capacity scaling in MIMO communication systems when the transmitters send with equal signal power. We have showed that a variation of the number of antennas in a MIMO system with invariant channel matrix affects the capacity at asymptotically large SNR in the following way: If the minimum number of antennas at transmitter and receiver sides stay unaltered, the change of capacity depends only on the system dimensions, but *not on the singular values of the channel matrix*. In the large-system limit, this change of capacity can be expressed in a compact closed form involving only the binary entropy functions of the two aspect ratios of the channel matrices (the one before and the one after the variation of the number of antennas). Moreover, capacity grows only approximately linearly with the minimum of the system dimensions even at high SNR. The deviation from the linear growth, i.e. the deviation of the linear approximation, does depend on the singular values of the channel matrix. It can be quantified and has the following remarkable property in the large-system limit: For certain MIMO channel matrices that can be factored, it is the sum of the respective deviations associated with the factor matrices. The results are derived for the asymptotic SNR regime. However, they provide least upper bounds over the whole SNR range. Finally, a fundamental relation between capacity and its affine approximation (the multiplexing rate) was unveiled. This relation can be conveniently described via the S-transform.

Chapter 4

Self-Averaging Expectation Propagation

This chapter is based directly on

Burak Çakmak, Manfred Opper, Bernard H. Fleury and Ole Winther, "Self-averaging expectation propagation," arXiv preprint arXiv: 1608.06602, August 2016.

1 Introduction

Expectation propagation [21], [20] (EP) is a typically highly accurate method for approximate probabilistic and Bayesian inference which is applicable to both discrete and continuous random variables as well as hybrid models. Especially Gaussian EP which approximates intractable posterior distributions by multivariate Gaussian densities was found to give excellent approximations not only to posterior marginal moments but also to the free energy (i.e. the negative logarithm of the marginal pdf of the observed variables) [80].

Unfortunately, the advantage of Gaussian EP – which takes dependencies between variables into account over other methods which are based on simpler approximations with factorizing densities – becomes a problem when the number of random variables is large. This stems from the fact that EP requires frequent matrix inversions related to the update of variance parameters, called cavity variances, of the Gaussian approximations. This makes a direct application of EP to large systems problematic.

On the other hand, there are other approaches to approximate inference which explicitly take advantage of the fact that the number of random variables in the model is large. Central limit theory arguments applied to linear combinations of random variables have frequently been used to facilitate approximate inference [22], [23], [25]. This idea is also very much at the heart of the so-called TAP approach originally developed in the field

of statistical physics [26] and also frequently applied to probabilistic inference [20], [81], [82]. These approaches lead to Gaussian approximations but with a typically simpler parameterization that avoids costly matrix inversions, see also the method of "diagonal restricted" expectation consistency [83]. This idea has been used e.g. to develop tractable approximations to loopy BP when the connectivity of the graphical model becomes large. The so-called AMP technique – originally developed in the context of CDMA communication problem [22] – has been successfully applied to problems in compressed sensing [23–25]. This approach relies on statistical assumptions on data matrices, assuming that they are random matrices with zero-mean iid entries and vanishing variances (as the system dimensions tend to infinity). Under this assumption, the variance parameters of the Gaussian random variables become asymptotically non-fluctuating and are the same for each variable. This *self-averaging* value can be explicitly computed for the simple random matrix ensemble with zero-mean iid entries and vanishing variances.

In this chapter, we show that under certain statistical assumptions on the transformation matrix, the cavity variances computed by EP become self-averaging and can be computed without costly inversions when the matrix dimensions grow large. The novel aspect of the subsequent work is to go beyond the simple iid case based on which AMP is derived and allows for more general types of dependencies between the entries of the matrices. We develop expressions for the cavity variances of EP in terms of specific generating functions of the matrix statistics via the R- and S-transforms in free probability. Our approach is based the concept of *asymptotic freeness* of random matrices, see Chapter 2. The asymptotic regime considered here is that when both the numbers of rows and columns of the transformation matrix grow to infinity with their ratio (the matrix aspect ratio) kept fixed. Moreover, we are also not concerned with specific iterative algorithms that solve the EP fixed-point equations. Instead, we focus our analysis on the properties of EP fixed points.

Essentially, our technical assumptions imply that all latent variables contribute to the data equally in a statistical sense. In fact, such assumption is important for EP to operate effectively, because EP approximates the so-called cavity fields by Gaussians, i.e. it implicitly assumes a central limit theorem to hold. This is again assuming the same kind of everything contributes equally. Hence, we expect that in the cases where EP works well the self-averaging assumption will also be justified.

The chapter is organized as follows: Section 2 introduces the inference problem and its EP fixed-point equations. Section 3 presents a brief summary of the concepts of random matrix theory needed for our approach together with our main mathematical result. Section 4 uses this result to define the self-averaging EP method. In Section 5 we demonstrate the performance of self-averaging EP on a signal recovery problem from nonlinear compressed

sensing and compare it with that of standard EP. Conclusions are outlined in Section 6. The technical lemmas and the proofs are located in Appendix C.

2 Inference Problem and EP Approximation

We apply approximate Bayesian inference to the general observation model described in Subsection 2.2 of Chapter 1. For the sake of completeness, let us recall the observation model: a K-dimensional real, or complex, input vector $\boldsymbol{x}$ – which is generated according to a prior pdf $f(\boldsymbol{x})$ – is linearly transformed with an $N \times K$ real, or complex, matrix as $\boldsymbol{z} \triangleq \boldsymbol{H}\boldsymbol{x}$. Then, the vector $\boldsymbol{z}$ is mapped to the output vector $\boldsymbol{y}$ of the system. This mapping is characterized by the conditional pdf $f(\boldsymbol{y}|\boldsymbol{z})$. We assume that the prior and the conditional pdfs are both separable and symmetric, i.e.

$$f(\boldsymbol{x}) = \prod_{k=1}^{K} f(x_k) \tag{4.1}$$

$$f(\boldsymbol{y}|\boldsymbol{z}) = \prod_{n=1}^{N} f(y_n|z_n). \tag{4.2}$$

As a matter of fact, the separability and symmetry assumptions regarding these pdfs are irrelevant in the derivation of the EP fixed-point equations. However, they are necessary assumptions in our "self-averaging ansatz" which requires the system model to obey the democratic order introduced in Chapter 1. In other words, the latent variables contribute equally to the system in a statistical sense.

To apply EP to this problem, it is useful to introduce the variable $\boldsymbol{H}\boldsymbol{x}$ as an auxiliary variable $\boldsymbol{z}$ and study the joint posterior pdf of vector $\boldsymbol{s} \triangleq (\boldsymbol{x}, \boldsymbol{z})$ as

$$f(\boldsymbol{s}|\boldsymbol{y}, \boldsymbol{H}) \propto f(\boldsymbol{s})\delta(\boldsymbol{z} - \boldsymbol{H}\boldsymbol{x}) \tag{4.3}$$

where $f(\boldsymbol{s}) \triangleq f(\boldsymbol{x})f(\boldsymbol{y}|\boldsymbol{z})$. EP approximates the posterior pdf $f(\boldsymbol{s}|\boldsymbol{y}, \boldsymbol{H})$ in (4.3) with a Gaussian pdf by substituting the typically non-Gaussian factor $f(\boldsymbol{s})$ with a separable Gaussian term. Doing so yields the approximation

$$q(\boldsymbol{s}) \propto e^{-\frac{\beta}{2}\boldsymbol{s}^\dagger \boldsymbol{\Lambda} \boldsymbol{s} + \beta \mathbb{R}\{\boldsymbol{\gamma}^\dagger \boldsymbol{s}\}}\ \delta(\boldsymbol{z} - \boldsymbol{H}\boldsymbol{x}) \tag{4.4}$$

where $\boldsymbol{\Lambda}$ is diagonal and $\beta = 1$ when the signal model is real-valued and $\beta = 2$ when it is complex-valued. The parameters $\boldsymbol{\gamma}$ and $\boldsymbol{\Lambda}$ are computed in an iterative way such that for all i the first and second moments of the marginal $q_i(s_i)$ of the Gaussian pdf $q(\boldsymbol{s})$ agree with those of the *tilted pdf*, say $\tilde{q}_i(s_i)$, which results from replacing in (4.4) the Gaussian factor

$$\exp\left(-\frac{\beta}{2}\Lambda_{ii}|s_i|^2 + \beta \mathbb{R}\{\gamma_i s_i\}\right) \tag{4.5}$$

with the (non-Gaussian) pdf $f_i(s_i)$ and integrating over all variables but s_i:

$$\begin{aligned}\tilde{q}_i(s_i) &\propto f_i(s_i) \int e^{\frac{\beta}{2}\Lambda_{ii}|s_i|^2 - \beta\Re\{\gamma_i s_i\}} q(\boldsymbol{s})\, \mathrm{d}\boldsymbol{s}_{\setminus i} \\ &\propto f_i(s_i) \exp\left(-\frac{\beta}{2}\mathrm{V}_{ii}|s_i|^2 + \beta\mathbb{R}\{\rho_i s_i\}\right) . \end{aligned} \tag{4.6}$$

Here V_{ii} is referred to as the *cavity* variance of the cavity distribution[1]. Note also that (4.6) implies

$$q_i(s_i) = \int q(\boldsymbol{s})\, \mathrm{d}\boldsymbol{s}_{\setminus i} \tag{4.7}$$

$$\propto \exp\left(-\frac{\beta}{2}(\Lambda_{ii} + \mathrm{V}_{ii})|s_i|^2 + \beta\mathbb{R}\{(\rho_i + \gamma_i)s_i\}\right). \tag{4.8}$$

For notational convenience, we write the diagonal matrices $\boldsymbol{\Lambda}$ and $\mathbf{V}$ and the vectors γ and $\boldsymbol{\rho}$ in the forms

$$\boldsymbol{\Lambda} = \begin{pmatrix} \boldsymbol{\Lambda}_{\mathrm{x}} & \mathbf{0} \\ \mathbf{0} & \boldsymbol{\Lambda}_{\mathrm{z}} \end{pmatrix}, \quad \gamma = (\gamma_{\mathrm{x}}, \gamma_{\mathrm{z}}) \tag{4.9}$$

$$\mathbf{V} = \begin{pmatrix} \mathbf{V}_{\mathrm{x}} & \mathbf{0} \\ \mathbf{0} & \mathbf{V}_{\mathrm{z}} \end{pmatrix}, \quad \boldsymbol{\rho} = (\boldsymbol{\rho}_{\mathrm{x}}, \boldsymbol{\rho}_{\mathrm{z}}). \tag{4.10}$$

By using standard Gaussian integral identities [84] we obtain

$$q(\boldsymbol{x}) = N(\boldsymbol{x}|\boldsymbol{\mu}_{\mathrm{x}}, \boldsymbol{\Sigma}_{\mathrm{x}}) \tag{4.11}$$

$$q(\boldsymbol{z}) = N(\boldsymbol{z}|\boldsymbol{H}\boldsymbol{\mu}_{\mathrm{x}}, \boldsymbol{H}\boldsymbol{\Sigma}_{\mathrm{x}}\boldsymbol{H}^{\dagger}) \tag{4.12}$$

where we introduce

$$\boldsymbol{\Sigma}_{\mathrm{x}} \triangleq (\boldsymbol{\Lambda}_{\mathrm{x}} + \boldsymbol{H}^{\dagger}\boldsymbol{\Lambda}_{\mathrm{z}}\boldsymbol{H})^{-1} \tag{4.13}$$

$$\boldsymbol{\mu}_{\mathrm{x}} \triangleq \boldsymbol{\Sigma}_{\mathrm{x}}(\gamma_{\mathrm{x}} + \boldsymbol{H}^{\dagger}\gamma_{\mathrm{z}}). \tag{4.14}$$

Then, by equating the first- and second-order moments of the pdfs $q_i(s_i)$ and $\tilde{q}_i(s_i)$, we obtain the fixed-point equations of EP for (4.3):

$$\eta_i = \frac{\gamma_i + \rho_i}{\mathrm{V}_{ii} + \Lambda_{ii}} = \begin{cases} [\boldsymbol{\mu}_{\mathrm{x}}]_{ii} & \Lambda_{ii} = [\boldsymbol{\Lambda}_{\mathrm{x}}]_{ii} \\ [\boldsymbol{H}\boldsymbol{\mu}_{\mathrm{x}}]_{jj} & \Lambda_{ii} = [\boldsymbol{\Lambda}_{\mathrm{z}}]_{jj} \end{cases} \tag{4.15a}$$

$$\chi_i = \frac{1}{\Lambda_{ii} + \mathrm{V}_{ii}} = \begin{cases} [\boldsymbol{\Sigma}_{\mathrm{x}}]_{ii} & \Lambda_{ii} = [\boldsymbol{\Lambda}_{\mathrm{x}}]_{ii} \\ [\boldsymbol{H}\boldsymbol{\Sigma}_{\mathrm{x}}\boldsymbol{H}^{\dagger}]_{jj} & \Lambda_{ii} = [\boldsymbol{\Lambda}_{\mathrm{z}}]_{jj} \end{cases}. \tag{4.15b}$$

The terms η_i and χ_i are the mean and the variance, respectively, of the pdf $\tilde{q}_i(s_i)$ in (4.6). By solving for η_i via (4.15) for each i we obtain an approximate of the minimum mean-square error estimator of s_i, i.e. $\langle s_i \rangle_{f(\boldsymbol{s}|\boldsymbol{y},\boldsymbol{H})} \approx \eta_i$.

[1]Specifically, following [81] one can introduce a cavity pdf $f(h_i)$ through the relationship $f(s_i|\boldsymbol{y},\boldsymbol{H}) = \frac{1}{Z} f_i(s_i) \int \exp(s_i h_i) f(h_i) \mathrm{d}h_i$.

2.1 TAP-like equations

One can design numerous fixed-point algorithms that solve (4.15). In this work we restrict our attention to TAP-like algorithms, see e.g. [20, 22, 23, 25, 81]. Specifically, we appropriately re-parameterize (4.15) whose form is similar to the TAP-like fixed-point equations. This is essentially carried out by bypassing the need for the vector γ in (4.15). We leave (4.15b) unchanged and keep the variables η and χ because these variables are expressed through the variables $\rho, \mathbf{V}, \Lambda$ only. Moreover, from (4.15a) we note that $\mu_{\mathrm{x}} = \eta_{\mathrm{x}}$ with $\eta = (\eta_{\mathrm{x}}, \eta_{\mathrm{z}})$. Hence, we solely need to bypass γ in the expression of ρ as a function of the other parameters. Combining (4.13) and (4.14) we write

$$\gamma_{\mathrm{x}} = -\boldsymbol{H}^{\mathsf{T}}\gamma_{\mathrm{z}} + (\boldsymbol{\Lambda}_{\mathrm{x}} + \boldsymbol{H}^{\mathsf{T}}\boldsymbol{\Lambda}_{\mathrm{z}}\boldsymbol{H})\boldsymbol{\mu}_{\mathrm{x}}. \tag{4.16}$$

The first equality in (4.15a) for all $\Lambda_{ii} = [\boldsymbol{\Lambda}_{\mathrm{x}}]_{ii}$ is equivalent to $\gamma_{\mathrm{x}} + \boldsymbol{\rho}_{\mathrm{x}} = (\boldsymbol{\Lambda}_{\mathrm{x}} + \mathbf{V}_{\mathrm{x}})\boldsymbol{\mu}_{\mathrm{x}}$. Inserting (4.19) we solve for $\boldsymbol{\rho}_{\mathrm{x}}$:

$$\begin{aligned}
\boldsymbol{\rho}_{\mathrm{x}} &= \boldsymbol{H}^{\mathsf{T}}\gamma_{\mathrm{z}} - (\boldsymbol{\Lambda}_{\mathrm{x}} + \boldsymbol{H}^{\mathsf{T}}\boldsymbol{\Lambda}_{\mathrm{z}}\boldsymbol{H})\boldsymbol{\mu}_{x} + (\boldsymbol{\Lambda}_{\mathrm{x}} + \mathbf{V}_{\mathrm{x}})\boldsymbol{\mu}_{\mathrm{x}} && (4.17)\\
&= \boldsymbol{H}^{\mathsf{T}}(\gamma_{\mathrm{z}} - \boldsymbol{\Lambda}_{\mathrm{z}}\boldsymbol{H}\boldsymbol{\mu}_{\mathrm{x}}) + \mathbf{V}_{\mathrm{x}}\boldsymbol{\mu}_{\mathrm{x}} && (4.18)\\
&= \boldsymbol{H}^{\mathsf{T}}\boldsymbol{m} + \mathbf{V}_{\mathrm{x}}\boldsymbol{\mu}_{\mathrm{x}} \quad \text{with} \quad \boldsymbol{m} \triangleq \gamma_{\mathrm{z}} - \boldsymbol{\Lambda}_{\mathrm{z}}\boldsymbol{H}\boldsymbol{\mu}_{\mathrm{x}}. && (4.19)
\end{aligned}$$

The second equality in (4.15a) for all $\Lambda_{ii} = [\boldsymbol{\Lambda}_{\mathrm{z}}]_{jj}$ is equivalent to $\gamma_{\mathrm{z}} + \boldsymbol{\rho}_{\mathrm{z}} = (\boldsymbol{\Lambda}_{\mathrm{z}} + \mathbf{V}_{\mathrm{z}})\boldsymbol{H}\boldsymbol{\mu}_{\mathrm{x}}$. With this identity we recast $\boldsymbol{m}$ as

$$\begin{aligned}
\boldsymbol{m} &= (\boldsymbol{\Lambda}_{\mathrm{z}} + \mathbf{V}_{\mathrm{z}})\boldsymbol{H}\boldsymbol{\mu}_{\mathrm{x}} - \boldsymbol{\rho}_{\mathrm{z}} - \boldsymbol{\Lambda}_{\mathrm{z}}\boldsymbol{H}\boldsymbol{\mu}_{\mathrm{x}} && (4.20)\\
&= \mathbf{V}_{\mathrm{z}}\boldsymbol{H}\boldsymbol{\mu}_{\mathrm{x}} - \boldsymbol{\rho}_{\mathrm{z}}. && (4.21)
\end{aligned}$$

Combining (4.19), (4.21) and the identities $\eta_{\mathrm{x}} = \boldsymbol{\mu}_{\mathrm{x}}$ and $\eta_{\mathrm{z}} = \boldsymbol{H}\boldsymbol{\mu}_{\mathrm{x}}$ (see (4.15a)) we obtain

$$\begin{aligned}
\boldsymbol{\rho}_{\mathrm{z}} &= \mathbf{V}_{\mathrm{z}}\boldsymbol{H}\boldsymbol{\eta}_{\mathrm{x}} - \boldsymbol{m} && (4.22a)\\
\boldsymbol{m} &= \mathbf{V}_{\mathrm{z}}\boldsymbol{\eta}_{\mathrm{z}} - \boldsymbol{\rho}_{\mathrm{z}} && (4.22b)\\
\boldsymbol{\rho}_{\mathrm{x}} &= \mathbf{V}_{\mathrm{x}}\boldsymbol{\eta}_{\mathrm{x}} + \boldsymbol{H}^{\mathsf{T}}\boldsymbol{m}. && (4.22c)
\end{aligned}$$

Here one may argue that the characterization of $\boldsymbol{\rho}_{\mathrm{z}}$ provided by (4.22) via the identity $\boldsymbol{\eta}_{\mathrm{z}} = \boldsymbol{H}\boldsymbol{\eta}_{\mathrm{x}}$ may not be unique. However, for any i $[\boldsymbol{\eta}_{\mathrm{z}}]_i$ is a strictly increasing function of $[\boldsymbol{\rho}_{\mathrm{z}}]_i$ and thereby is bijective. Hence, the characterization is unique. The TAP-like form of the EP fixed-point equations consists of (4.22) and (4.15b).

2.2 The AMP algorithm

The AMP algorithm was originally derived in the context of CDMA [22]. It re-appeared later in the context of compressed sensing [23]. Later on, it

was generalized for the model (1.1) [25]. Essentially, the AMP algorithm is obtained as a large-system limit of heuristic loopy BP where the central limit theorem can be applied when the underlying measurement matrix has iid entries with zero mean and variance $1/K$. The AMP algorithm proceeds the following iterative equations

$$\boldsymbol{\rho}_{\mathrm{z}}(t) = \mathbf{V}_{\mathrm{z}}(t)\boldsymbol{H}\boldsymbol{\eta}_{\mathrm{x}}(t) - \boldsymbol{m}(t-1) \tag{4.23}$$

$$\boldsymbol{m}(t) = \mathbf{V}_{\mathrm{z}}(t)\boldsymbol{\eta}_{\mathrm{z}}(t) - \boldsymbol{\rho}_{\mathrm{z}}(t) \tag{4.24}$$

$$\boldsymbol{\rho}_{\mathrm{x}}(t+1) = \mathbf{V}_{\mathrm{x}}(t)\boldsymbol{\eta}_{\mathrm{x}}(t) + \boldsymbol{H}^{\dagger}\boldsymbol{m}(t). \tag{4.25}$$

Here $\boldsymbol{\eta}(t) \triangleq (\boldsymbol{\eta}_{\mathrm{x}}(t), \boldsymbol{\eta}_{\mathrm{z}}(t))$ denotes the mean vector of the pdf

$$\tilde{q}_t(\boldsymbol{s}) \propto f(\boldsymbol{s}) \left(-\frac{\beta}{2}\boldsymbol{s}^{\dagger}\mathbf{V}(t)\boldsymbol{s} + \mathbb{R}\{\boldsymbol{s}^{\dagger}\boldsymbol{\rho}(t)\} \right) \tag{4.26}$$

where $\boldsymbol{\rho}(t) = (\boldsymbol{\rho}_{\mathrm{x}}(t), \boldsymbol{\rho}_{\mathrm{z}}(t))$ and the diagonal matrix $\mathbf{V}(t)$ is the proper conjugation of the diagonal matrices $\mathbf{V}_{\mathrm{x}}(t)$ and $\mathbf{V}_{\mathrm{z}}(t)$, see (4.10). The cavity variances are updated according to $\mathbf{V}_{\mathrm{x}}(t) = v_{\mathrm{x}}(t)\mathbf{I}$ and $\mathbf{V}_{\mathrm{z}}(t) = v_{\mathrm{z}}(t)\mathbf{I}$ where

$$v_{\mathrm{x}}(t) = \frac{\alpha(1 - v_{\mathrm{z}}(t)\langle\boldsymbol{\chi}_{\mathrm{z}}(t)\rangle)}{\langle\boldsymbol{\chi}_{\mathrm{x}}(t)\rangle} \tag{4.27}$$

$$v_{\mathrm{z}}(t) = \frac{1}{\langle\boldsymbol{\chi}_{\mathrm{x}}(t)\rangle}. \tag{4.28}$$

Here $\alpha \triangleq N/K$ and $\boldsymbol{\chi}(t) \triangleq (\boldsymbol{\chi}_{\mathrm{x}}(t), \boldsymbol{\chi}_{\mathrm{z}}(t))$ (with $\boldsymbol{\chi}_{\mathrm{x}}(t)$ of dimension K) denotes the variance of $\tilde{q}_{t-1}(\boldsymbol{s})$.

2.3 Summary of the fixed-point equations of AMP and EP

AMP and EP share the fixed-point equations (4.22). The fixed-point equations of the cavity variances, differ however. Those of AMP read $\mathbf{V}_{\mathrm{x}} = v_{\mathrm{x}}\mathbf{I}$ and $\mathbf{V}_{\mathrm{z}} = v_{\mathrm{z}}\mathbf{I}$ where

$$v_{\mathrm{x}} = \frac{\alpha(1 - v_{\mathrm{z}}\langle\boldsymbol{\chi}_{\mathrm{z}}\rangle)}{\langle\boldsymbol{\chi}_{\mathrm{x}}\rangle} \tag{4.29}$$

$$v_{\mathrm{z}} = \frac{1}{\langle\boldsymbol{\chi}_{\mathrm{x}}\rangle}. \tag{4.30}$$

Those of EP are given by (4.15b), which we recast in a more explicit form

$$\chi_i = \frac{1}{\Lambda_{ii} + \mathrm{V}_{ii}} = \begin{cases} [(\boldsymbol{\Lambda}_{\mathrm{x}} + \boldsymbol{H}^{\dagger}\boldsymbol{\Lambda}_{\mathrm{z}}\boldsymbol{H})^{-1}]_{ii} & \Lambda_{ii} = [\boldsymbol{\Lambda}_{\mathrm{x}}]_{ii} \\ [\boldsymbol{H}(\boldsymbol{\Lambda}_{\mathrm{x}} + \boldsymbol{H}^{\dagger}\boldsymbol{\Lambda}_{\mathrm{z}}\boldsymbol{H})^{-1}\boldsymbol{H}^{\dagger}]_{jj} & \Lambda_{ii} = [\boldsymbol{\Lambda}_{\mathrm{z}}]_{jj} \end{cases}. \tag{4.31}$$

Hence, from an algorithmic point of view, the most expensive operations required in EP are related to the computation of the vector of cavity variances $\mathbf{V}$ in terms of $\boldsymbol{\Lambda}$ from (4.31). As we will see in the next section, we can overcome this difficulty by using the concept of asymptotic freeness of random matrices.

3 Random Matrix Treatment

We will use the fact that the equations (4.15b) are obtained as the stationary points of the objective function

$$C_{\boldsymbol{H}}(\boldsymbol{\Lambda}) = \ln|\boldsymbol{\Lambda}_x + \boldsymbol{H}^\dagger\boldsymbol{\Lambda}_z\boldsymbol{H}| - \ln|\boldsymbol{\Lambda} + \mathbf{v}|. \tag{4.32}$$

Under certain asymptotic freeness assumptions on the matrices, we will derive an asymptotic limiting expression for the first term in (4.32) which depends only on certain random matrix transforms. These involve the LED of $\boldsymbol{H}\boldsymbol{H}^\dagger$. The transforms can be precomputed before iterating the EP algorithm if the random matrix ensemble is explicitly given. In other cases, an approximation based on the empirical eigenvalue distribution of $\boldsymbol{H}$ can be used. Assuming that the deviation from the asymptotic objective function can also be neglected when we minimize (4.32) by taking derivatives, we will end up with a type of *self-averaging* EP that entirely avoids matrix inversions.

3.1 The asymptotic result

To approximate the term $\ln|\boldsymbol{\Lambda}_x + \boldsymbol{H}^\dagger\boldsymbol{\Lambda}_z\boldsymbol{H}|$ in the objective function $C_{\boldsymbol{H}}(\boldsymbol{\Lambda})$ in (4.32), we employ additive and multiplicative free convolutions. We will assume that $\boldsymbol{\Lambda}_x$ and $\boldsymbol{H}^\dagger\boldsymbol{\Lambda}_z\boldsymbol{H}$ have LEDs, are asymptotically free and use the result

$$\mathrm{R}_{\boldsymbol{\Lambda}_x+\boldsymbol{H}^\dagger\boldsymbol{\Lambda}_z\boldsymbol{H}}(\omega) = \mathrm{R}_{\boldsymbol{\Lambda}_x}(\omega) + \mathrm{R}_{\boldsymbol{H}^\dagger\boldsymbol{\Lambda}_z\boldsymbol{H}}(\omega). \tag{4.33}$$

The R-transform of the LED $\boldsymbol{H}^\dagger\boldsymbol{\Lambda}_z\boldsymbol{H}$ is still analytically intractable. If $\boldsymbol{\Lambda}_z$ and $\boldsymbol{H}^\dagger\boldsymbol{H}$ are asymptotically free, we can resolve these difficultly by making use of

$$\mathrm{S}_{\boldsymbol{\Lambda}_z\boldsymbol{H}\boldsymbol{H}^\dagger}(z) = \mathrm{S}_{\boldsymbol{\Lambda}_z}(z)\mathrm{S}_{\boldsymbol{H}\boldsymbol{H}^\dagger}(z). \tag{4.34}$$

Assumption 4.1. *In the large-system limit, let the matrices $\boldsymbol{\Lambda}_x$, $\boldsymbol{\Lambda}_z$ and $\boldsymbol{H}^\dagger\boldsymbol{H}$ have compactly supported LEDs, the LED of $\boldsymbol{\Lambda}_z$ have its support in $[0,\infty)$ and $\boldsymbol{H}$ have uniformly bounded spectral norm. Furthermore, let $\phi(\boldsymbol{\Lambda}_x) < \infty$, $\phi(\boldsymbol{\Lambda}_z) < \infty$ and $\phi(\boldsymbol{\Lambda}_x + \boldsymbol{H}^\dagger\boldsymbol{\Lambda}_z\boldsymbol{H})^{-1} < \phi(\boldsymbol{H}^\dagger\boldsymbol{\Lambda}_z\boldsymbol{H})^{-1}$ where by convention $\phi(\boldsymbol{X}^{-1}) = \infty$ if $\boldsymbol{X}$ is singular. Moreover,* (4.33) *and* (4.34) *hold.*

The restriction of non-negativeness of $\boldsymbol{\Lambda}_z$ can be relaxed in the analysis. However, based on numerical evidence and the so-called AT line of stability analysis in Appendix C.2 we conjecture that in practice any effective solution fulfills this condition when the dimensions are sufficiently large. Typically, $\alpha = N/K < 1$ and thereby $\phi(\boldsymbol{H}^\dagger\boldsymbol{\Lambda}_z\boldsymbol{H})^{-1} = \infty$, so that the last but one condition is fulfilled. As regards the final condition two points are worth noting. Firstly, if $\boldsymbol{H}$ is invariant from right and left, then (4.33) and (4.34) always

hold provided the matrices in Assumption 4.1 have compactly supported LEDs [41]. Secondly, depending on the application some of the matrices $\mathbf{\Lambda}_{\mathrm{x}}$, $\mathbf{\Lambda}_{\mathrm{z}}$, $\boldsymbol{H}\boldsymbol{H}^{\dagger}$ might be proportional to the identity matrix. For instance, in the context of (non)linear compressed sensing $\boldsymbol{H}$ might be row-orthogonal, i.e. $\boldsymbol{H}\boldsymbol{H}^{\dagger} = \mathbf{I}$ and thereby (4.34) always holds.

Theorem 4.1. *Let the matrices $\mathbf{\Lambda}_{\mathrm{x}}$, $\mathbf{\Lambda}_{\mathrm{z}}$ and $\boldsymbol{H}$ fulfill the conditions stated in Assumption 4.1 and $(\mathbf{\Lambda}_{\mathrm{x}} + \boldsymbol{H}^{\dagger}\mathbf{\Lambda}_{\mathrm{z}}\boldsymbol{H})$ be positive definite. Then, for sufficiently large N, K there exist positive quantities χ_{a}, v_{a} and λ_{a} for $\mathrm{a} \in \{\mathrm{x}, \mathrm{z}\}$ such that*

$$\begin{aligned}\ln|\mathbf{\Lambda}_{\mathrm{x}} + \boldsymbol{H}^{\dagger}\mathbf{\Lambda}_{\mathrm{z}}\boldsymbol{H}| &= \ln|\mathbf{\Lambda}_{\mathrm{x}} + v_{\mathrm{x}}\mathbf{I}| + \ln|\mathbf{\Lambda}_{\mathrm{z}} + v_{\mathrm{z}}\mathbf{I}| \\ &\quad + \ln|\lambda_{\mathrm{x}}\mathbf{I} + \lambda_{\mathrm{z}}\boldsymbol{H}^{\dagger}\boldsymbol{H}| + K\ln\chi_{\mathrm{x}} + N\ln\chi_{\mathrm{z}} + \epsilon \end{aligned} \tag{4.35}$$

where $\epsilon = O(1)$ is a bounded function of N. The quantities in (4.35) *are uniquely characterized by the implicit equations*

$$v_{\mathrm{x}} = \lambda_{\mathrm{z}}\mathrm{R}^{K}_{\boldsymbol{H}^{\dagger}\boldsymbol{H}}(-\lambda_{\mathrm{z}}\chi_{\mathrm{x}}) \tag{4.36}$$

$$v_{\mathrm{z}} = \lambda_{\mathrm{x}}\mathrm{S}^{N}_{\boldsymbol{H}\boldsymbol{H}^{\dagger}}(-\lambda_{\mathrm{z}}\chi_{\mathrm{z}}) \tag{4.37}$$

where $\chi_{\mathrm{a}} = \mathrm{Tr}(\mathbf{\Lambda}_{\mathrm{a}} + v_{\mathrm{a}}\mathbf{I})^{-1}$ and $\lambda_{\mathrm{a}} = \chi_{\mathrm{a}}^{-1} - v_{\mathrm{a}}$ for $\mathrm{a} \in \{\mathrm{x}, \mathrm{z}\}$. Moreover, we have the limiting approximations $\chi_{\mathrm{x}} \simeq \mathrm{Tr}(\mathbf{\Lambda}_{\mathrm{x}} + \boldsymbol{H}^{\dagger}\mathbf{\Lambda}_{\mathrm{z}}\boldsymbol{H})$ and

$$v_{\mathrm{x}} \simeq \lambda_{\mathrm{z}}\mathrm{R}_{\boldsymbol{H}^{\dagger}\boldsymbol{H}}(-\lambda_{\mathrm{z}}\chi_{\mathrm{x}}) \tag{4.38}$$

$$v_{\mathrm{z}} \simeq \lambda_{\mathrm{x}}\mathrm{S}_{\boldsymbol{H}\boldsymbol{H}^{\dagger}}(-\lambda_{\mathrm{z}}\chi_{\mathrm{z}}). \tag{4.39}$$

Proof: See Appendix C. 1.

4 Self-Averaging EP Framework

To characterize the cost function (4.32) with respect to $\{\Lambda_{ii}\}$, we use Theorem 4.1 as follows:

$$\begin{aligned}\frac{\partial \ln|\mathbf{\Lambda}_{\mathrm{x}} + \boldsymbol{H}^{\dagger}\mathbf{\Lambda}_{\mathrm{z}}\boldsymbol{H}|}{\partial\Lambda_{ii}} = \frac{1}{\Lambda_{ii}+v} + \frac{\partial\epsilon}{\partial\Lambda_{ii}} &+ K\chi_{\mathrm{x}}\frac{\partial v_{\mathrm{x}}}{\partial\Lambda_{ii}} + N\chi_{\mathrm{z}}\frac{\partial v_{\mathrm{z}}}{\partial\Lambda_{ii}} + K\chi_{\mathrm{x}}\frac{\partial\lambda_{\mathrm{x}}}{\partial\Lambda_{ii}} \\ &\underbrace{+N\chi_{\mathrm{z}}\frac{\partial\lambda_{\mathrm{z}}}{\partial\Lambda_{ii}} + K\frac{1}{\chi_{\mathrm{x}}}\frac{\partial\chi_{\mathrm{x}}}{\partial\Lambda_{ii}} + N\frac{1}{\chi_{\mathrm{z}}}\frac{\partial\chi_{\mathrm{z}}}{\partial\Lambda_{ii}}}_{=0}\end{aligned} \tag{4.40}$$

where by abuse of notation we write $v = v_{\mathrm{x}}$ for $\Lambda_{ii} = [\mathbf{\Lambda}_{\mathrm{x}}]_{ii}$ and $v = v_{\mathrm{z}}$ for $\Lambda_{ii} = [\mathbf{\Lambda}_{\mathrm{z}}]_{jj}$. The fact that the sum of the last six terms vanishes is an immediate consequence of the definition of the variables χ_{a}, λ_{a} for $\mathrm{a} \in \{\mathrm{x}, \mathrm{z}\}$

in Theorem 4.1. Taking the partial derivative of the left-hand term in (4.40) and making use of (4.15b) we obtain

$$\frac{1}{\Lambda_{ii}+\mathrm{V}_{ii}} = \frac{1}{\Lambda_{ii}+v} + \frac{\partial \epsilon}{\partial \Lambda_{ii}}. \tag{4.41}$$

An explicit analysis of the derivative of the asymptotic correction term $\frac{\partial \epsilon}{\partial \Lambda_{ii}}$ requires an extensive random matrix study. Instead, we consider the following heuristic argument: Firstly, we recall approximation $\chi_{\mathrm{x}} \simeq \mathrm{Tr}(\boldsymbol{\Lambda}_{\mathrm{x}} + \boldsymbol{H}^{\dagger}\boldsymbol{\Lambda}_{z}\boldsymbol{H})^{-1}$ of Theorem 4.1. Thereby, we have

$$\sum_{i} \frac{\partial \epsilon}{\partial [\boldsymbol{\Lambda}_{\mathrm{x}}]_{ii}} = O(1). \tag{4.42}$$

Then, we consider the implicit assumption that "*everything contributes in a democratic fashion*", specifically there is no dominant individual term in the sum (4.42). So, we have

$$\frac{\partial \epsilon}{\partial [\boldsymbol{\Lambda}_{\mathrm{x}}]_{ii}} = O\left(\frac{1}{N}\right). \tag{4.43}$$

Secondly, from (4.43) and using Theorem 4.1 one can show that

$$\chi_{\mathrm{z}} \simeq \mathrm{Tr}(\boldsymbol{H}(\boldsymbol{\Lambda}_{\mathrm{x}} + \boldsymbol{H}^{\dagger}\boldsymbol{\Lambda}_{z}\boldsymbol{H})^{-1}\boldsymbol{H}^{\dagger}). \tag{4.44}$$

Thereby, we have

$$\sum_{j} \frac{\partial \epsilon}{\partial [\boldsymbol{\Lambda}_{\mathrm{z}}]_{jj}} = O(1). \tag{4.45}$$

Similarly, we assume that "*everything contributes in a democratic fashion*", specifically there is no dominant individual term in the sum (4.45). Thus, we have

$$\frac{\partial \epsilon}{\partial [\boldsymbol{\Lambda}_{\mathrm{z}}]_{jj}} = O\left(\frac{1}{N}\right). \tag{4.46}$$

In summary, we conclude that we have $\mathbf{V}_{\mathrm{x}} \simeq v_{\mathrm{x}}\mathbf{I}$ and $\mathbf{V}_{\mathrm{z}} \simeq v_{\mathrm{z}}\mathbf{I}$. This means that the diagonal elements of $\mathbf{V}_{\mathrm{x}}$ and $\mathbf{V}_{\mathrm{z}}$ are asymptotically self-averaging.

4.1 Summary of self-averaging EP

For convenience, we first factorize the *tilted* pdf $\tilde{q}(\boldsymbol{s}) = \prod_i \tilde{q}_i(s_i)$ in (4.6) as $\tilde{q} = \tilde{q}_{\mathrm{x}} \cdot \tilde{q}_{\mathrm{z}}$ where

$$\tilde{q}_{\mathrm{x}}(\boldsymbol{x}) \propto f(\boldsymbol{x}) e^{-\frac{\beta}{2} v_{\mathrm{x}} \boldsymbol{x}^{\dagger}\boldsymbol{x} + \beta \mathbb{R}\{\boldsymbol{x}^{\dagger}\boldsymbol{\rho}_{\mathrm{x}}\}} \tag{4.47}$$

$$\tilde{q}_{\mathrm{z}}(\boldsymbol{z}) \propto f(\boldsymbol{y}|\boldsymbol{z}) e^{-\frac{\beta}{2} v_{\mathrm{z}} \boldsymbol{z}^{\dagger}\boldsymbol{z} + \beta \mathbb{R}\{\boldsymbol{z}^{\dagger}\boldsymbol{\rho}_{\mathrm{z}}\}}. \tag{4.48}$$

Moreover, for $\mathrm{a} \in \{\mathrm{x}, \mathrm{z}\}$ let $\boldsymbol{\eta}_{\mathrm{a}}$ and $\boldsymbol{\chi}_{\mathrm{a}}$ be the mean and variance vectors of the pdf q_{a}, respectively. Thus, we have $\chi_{\mathrm{a}} \simeq \langle \boldsymbol{\chi}_{\mathrm{a}} \rangle$ where χ_{a} is given in

Theorem 4.1. Thereby, from (4.22) the self-averaging EP fixed-point equations are given by

$$\boldsymbol{\rho}_{\mathrm{z}} = v_{\mathrm{z}}\boldsymbol{H}\boldsymbol{\eta}_{\mathrm{x}} - \boldsymbol{m} \tag{4.49a}$$
$$\boldsymbol{m} = v_{\mathrm{z}}\boldsymbol{\eta}_{\mathrm{z}} - \boldsymbol{\rho}_{\mathrm{z}} \tag{4.49b}$$
$$\boldsymbol{\rho}_{\mathrm{x}} = v_{\mathrm{x}}\boldsymbol{\eta}_{\mathrm{x}} + \boldsymbol{H}^{\mathsf{T}}\boldsymbol{m} \tag{4.49c}$$
$$v_{\mathrm{x}} = \lambda_{\mathrm{z}}\mathrm{R}_{\boldsymbol{H}^{\mathsf{T}}\boldsymbol{H}}(-\lambda_{\mathrm{z}}\langle\boldsymbol{\chi}_{\mathrm{x}}\rangle) \tag{4.49d}$$
$$v_{\mathrm{z}} = \lambda_{\mathrm{x}}\mathrm{S}_{\boldsymbol{H}\boldsymbol{H}^{\mathsf{T}}}(-\lambda_{\mathrm{z}}\langle\boldsymbol{\chi}_{\mathrm{z}}\rangle) \tag{4.49e}$$
$$\lambda_{\mathrm{x}} = 1/\langle\boldsymbol{\chi}_{\mathrm{x}}\rangle - v_{\mathrm{x}} \tag{4.49f}$$
$$\lambda_{\mathrm{z}} = 1/\langle\boldsymbol{\chi}_{\mathrm{z}}\rangle - v_{\mathrm{z}}. \tag{4.49g}$$

Also, one can alternatively consider the characterization of v_{x} in (4.49d) as (see Appendix C.1)

$$v_{\mathrm{x}} = \frac{\alpha(1 - v_{\mathrm{z}}\langle\boldsymbol{\chi}_{\mathrm{z}}\rangle)}{\langle\boldsymbol{\chi}_{\mathrm{x}}\rangle}. \tag{4.50}$$

When the analytical expression of either the R-transform or the S-transform in the above expressions is known, while the other is unknown, we can use (2.65) to express the cavity variances as a function of the known transform. For example, by using (2.65) we can write (4.49e) in the form

$$v_{\mathrm{z}} = \frac{\lambda_{\mathrm{x}}}{\mathrm{R}_{\boldsymbol{H}\boldsymbol{H}^{\mathsf{T}}}(-v_{\mathrm{z}}(1 - v_{\mathrm{z}}\langle\boldsymbol{\chi}_{\mathrm{z}}\rangle)/\lambda_{\mathrm{x}})}. \tag{4.51}$$

It might be the case that the analytical expressions of both the R-transform and the S-transform are unknown. In fact, the LEDs themselves might be even unknown. In such cases, the simplest approach would be to use the R-transform $\mathrm{R}^{K}_{\boldsymbol{H}^{\mathsf{T}}\boldsymbol{H}}$ and S-transform $\mathrm{S}^{N}_{\boldsymbol{H}\boldsymbol{H}^{\mathsf{T}}}$ of the *empirical* eigenvalue distribution of the matrices $\boldsymbol{H}^{\mathsf{T}}\boldsymbol{H}$ and $\boldsymbol{H}\boldsymbol{H}^{\mathsf{T}}$, respectively. Using the definitions of the transforms, this leads to the fixed-point equations

$$\langle\boldsymbol{\chi}_{\mathrm{a}}\rangle = \frac{1}{\lambda_{\mathrm{a}} + v_{\mathrm{a}}} = \begin{cases} \mathrm{Tr}(\lambda_{\mathrm{x}}\mathbf{I} + \lambda_{\mathrm{z}}\boldsymbol{H}^{\mathsf{T}}\boldsymbol{H})^{-1} & \mathrm{a} = \mathrm{x} \\ \mathrm{Tr}(\boldsymbol{H}(\lambda_{\mathrm{x}}\mathbf{I} + \lambda_{\mathrm{z}}\boldsymbol{H}^{\mathsf{T}}\boldsymbol{H})^{-1}\boldsymbol{H}^{\mathsf{T}}) & \mathrm{a} = \mathrm{z} \end{cases}. \tag{4.52}$$

We can iteratively solve these fixed-point equations without the need for a matrix inversion. The singular values of $\boldsymbol{H}$, which are required in the iterations, are precomputed. Finally, it is also important to note that the resulting solutions for λ_{x} and λ_{z} in self-averaging EP should be positive. Otherwise, they may lead to an instability of the algorithm and yield incorrect solutions for the cavity variances.

5 Numerical Results

To illustrate our analysis we consider a signal recovery problem from one-bit compressed sensing, see [85] and the references therein. Specifically, the signal model reads

$$\boldsymbol{y} = \mathrm{sign}(\boldsymbol{H}\boldsymbol{x}) \tag{4.53}$$

where the entries of $\boldsymbol{x}$ are drawn independently from a standard Bernoulli-Gaussian, specifically, with a prior pdf of the *spike and slab* form

$$f(\boldsymbol{x}) = (1-\rho)\delta(\boldsymbol{x}) + \rho\mathcal{N}(\boldsymbol{x}|\boldsymbol{0}, \tau\mathbf{I}). \tag{4.54}$$

We restrict ourselves to simulated data. We consider two classical random matrix models in compressed sensing:

(i) the entries of $\boldsymbol{H} \in \mathbb{R}^{N\times K}$ are iid Gaussian with zero mean and variance $1/K$;

(ii) a random row-orthogonal model [9, 10, 74], where the rows of $\boldsymbol{H}$ are drawn from a randomly permuted discrete cosine transform (DCT) matrix. Specifically, $\boldsymbol{H} = \boldsymbol{P}_\alpha(\boldsymbol{P}_\pi \boldsymbol{\Psi} \boldsymbol{P}_\pi^\dagger)$ where $\boldsymbol{P}_\alpha \in \{0,1\}^{N\times K}$ with ones on the diagonal and zeros elsewhere, $\boldsymbol{P}_\pi$ is a $K \times K$ permutation matrix associated with the permutation π which is drawn uniformly from the set of permutations $(1, \cdots, K) \to (1, \cdots, K)$ and $\boldsymbol{\Psi}$ is the $K \times K$ DCT matrix.

To solve the EP and self-averaging EP fixed-point equations we consider AMP-like iterative equations. Specifically, the iterative equations (4.23)-(4.25) are common to EP and self-averaging EP. The iterative equations for the cavity variances $[\mathbf{V}_\mathrm{x}(t)]_{ii}$ and $[\mathbf{V}_\mathrm{z}(t)]_{jj}$ in EP are readily obtained from (4.31), see Appendix E. The cavity variances in self-averaging EP, i.e. $[\mathbf{V}_\mathrm{x}(t)]_{ii} = v_\mathrm{x}(t)$ and $[\mathbf{V}_\mathrm{z}(t)]_{jj} = v_\mathrm{z}(t)$, are updated according to

$$v_\mathrm{z}(t) = \left(\frac{1}{\langle \boldsymbol{\chi}_\mathrm{x}(t)\rangle} - v_\mathrm{x}(t-1)\right) \mathrm{S}_{\boldsymbol{H}\boldsymbol{H}^\dagger}\left(-\frac{v_\mathrm{x}(t-1)\langle \boldsymbol{\chi}_\mathrm{x}(t)\rangle}{\alpha}\right) \tag{4.55}$$

$$v_\mathrm{x}(t) = \frac{\alpha(1 - v_\mathrm{z}(t)\langle \boldsymbol{\chi}_\mathrm{z}(t)\rangle)}{\langle \boldsymbol{\chi}_\mathrm{x}(t)\rangle}. \tag{4.56}$$

For random matrix model (i) we have

$$\mathrm{S}_{\boldsymbol{H}\boldsymbol{H}^\dagger}(z) = \frac{1}{1+\alpha z} \tag{4.57}$$

and thereby $v_\mathrm{z}(t) = 1/\langle \boldsymbol{\chi}_\mathrm{x}(t)\rangle$. Hence, we have exactly the AMP algorithm, see (4.28). For random matrix model (ii) we have $\boldsymbol{H}^\dagger\boldsymbol{H} = \mathbf{I}$ and thereby

$$\mathrm{S}_{\boldsymbol{H}\boldsymbol{H}^\dagger}(z) = 1. \tag{4.58}$$

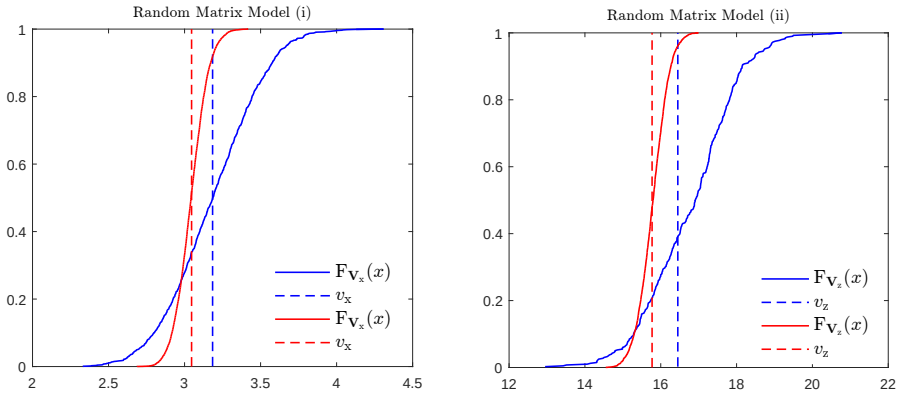

Fig. 4.1: Empirical cumulative distribution function of the cavity variances. The dimensions of $\boldsymbol{H}$ are $K/3 \times K$, $\rho = 0.1$ and $\tau = 1$. Blue curves are for $K = 1200$ and red curves are for $K = 9600$. The quantities v_x and v_z are obtained from the stable solutions of self-averaging EP.

Figure 4.1 illustrates the convergence of the empirical distributions of the cavity variances i.e. the diagonal entries of $\mathbf{V}_x$ and $\mathbf{V}_z$, e.g.

$$\mathrm{F}_{\mathrm{v_x}}(x) = \frac{1}{K} \left| \{ v \in \{ [\mathbf{V}_x]_{ii} : \forall i \} : v \leq x \} \right|, \tag{4.59}$$

as the dimensions of the system increase. The numerical results show that the cavity variances converge towards their self-averaging EP values as the system dimensions increase.

In Figure 4.2, we compare the performance of EP and self-averaging EP through their mean square error in predicting the signals. The results show that both algorithms provide the same performance, but the latter is outstandingly less complex than the former.

The provided algorithm for EP is naive and it has poor convergence because it requires a proper iterative scheme for solving a *large number of variables*, i.e. the diagonal entries of $\boldsymbol{\Lambda}_x$ and $\boldsymbol{\Lambda}_z$, instead of two scalars as in self-averaging EP, i.e. λ_x and λ_z. One may need to adaptively select the initialization of the EP algorithm to the given parameter values of the system model. On the other hand, self-averaging EP shows excellent convergence for both random matrix models. This can be explained as follows. Recall first that self-averaging EP for random matrix model (i) coincides with AMP, which is known to have fast convergence. Moreover, we can consider that random matrix model (ii) *asymptotically* behaves as an $N \times K$ corner of a (real) Haar matrix with $N, K \to \infty$. It is known that the entries of a Haar matrix have zero mean with variance $1/K$, but they are (weakly) correlated, see Lemma 2.1. In other words, random matrix model (ii) has statistical characteristics approximately similar to those of model (i). Figure 4.2 also confirms

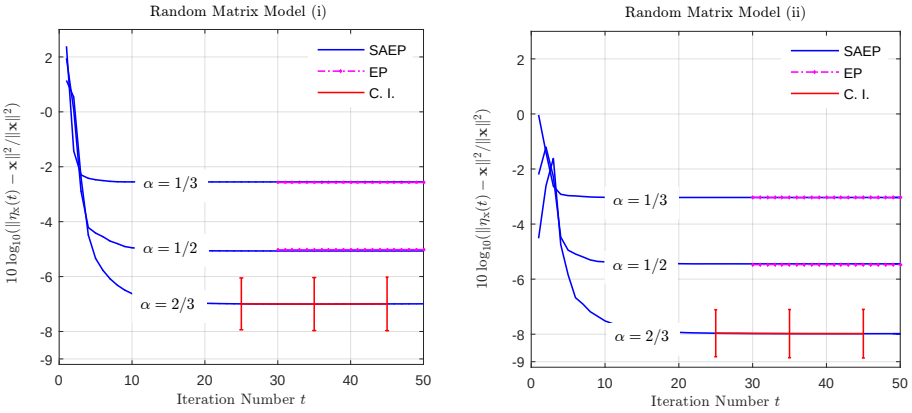

Fig. 4.2: Mean square error of EP and self-averaging EP (SAEP) versus number of iterations: $\boldsymbol{H}$ has dimensions $\alpha 1200 \times 1200$, $\rho = 0.1$ and $\tau = 1$. The reported figures are empirical averages over 100 and 1000 trials for $\alpha \in \{1/3, 1/2\}$ and $\alpha = 2/3$ respectively. C.I. denotes the confidence interval in dB.

this similarity: both algorithms show similar performance for both models. Thereby, it is reasonable to expect that self-averaging EP for matrix model (ii) with iterative equations similar to AMP exhibits a good convergence behavior as well. A similar trick is used in a linear compressed sensing problem in our contribution [86].

6 Conclusions

We have investigated the problem of approximate inference using EP for large systems. EP applied to large systems requires tremendous computational complexity. We have introduced a theoretical framework – called self-averaging EP – that transforms the large-system challenge into an opportunity provided the underlying transformation matrix fulfills certain asymptotic freeness conditions. Self-averaging EP extends AMP – whose optimality is valid only for the classical iid random matrix ensemble – to a general class of random matrix ensembles. We have restricted ourselves to cases where the random matrix ensemble is known explicitly. This is typically the case for applications in compressed sensing. But we expect that self-averaging EP can be applied to a large class of models in which latent variables equally contribute in a statistical sense to the data. It would then be important to have an estimator of the R-transform (or the S-transform) that is computationally more efficient than the simple one in (4.52). This estimator could e.g. be based on spectral moments $\mathrm{Tr}((\boldsymbol{H}^\dagger \boldsymbol{H})^k)$ up to some order, see Subsection 4.2 of Chapter 2.

Chapter 5

A Theory of Solving the TAP Equations for the Ising Model

This chapter is based directly on

Manfred Opper, Burak Çakmak and Ole Winther, "A theory of solving TAP equations for Ising model with general invariant random matrices," Journal of Physics A: Mathematical and Theoretical, vol. 49, no. 11, February 2016,

1 Introduction

While the TAP fixed point equations can be derived in a systematic way by combining EP and free probability frameworks, it is not necessarily clear how the resulting system of nonlinear equations can be solved efficiently. A naive algorithm based on a simple iteration of the equations usually fails to achieve convergence. This problem has been addressed in a paper by Bolthausen for the case of the SK model [33]. He has analyzed the dynamics of the iterations rigorously and shown how the iterations can be altered to achieve exponential convergence (above the AT line of stability). Other ideas to arrive at a convergent method are based on taking the asymptotic limit of dense coupling matrices in BP algorithms, see [22], [23], and [24], (for rigorous analyses [87] and [88]). Unfortunately, in this approach, it is necessary to augment the original variables by auxiliary ones, such that the interactions in the new model are independent. For example, the Hopfield model can be represented by a bipartite graph of Ising spins and continuous variables. It is not clear how such a method should be set up for a matrix of interactions

with more general statistical dependencies. Also, AMP – which is valid for problems involving a sparse coupling matrix – will not always lead to the correct algorithms for dense coupling matrices. Here we will construct a theory for the dynamics of iterative algorithms using dense coupling matrices as the starting point.

In this chapter, we will address the problem of solving TAP equations for the Ising model with an arbitrary invariant random coupling matrix. Our analysis is based on the dynamical functional theory which allows for studying the dynamics of iterative algorithms in the large-system limit by a suitable average over the coupling matrix ensemble. It turns out that by including certain memory terms in the iteration, the effective field in the dynamics becomes a simple Gaussian random variable suggesting that the algorithm might converge. The explicit form of the memory terms depends on the coupling matrix ensembles. We show that our method reproduces previous convergent algorithms for SK and Hopfield models. We also work out the details of our theory for the spin model with orthogonal random coupling matrix [6], [66]. Simulations of the resulting algorithms show exponential convergence above a line of stability which can be identified with the so-called AT line.

The chapter is organized as follows. In Section 2 we introduce the general random matrix formulation for the TAP equations. In Section 3 we present the results of the dynamical functional theory. In Section 4, we introduce "the single-step memory construction" based iterative algorithm for solving the TAP equations. Section 5 is devoted to the derivation of the AT stability condition. Conclusions are outlined in Section 6. Lengthy technical derivations are deferred to Appendix D.

2 Invariant Random Matrices

We consider the standard Ising model with pairwise interactions given by the Gibbs distribution for the spins $\boldsymbol{x} = (x_1, \ldots, x_N)$ (see e.g. [26, 27])

$$f(\boldsymbol{x}) = \frac{1}{Z} \exp\left[\sum_{i<j}^{N} J_{ij} x_i x_j + h \sum_{i=1}^{N} x_i\right] \tag{5.1}$$

with Z denoting the normalization constant. We are interested in the case, where J_{ij}, $i < j$ are random and identically distributed but not necessarily independent. A mathematically simple way for defining such entries is via invariant matrix ensembles: let the $N \times N$ matrix $\tilde{\boldsymbol{J}} = \tilde{\boldsymbol{J}}^{\dagger}$ be invariant. Then, we define the random coupling matrix $\boldsymbol{J}$ with entries

$$J_{ij} = \begin{cases} \beta \tilde{J}_{ij} & i \neq j \\ 0 & i = j \end{cases} . \tag{5.2}$$

In (5.2) we have included an inverse temperature factor β in the definition. The coupling matrices of the standard SK and Hopfield models can be defined as above: in the first case $-\tilde{\boldsymbol{J}}$ is the Gaussian Wigner matrix, in the second case $-\tilde{\boldsymbol{J}}$ is the null Wishart matrix. We assume that $\tilde{\boldsymbol{J}}$ has uniformly bounded spectral norm and a LED in the large-system limit. Thereby, the diagonal elements of $\tilde{\boldsymbol{J}}$ converge to the same deterministic limit as $N \to \infty$, see Theorem 2.1. This implies that we can treat $\boldsymbol{J}$ as asymptotically invariant.

2.1 The asymptotic Itzykson-Zuber integral

We will later need the asymptotic Itzykson-Zuber integral

$$\lim_{N\to\infty} \frac{1}{N} \ln \left\langle e^{\frac{N}{2}\mathrm{tr}(\boldsymbol{Q}\boldsymbol{J})} \right\rangle_{\boldsymbol{J}} = \frac{1}{2} \sum_{n=1}^{\infty} \frac{c_n}{n} \mathrm{tr}(\boldsymbol{Q}^n) \tag{5.3}$$

whenever the right-hand side of (5.3) exists, see Subsection 2.5 of Chapter 2. Here, $\boldsymbol{Q} = \boldsymbol{U}\boldsymbol{\Lambda}\boldsymbol{U}^\dagger$ is $N \times N$ dimensional with the matrices $\boldsymbol{U}$ and $\boldsymbol{\Lambda}$ being orthogonal and diagonal, respectively, and has an asymptotically finite rank. Moreover, c_n is the nth order free cumulant of the LED of $\boldsymbol{J}$. To keep the notation short, in this chapter we denote the R-transform (see Section 4 of Chapter 2) of the LED of $\boldsymbol{J}$ by R. At this stage we first point out the simple identity

$$\mathrm{R}(\omega) = \beta \tilde{\mathrm{R}}(\beta\omega) - \beta \tilde{c}_1. \tag{5.4}$$

In this expression $\tilde{\mathrm{R}}$ denotes the R-transform of the LED of $\tilde{\boldsymbol{J}}$ and $\tilde{c}_1 = \tilde{\mathrm{R}}(0)$. We next provide the explicit form of $\mathrm{R}(\omega)$ for the SK, Hopfield and random orthogonal [6] models:

(i) SK model: $\tilde{\boldsymbol{J}}$ is a Gaussian Wigner matrix, i.e. its entries are iid Gaussian with zero mean and variance β^2/N. In this case, we have $\phi(\tilde{\boldsymbol{J}}) = 0$, so that $\mathrm{R}(\omega) = \tilde{\mathrm{R}}(\omega) = \beta^2\omega$ [12].

(ii) Hopfield model: $\tilde{\boldsymbol{J}} = -\boldsymbol{H}^\dagger\boldsymbol{H}$ where $\boldsymbol{H}$ is an $(N/\alpha) \times N$ matrix whose entries are iid and Gaussian with zero mean and variance α/N, i.e. $(-\tilde{\boldsymbol{J}})$ is a null Wishart matrix whose LED is the Marčenko-Pastur distribution. By invoking the R-transform of the Marčenko-Pastur distribution, we then have

$$\mathrm{R}(\omega) = \frac{\beta^2\alpha\omega}{1+\beta\alpha\omega}. \tag{5.5}$$

(iii) Random orthogonal model: $\tilde{\boldsymbol{J}} = \boldsymbol{O}^\dagger\boldsymbol{\Lambda}\boldsymbol{O}$. The diagonal entries of the diagonal matrix $\boldsymbol{\Lambda}$ are composed of ± 1 such that $\phi(\boldsymbol{\Lambda}) = 0$. One can easily show that

$$\mathrm{R}(\omega) = \frac{-1+\sqrt{1+4\beta^2\omega^2}}{2\omega}. \tag{5.6}$$

2.2 TAP equations for general invariant coupling matrices

TAP equations form a set of self-consistent equations for the vector of magnetizations $\boldsymbol{m} = \langle \boldsymbol{x} \rangle$ where the brackets denote expectation with respect to the Gibbs distribution (5.1). For invariant ensembles, they have been conjectured in [6]. Note also that in Chapter 4 we generalized the TAP equations for the general probabilistic model (4.3) by combining EP and free probability framework. The resulting TAP equations for the Ising model (5.1) read [6]

$$\boldsymbol{m} = \tanh(\boldsymbol{\psi}) \tag{5.7a}$$

$$\boldsymbol{\psi} = \boldsymbol{h} + \boldsymbol{J}\boldsymbol{m} - \mathrm{R}(1-q)\boldsymbol{m} \tag{5.7b}$$

where $q \triangleq \frac{1}{N}\boldsymbol{m}^\intercal \boldsymbol{m}$ and $h_i = h, \forall i$[1] is the non-random external field. Note, that the only dependency on the random matrix ensemble is via the R-transform $\mathrm{R}(1-q)$ in the so-called Onsager term which is a correction to the naive mean field term $\boldsymbol{J}\boldsymbol{m}$. One can show that $\boldsymbol{\psi}$ is the vector of means of the cavity field. Furthermore, following the calculations of [81] one finds using a "replica-symmetric ansatz" that ψ_i is Gaussian distributed (in the large-system limit) with respect to the (random) coupling matrix $\boldsymbol{J}$ with mean h and variance

$$\left\langle (\psi_i - h)^2 \right\rangle \simeq q\mathrm{R}'(1-q). \tag{5.8}$$

Hence, subtracting the Onsager term $\mathrm{R}(1-q)\boldsymbol{m}$ from the mean field $\boldsymbol{J}\boldsymbol{m}$ makes the difference Gaussian. We will next transfer the idea of a Gaussian field from the static solutions to the dynamics of an algorithm.

3 Results from Dynamical Functional Theory

Dynamical properties of disordered systems can be computed by the method of dynamical functionals [30]. In the large-system limit (in the thermodynamic limit, more precisely) this method provides us with *exact* results for the marginal distribution of the trajectory of a single variable (in our case a magnetization $m_i(t)$) when we define a dynamical system that solves the TAP equations. As a typical result of such a calculation, one finds that the "field" $\boldsymbol{J}\boldsymbol{m}(t)$ becomes a sum of a Gaussian term and a memory term which includes the magnetizations at all previous times. This memory often makes the dynamical disordered systems highly complex allowing e.g. for a persistent dependency on the initial conditions and thus a failure to converge to a unique fixed point. Hence, we propose to introduce *explicit* memory terms which are chosen to cancel the *implicit* memory terms derived from the dynamical functional theory. In such a way, at each time step, the update of the magnetization computed by the algorithm involves a Gaussian

[1] As a matter of fact in our derivations we do not consider the restriction $h_i = h, \forall i$.

distributed random field only and we expect that we might obtain good convergence results. This Gaussian property of the effective dynamical field was already shown for a Hopfield model in [22] and [23] (and proved in [87]) and reappeared in Bolthausen's iterative construction of solutions to the TAP equations for the SK model in [33].

We start with defining a set of dynamical equations which could serve as a candidate algorithm for solving the TAP equations (5.7). For $\tau = 0, \dots, t$ let us define

$$\boldsymbol{m}(t) = f_t\left(\{\boldsymbol{\gamma}(\tau), \boldsymbol{m}(\tau)\}_{\tau=0}^{t-1}\right) \tag{5.9a}$$

$$\boldsymbol{\gamma}(t) = \boldsymbol{h} + \boldsymbol{J}\boldsymbol{m}(t). \tag{5.9b}$$

Clearly, $\boldsymbol{m}(t)$ depends on the field $\boldsymbol{J}\boldsymbol{m}(t)$ and the previous local magnetizations $\boldsymbol{m}(\tau)$. Here f_t is an appropriate sequence of nonlinear scalar functions. Our goal is to get the statistics of a single trajectory of (5.9), when $\boldsymbol{J}$ is a random matrix with generating function (5.3). To do so, we make use of the dynamical functional theory as described in [31, 32] which is a discrete time version of the method of [30]. We also refer the reader to [89] where the dynamical functional theory was used to analyze the AMP algorithm in the context of the CDMA communication.

We introduce the generating functional corresponding to the dynamical equations (5.9) as

$$Z(\{\boldsymbol{l}(t)\}) = \int \prod_{t=0}^{T-1} \Big\{ \delta\left(\boldsymbol{m}(t) - f_t\left(\{\boldsymbol{\gamma}(\tau), \boldsymbol{m}(\tau)\}_{\tau=0}^{t-1}\right)\right) \\ \delta(\boldsymbol{\gamma}(t) - \boldsymbol{h} - \boldsymbol{J}\boldsymbol{m}(t)) e^{i\boldsymbol{\gamma}(t)^\dagger \boldsymbol{l}(t)}\, \mathrm{d}\boldsymbol{m}(t)\mathrm{d}\boldsymbol{\gamma}(t)\Big\}. \tag{5.10}$$

Notice that $Z(\{\boldsymbol{l}(t) = \boldsymbol{0}\}) = 1$. Thus, the statistics of the variables can be computed from the averaged generating functional $\langle Z(\{\boldsymbol{l}(t)\})\rangle_{\boldsymbol{J}}$. By making use of the asymptotic Itzykson-Zuber integral (5.3) and the saddle-point method (see [90, Section 4.3]) we obtain in Appendix D.1 that

$$\langle Z(\{\boldsymbol{l}(t)\})\rangle_{\boldsymbol{J}} = \prod_{n=1}^{N} \int \mathrm{d}\mathcal{N}(\{\phi_n(t)\}; 0, \mathcal{C}_\phi) \prod_{t=0}^{T-1} \Big\{ \delta(m_n(t) - f_t\left\{m_n(\tau), \gamma_n(\tau)\right\}_{\tau=0}^{t-1}) \\ \delta\left(\gamma_n(t) - h_n - \sum_{s<t} \hat{\mathcal{G}}(t,s) m_n(s) - \phi_n(t)\right) e^{i\gamma_n(t) l_n(t) + O(N^{-1})}\, \mathrm{d}m_n(t)\mathrm{d}\gamma_n(t) \Big\}. \tag{5.11}$$

This result shows that as N tends to infinity, the trajectories can be treated as independent stochastic dynamical processes described by the following

equations

$$\boldsymbol{m}(t) = f_t\left(\{\boldsymbol{\gamma}(\tau), \boldsymbol{m}(\tau)\}_{\tau=0}^{t-1}\right) \tag{5.12}$$

$$\boldsymbol{\gamma}(t) = \boldsymbol{h} + \sum_{\tau=0}^{t-1} \hat{\mathcal{G}}(t,s)\boldsymbol{m}(\tau) + \boldsymbol{\phi}(t)\ . \tag{5.13}$$

Here $\boldsymbol{\phi}(t)$ is a vector of independent Gaussian random variables with covariance matrix $\mathcal{C}_\phi$ given by

$$\mathcal{C}_\phi = \sum_{n=1}^{\infty} c_n \sum_{k=0}^{n-2} \mathcal{G}^k \mathcal{C} (\mathcal{G}^\intercal)^{n-2-k} \tag{5.14}$$

where $\mathcal{G}$ and $\mathcal{C}$ are the $T \times T$ response and correlation matrices, respectively. With slight abuse of notation, their $(t+1, \tau+1)$th entries are given by

$$\mathcal{G}(t,\tau) = \frac{1}{N}\sum_{i=1}^{N} \left\langle \frac{\partial m_i(t)}{\partial \phi_i(\tau)} \right\rangle_{\phi_i} \tag{5.15}$$

$$\mathcal{C}(t,\tau) = \frac{1}{N}\sum_{i=1}^{N} \langle m_i(t) m_i(\tau)\rangle_{\phi_i}\,. \tag{5.16}$$

The random matrix ensemble $\boldsymbol{J}$ enters the right-hand terms in (5.15) and (5.16) through the free cumulants c_n, and the memory matrix $\hat{\mathcal{G}}$

$$\hat{\mathcal{G}} = \mathrm{R}(\mathcal{G}). \tag{5.17}$$

So far we have not yet referred to the TAP equations in the dynamical functional theory analysis. Instead, we have considered a somewhat general dynamical system with disorder and memory. Such a formulation gives us enough freedom to construct convenient dynamical equations which asymptotically converges to the solution of the TAP equations. We will define the dynamical equations to be of the form

$$\boldsymbol{m}(t+1) = \tanh(\boldsymbol{\psi}(t)) \tag{5.18}$$

where the variables $\psi_i(t)$ must be chosen to become independent Gaussian fields in the resulting effective single variable dynamical equations (5.13). There are actually various methods for doing this. In the sequel, we will limit our attention to a method that we call the *single-step memory* construction.

4 Single-Step Memory Construction

In the single-step memory algorithm, we construct the update in such a way that the resulting memory matrix (5.17) satisfies the equation

$$\hat{\mathcal{G}}(t,\tau) = 0,\ \forall \tau \neq t-1. \tag{5.19}$$

Hence, if (5.19) holds, then using (5.13) we find that the vector

$$\gamma(t) - \hat{\mathcal{G}}(t, t-1)\boldsymbol{m}(t-1) = \boldsymbol{\phi}(t) + \boldsymbol{h} \tag{5.20}$$

becomes a Gaussian field. We will choose the field $\boldsymbol{\psi}(t)$ in (5.18) to be a linear combination of the Gaussian fields $\boldsymbol{\phi}(\tau)$, $\tau = 1, \ldots, t$, i.e.

$$\boldsymbol{\psi}(t) = \sum_{\tau=0}^{t} \mathcal{A}(t+1, \tau)(\boldsymbol{\phi}(\tau) + \boldsymbol{h}). \tag{5.21}$$

We have to construct the non-random terms $\mathcal{A}(t+1, \tau)$ to make the dynamical order parameters consistent with the single-step memory condition (5.19). From (5.18) we obtain for the response function (5.15)

$$\mathcal{G}(t, \tau) = \frac{1}{N} \sum_i \left\langle (1 - m_i^2(t)) \frac{\partial \psi_i(t-1)}{\partial \phi_i(\tau)} \right\rangle \tag{5.22}$$

$$= (1 - q(t))\mathcal{A}(t, \tau) \tag{5.23}$$

with $q(t) \triangleq \frac{1}{N}\boldsymbol{m}(t)^\intercal \boldsymbol{m}(t)$. Thus we have the explicit result

$$\mathcal{A}(t, \tau) = \frac{\mathcal{G}(t, \tau)}{1 - q(t)}. \tag{5.24}$$

Finally, using (5.17) we get an explicit result for the response function in terms of the memory terms $\hat{\mathcal{G}}(t, t-1)$. Note that by construction of the single-step memory matrix $\hat{\mathcal{G}}$ (5.19) we can write (5.17) as

$$\mathcal{G}(t, \tau) = a_{t-\tau} \prod_{s=\tau+1}^{t} \hat{\mathcal{G}}(s, s-1) \tag{5.25}$$

where the coefficients a_n are obtained from the power series expansion of the composition inverse of the R-transform of the LED of $\boldsymbol{J}$:

$$\mathrm{R}^{-1}(z) = \sum_{n=1}^{\infty} a_n z^n. \tag{5.26}$$

By definition the trace of $\boldsymbol{J}$ is zero, i.e. $\mathrm{R}(0) = 0$. Hence, the power series expansion in (5.26) starts from the first order term.

To complete the specification of the single-step memory construction we only need to specify $\hat{\mathcal{G}}(t, t-1)$. This will be done in such a way the method is asymptotically consistent with the static TAP equations. Specifically, from (5.7b) we have

$$\lim_{t \to \infty} \hat{\mathcal{G}}(t, t-1) = \mathrm{R}(1 - q). \tag{5.27}$$

We choose the explicit form

$$\hat{\mathcal{G}}(t,t-1) = \frac{1-q(t)}{1-q(t-1)}\mathrm{R}(1-q(t-1)). \tag{5.28}$$

By assuming $q(t) \to q$ as $t \to \infty$, (5.28) leads to (5.27) as $t \to \infty$. This form has also the advantage that in (5.24) an unwanted factor $1-q(t)$ – which would make $\boldsymbol{\psi}(t-1)$ depending on the future state $\boldsymbol{m}(t)$ – cancels.

4.1 Summary

Putting everything together the single-step memory algorithm for $t \geq 0$ is defined as follows:

$$\boldsymbol{m}(t+1) = \tanh(\boldsymbol{\psi}(t)) \tag{5.29}$$

$$\boldsymbol{\psi}(t) = Q(t)\sum_{\tau=0}^{t} a_{t+1-\tau}\boldsymbol{u}(\tau) \tag{5.30}$$

$$\boldsymbol{u}(t) = \frac{\boldsymbol{h} + \boldsymbol{J}\boldsymbol{m}(t) - \hat{\mathcal{G}}(t,t-1)\boldsymbol{m}(t-1)}{Q(t-1)(1-q(t))} \tag{5.31}$$

where the coefficients a_n are obtained from the power series (5.26) and we introduce

$$Q(t) = \prod_{\tau=0}^{t}\mathrm{R}(1-q(\tau)) = Q(t-1)\mathrm{R}(1-q(t)) \tag{5.32}$$

such that $Q(-1) = 1$. The memory term $\hat{\mathcal{G}}(t,t-1)$ is given by (5.28). Moreover, the algorithm initializes with $\boldsymbol{m}(t) = \boldsymbol{0}$ for $t \in \{-1, 0\}$.

4.2 Asymptotic consistency with the TAP equations

We next show that if the single-step memory algorithm (5.29)-(5.31) converges, it solves the TAP equations (5.7). Let us first assume that $\boldsymbol{m}(t) \to \boldsymbol{m}$ as $t \to \infty$. To have the convergence to the TAP equations we solely need to show that the sum in (5.30) converges to the proper limit. From (5.21) and (5.24) we must have

$$Q(t)\sum_{\tau=0}^{t}\frac{a_{t+1-\tau}}{(1-q(\tau))Q(\tau-1)} = \frac{1}{1-q(t+1)}\sum_{\tau=0}^{t}\mathcal{G}(t+1,\tau) \to 1. \tag{5.33}$$

We make the so-called weak long-term response assumption [91] that

$$\lim_{t\to\infty}\mathcal{G}(t,\tau) = 0, \quad \forall \text{ finite } \tau. \tag{5.34}$$

Thus, for sufficiently large t and $\tau' < t$ while $t/\tau' = O(1)$, we can write

$$\sum_{\tau=0}^{t} \mathcal{G}(t+1,\tau) \simeq \sum_{\tau=\tau'}^{t} \mathcal{G}(t+1,\tau) \tag{5.35}$$

$$\simeq \sum_{\tau=\tau'}^{t} a_{t+1-\tau} \mathrm{R}\,(1-q)^{t+1-\tau} \tag{5.36}$$

$$\simeq \sum_{n=1}^{\infty} a_n \mathrm{R}(1-q)^n \tag{5.37}$$

$$= \mathrm{R}^{-1}(\mathrm{R}(1-q)) = 1-q. \tag{5.38}$$

Next we provide the details of the single-step memory algorithm for the SK, Hopfield and random orthogonal models.

4.3 Example 1 – SK model

Recall that, for the standard SK model we have $\mathrm{R}(\omega) = \beta^2\omega$ so that $\mathrm{R}^{-1}(z) = z/\beta^2$. Hence, $a_1 = 1/\beta^2$ and $a_n = 0$ for $n > 1$. Thus, the single-step memory algorithm may be written as

$$\boldsymbol{m}(t+1) = \tanh(\boldsymbol{\psi}(t)) \tag{5.39}$$

$$\boldsymbol{\psi}(t) = \boldsymbol{h} + \boldsymbol{J}\boldsymbol{m}(t) - \beta^2(1-q(t))\boldsymbol{m}(t-1). \tag{5.40}$$

At first glance, these dynamical equations are similar but not exactly equal to those proposed by Bolthausen [33]. The difference is that instead of the dynamical order parameter $q(t)$ the fixed point solution of q appears. Using the explicit form of the covariance of the field $\psi_i(t)$ given by (5.54) in the next section, one finds for the field variance $\langle(\psi_i(t) - \langle\psi_i(t)\rangle)^2\rangle = \beta^2 q(t)$. Hence, if we start the iteration (as in [33]) with $m_i(1) = \sqrt{q}$ such that $q(1) = q$, then we find that in the large N limit, we also have $q(t) = \left\langle \tanh^2(\psi_i(t-1)) \right\rangle = q$ for all times t and we get the agreement with [33].

4.4 Example 2 – Hopfield model

For the Hopfield model from (5.5), we have

$$\mathrm{R}^{-1}(z) = \frac{1}{\beta\alpha}\frac{z}{\beta - z}. \tag{5.41}$$

Thus, the memory coefficients are given as $a_n = 1/(\alpha\beta^{n+1})$ for $n \geq 1$. In the sequel we show that the single-step memory algorithm for the Hopfield

model coincides with the AMP algorithm [22, 23]. From (5.30) we first write

$$\boldsymbol{\psi}(t) = \frac{Q(t)}{\alpha\beta^2}\boldsymbol{u}(t) + \frac{Q(t)}{\alpha\beta^{t+2}}\sum_{\tau=0}^{t-1}\beta^{\tau}\boldsymbol{u}(\tau) \tag{5.42}$$

$$= \frac{Q(t)}{\alpha\beta^2}\boldsymbol{u}(t) + \frac{1}{\beta}\mathrm{R}(1-q(t))\boldsymbol{\psi}(t-1). \tag{5.43}$$

For convenience we introduce

$$A(t) \triangleq \frac{\mathrm{R}(1-q(t))}{\beta\alpha(1-q(t))} = \frac{\beta}{1+\beta\alpha(1-q(t))}. \tag{5.44}$$

Notice that from (5.31) we may write (5.43) in the form of

$$\boldsymbol{\psi}(t) = \frac{1}{\beta}A(t)[\boldsymbol{h}+\boldsymbol{J}\boldsymbol{m}(t)] + \alpha(1-q(t))A(t)[\boldsymbol{\psi}(t-1) - A(t-1)\boldsymbol{m}(t-1)]. \tag{5.45}$$

Then, defining $\boldsymbol{z}(t) \triangleq \boldsymbol{\psi}(t) - A(t)\boldsymbol{m}(t)$, we write the single-step memory algorithm as

$$\boldsymbol{m}(t+1) = \tanh(\boldsymbol{z}(t) + A(t)\boldsymbol{m}(t)) \tag{5.46}$$

$$\boldsymbol{z}(t) = \frac{1}{\beta}A(t)[\boldsymbol{h} + (\boldsymbol{J}-\beta\mathbf{I})\boldsymbol{m}(t)] + \alpha(1-q(t))A(t)\boldsymbol{z}(t-1) \tag{5.47}$$

where $\mathbf{I}$ is the identity matrix of appropriate dimension. Note, that $(\mathbf{I} - \boldsymbol{J}/\beta)$ asymptotically coincides with the null-Wishart matrix (see Section 2). Thereby, we exactly obtain the AMP algorithm as introduced in [22]. We also refer the reader to the related works [87] and [89], where the dynamics of the AMP algorithm is analyzed by means of dynamical functional theory and Bolthausen's conditioning technique [33], respectively.

Bolthausen's conditioning technique for the SK model [33] and the Hopfield model [87] are based on the assumption that the entries of the underlying coupling matrix are defined via zero-mean iid and *Gaussian distributed* random variables, see Subsection 2.1. Recently, it has been shown in [88] that the same analyses can be obtained with the *Gaussian distribution* assumption relaxed by a sub-Gaussian tail condition on the distribution. Indeed, by invoking the central limit theorem, one can show that the generating function (5.3) also yields the same result regardless of whether the *Gaussian distribution* assumption is considered or not, see [92, Section 5].

4.5 Example 3 – Random orthogonal model

For the random orthogonal model from (5.6) we have $\mathrm{R}^{-1}(z) = z/(\beta^2 - z^2)$. This yields the memory coefficients

$$a_n = \begin{cases} \frac{1}{\beta^{n+1}} & n \text{ is odd} \\ 0 & n \text{ is even.} \end{cases} \tag{5.48}$$

In Figure 5.1 and Figure 5.2 we illustrate the convergence of the single-step memory algorithm for the random orthogonal model obtained by running simulations. Notice that after few iteration steps the convergence becomes exponentially fast. The flat lines around (-300)dB, i.e. 10^{-30}, are the consequence of the machine precision of the computer which was used.

The convergence improves with increasing temperature parameter $1/\beta$. On the other hand, for large enough β, the algorithm fails to converge. To estimate the critical value of β, we study the inverse decay time measured by the angle θ as illustrated in Figure 5.3 and extrapolate the simulational data to $\theta = 0$ using a suitable range of β. One might expect that the critical value of β would coincide with the one obtained from the Almeida-Thouless (AT) stability condition. The AT line is given by the equation (see (C.34))

$$\alpha \mathrm{R}'(1-q) = 1 \quad \text{with} \quad \alpha \triangleq \frac{1}{N}\sum_{i=1}^{N} \Big\langle (1 - \tanh^2(\psi_i))^2 \Big\rangle \tag{5.49}$$

where the random variable ψ_i is Gaussian with mean h_i and variance $q\mathrm{R}'(1-q)$. In Figure 5.3 we present a comparison between the simulation results and (5.49). The observed coincidence can be understood from a dynamical point of view by analyzing the stability of the dynamics close to the fixed point. The details are postponed to Section 5. Finally, it also worth noting that the trajectories of the algorithm show a self-averaging behavior above the AT line. On the other hand, we find that below the AT line, there are strong sample-to-sample fluctuations. However, by averaging the dynamical order parameters over many samples, we get a good agreement with the theory.

4.6 Field covariance matrix

In order to compare simulation results with analytical results obtained from the dynamical functional theory approach and to study the stability of the TAP fixed points, we have to perform expectations over the Gaussian random variables $\psi_i(t)$, see (5.21). Specifically, we write

$$\frac{1}{N}\langle \|\boldsymbol{m}(t) - \boldsymbol{m}(t-1)\|^2 \rangle_{\boldsymbol{J}} \simeq q(t) + q(t-1) - 2\mathcal{C}(t, t-1) \tag{5.50}$$

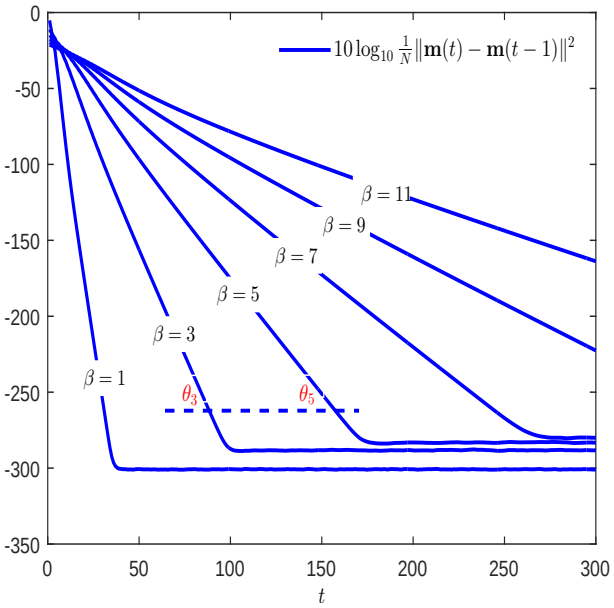

Fig. 5.1: Convergence of the single-step memory algorithm: Random orthogonal model with $\beta \in \{1,3,...,9,11\}$, $h_i = 1$ and $N = 2^{14}$. Here e.g. $\theta \in \{\theta_3, \theta_5\}$ represents the respective linear decay time (in the log-domain), i.e. the convergence is faster the larger θ is.

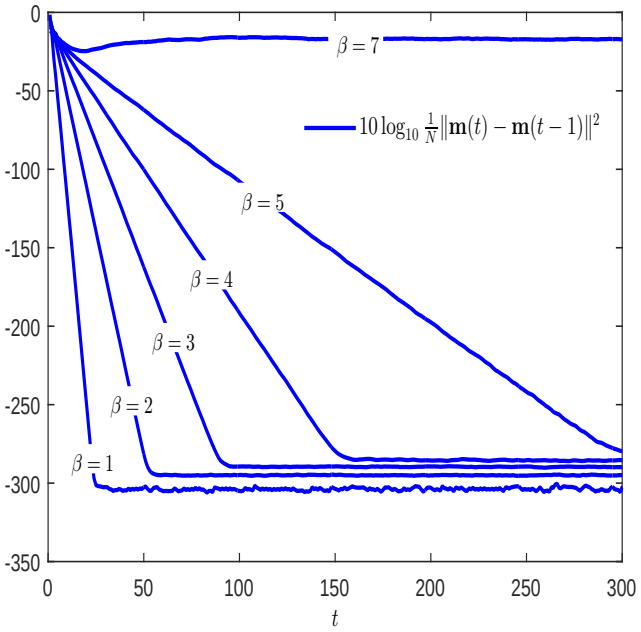

Fig. 5.2: Convergence of the single-step memory algorithm: Random orthogonal model with $\beta \in \{1,...,5,7\}$, $h_i = 2$ and $N = 2^{14}$. The inverse temperature $\beta = 6.9$ gives the AT line.

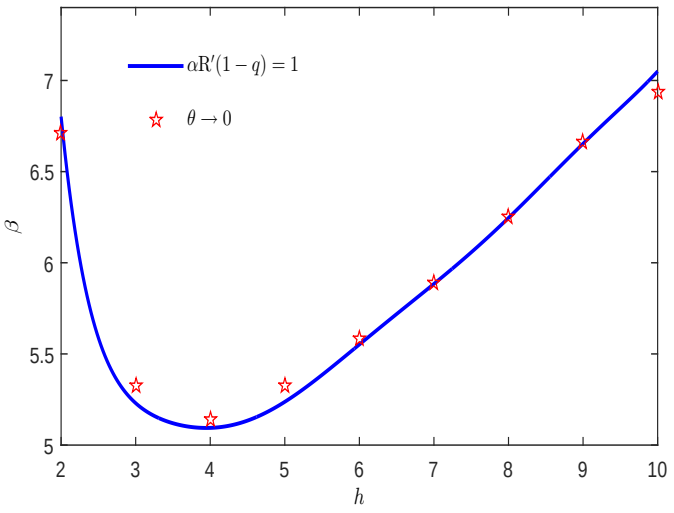

Fig. 5.3: Consistency of the diverging decay time with the AT line: Each simulated point is based on an average over ten realizations of $\boldsymbol{J}$ with $N = 2^{14}$.

where the order parameter $\mathcal{C}$ is given by

$$\mathcal{C}(t+1,t'+1) = \frac{1}{N}\sum_{i=1}^{N}\int \mathrm{dF}(x,y)\ \tanh(\langle\psi_i(t)\rangle + x)\tanh(\langle\psi_i(t')\rangle + y). \tag{5.51}$$

Here F is a two-dimensional Gaussian distribution with zero mean. The mean of the field $\psi_i(t)$ follows from (5.21) to be

$$\langle\psi_i(t)\rangle = \left\{ Q(t)\sum_{\tau=0}^{t}\frac{a_{t+1-\tau}}{(1-q(\tau))Q(\tau-1)}\right\} h_i. \tag{5.52}$$

Hence, we need to compute the corresponding covariance matrix which is defined as

$$\mathcal{C}_\psi(t,t') = \left\langle (\psi_i(t) - \langle\psi_i(t)\rangle)(\psi_i(t') - \langle\psi_i(t')\rangle)\right\rangle. \tag{5.53}$$

In Appendix D. 2 we derive the expression

$$\mathcal{C}_\psi(t,t') = Q(t)Q(t')\sum_{l\le t, m\le t'}\frac{\mathrm{Co}_{x^{t+1-l}y^{t'+1-m}}[\mathrm{A}(x,y)]\mathcal{C}(l,m)}{(1-q(l))(1-q(m))Q(l-1)Q(m-1)}. \tag{5.54}$$

In this expression, for a power series $f(x,y) = \sum_{n,k\ge 0} a_n b_k x^n y^k$, we have introduced the symbol $\mathrm{Co}_{x^n y^k}[f(x,y)] \triangleq a_n b_k$ for its coefficients. Moreover

the function A is defined as

$$\mathrm{A}(x,y) \triangleq \left(\frac{1}{\mathrm{R}^{-1}(x)} - \frac{1}{\mathrm{R}^{-1}(y)}\right)^{-1}(y-x). \tag{5.55}$$

The function A has a relatively simple form for the three random matrix ensembles considered in this chapter. For the SK and Hopfield models $\mathrm{A}(x,y) = xy/\beta^2$ and $\mathrm{A}(x,y) = xy/(\beta^2\alpha)$, respectively. For the random orthogonal model, from $\mathrm{R}^{-1}(x) = x/(\beta^2 - x^2)$ we have $\mathrm{Co}_{x^n y^k}[\mathrm{A}(x,y)] = \delta_{nk}(-1)^{n+1}/\beta^{2n}$. We next compare our simulation results with theoretical results. We used the initializations $\boldsymbol{m}(t) = \mathbf{0}$ for $t \in \{0,1\}$, hence we assign $\mathcal{C}(1,0) = 0$. In Figures 5.4 and 5.5 we show such a comparison above the AT line. Note, that no averaging over coupling matrices was used for the simulations. The integration over a two-dimensional correlated Gaussian distribution used to calculate $\mathcal{C}(t,t-1)$ was performed numerically. However the accuracy of the numerical method limits us from getting very precise results as t grows. In Figure 5.4 we illustrate the theoretical prediction of $\frac{1}{N}\boldsymbol{m}(t)^\intercal \boldsymbol{m}(m-1)$ by the order parameter $\mathcal{C}(t,t-1)$ for a large range of t. Below the AT line, the single-step memory algorithm diverges and simulated trajectories show strong sample-to-sample fluctuations. However, by taking an average over a large number of trajectories we obtain a good agreement with the theory (see Figure 5.6).

4.7 Asymptotic consistency with the cavity variance

In Subsection 4.2 we have demonstrated the convergence of the single-step memory algorithm to the TAP equations. In a similar way, one can show that (5.54) converges to the variance of the static field variance in (5.8) as t and t' tend to infinity. Specifically, by invoking the weak long-term response assumption (5.34) in (5.14) and following similar steps as in Appendix D.2, for sufficiently large t, $\tau < t$, t' and $\tau' < t'$ with $\tau/t = O(1)$ and $\tau'/t' = O(1)$, one can show that

$$\mathcal{C}_\psi(t,t') \simeq \frac{q}{(1-q)^2}\sum_{\tau\le t,\tau'\le t'} \mathrm{Co}_{x^{t+1-\tau}y^{t'+1-\tau'}}[\mathrm{A}(x,y)]\mathrm{R}(1-q)^{t+1-\tau}\mathrm{R}(1-q)^{t'+1-\tau'} \tag{5.56}$$

$$\simeq \frac{q}{(1-q)^2}\sum_{n,k\le 1} \mathrm{Co}_{x^n y^k}[\mathrm{A}(x,y)]\mathrm{R}(1-q)^n\mathrm{R}(1-q)^k \tag{5.57}$$

$$= \frac{q}{(1-q)^2}\mathrm{A}(\mathrm{R}(1-q),\mathrm{R}(1-q)). \tag{5.58}$$

In this expression, by abuse of notation, we denote $\lim_{y\to x}\mathrm{A}(x,y)$ by $\mathrm{A}(x,x)$. Its explicit form is given by

$$\lim_{y\to x}\mathrm{A}(x,y) = (\mathrm{R}^{-1}(x))^2\frac{1}{(\mathrm{R}^{-1}(x))'} = (\mathrm{R}^{-1}(x))^2\mathrm{R}'(\mathrm{R}^{-1}(x)). \tag{5.59}$$

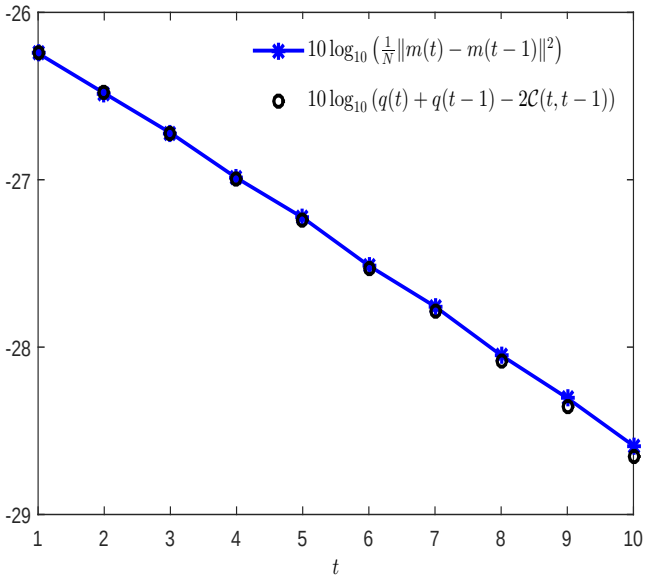

Fig. 5.4: The field covariance matrix above the AT line: Comparison of theoretical and simulation results for $\beta = 20$ and $h_i = 1$, $N = 2^{14}$.

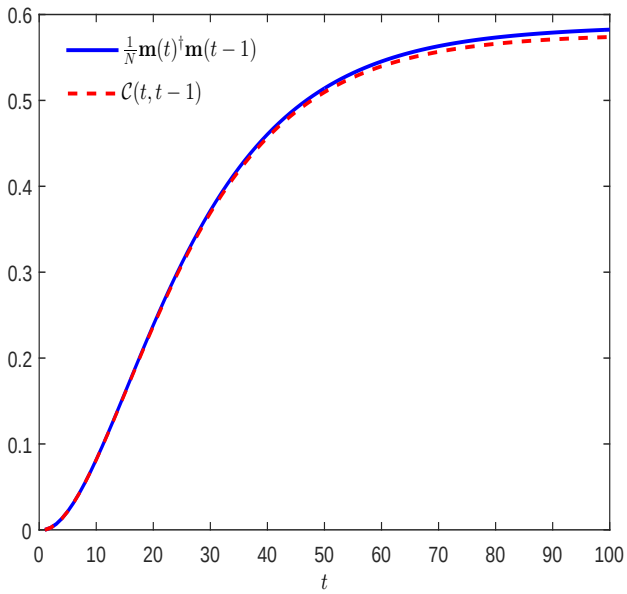

Fig. 5.5: The field covariance matrix above the AT line: Comparison of theoretical and simulation results for $\beta = 20$ and $h_i = 1$, $N = 2^{14}$.

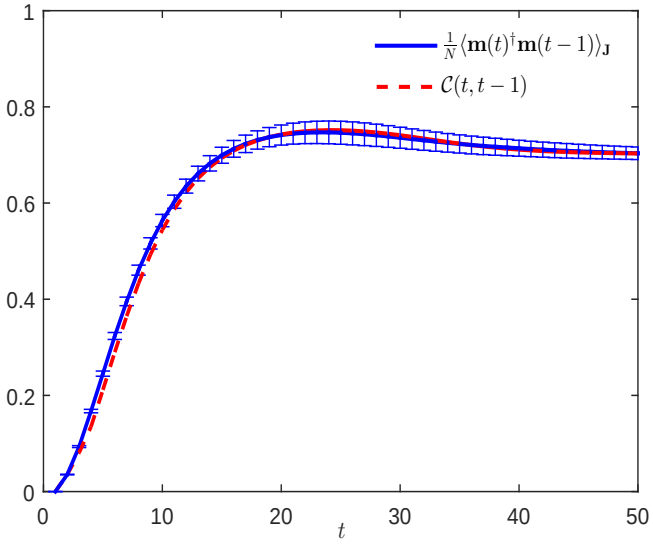

Fig. 5.6: The field covariance matrix below the AT line: Comparison of theoretical and simulation results for $\beta = 10$ and $h_i = 2$, $N = 2^{12}$. $\langle\cdot\rangle_J$ is obtained from 5×10^3 realizations of $\boldsymbol{J}$.

Hence we have

$$\lim_{t,t'\to\infty} \mathcal{C}_\psi(t,t') = \frac{q}{(1-q)^2}(\mathrm{R}^{-1}(\mathrm{R}(1-q)))^2\mathrm{R}'(\mathrm{R}^{-1}(\mathrm{R}(1-q))) \tag{5.60}$$

$$= q\mathrm{R}'(1-q). \tag{5.61}$$

5 Stability of the TAP Fixed Points

In order to analyze the stability of the fixed points of the single-step algorithm, we resort to a linear stability analysis. We add Gaussian white noise to the dynamical equations, i.e. we set $\psi_i(t) \to \psi_i(t) + \epsilon_i(t)$ with $\langle \epsilon_i(t)^2 \rangle = \epsilon$ and discuss the limit $\epsilon \to 0$. If the static TAP fixed points are stable, then the system should asymptotically show only small stationary fluctuations around the static solution so we can work in the Fourier domain. Hence, we assume

$$\mathcal{C}(t,t') = \frac{1}{2\pi}\int \mathrm{d}\omega\, \hat{\mathcal{C}}(\omega) e^{i\omega(t-t')} \tag{5.62}$$

$$\mathcal{C}_\psi(t,t') = \frac{1}{2\pi}\int \mathrm{d}\omega\, \hat{\mathcal{C}}_\psi(\omega) e^{i\omega(t-t')}. \tag{5.63}$$

Inserting into (5.54), for large t and t' we can write (see (5.56)-(5.58))

$$\hat{\mathcal{C}}_\psi(\omega) \simeq \sum_{l\le t, m\le t'} \frac{\mathrm{Co}_{x^{t'+1-l}y^{t'+1-m}}[\mathrm{A}(x,y)]\hat{\mathcal{C}}(\omega)e^{i\omega(l-t-(m-t'))}}{(1-q)^2\mathrm{R}(1-q)^{l-t-1}\mathrm{R}(1-q)^{m-t'-1}} \tag{5.64}$$

$$\simeq \frac{\mathrm{A}(e^{-i\omega}\mathrm{R}(1-q), e^{i\omega}\mathrm{R}(1-q))}{(1-q)^2}\hat{\mathcal{C}}(\omega). \tag{5.65}$$

For small noise $\epsilon \to 0$, the assumption of stability translates into small fluctuations around the static solution and we can write

$$\hat{\mathcal{C}}(\omega) \simeq 2\pi q\delta(\omega) + \epsilon\hat{c}(\omega) \tag{5.66}$$

$$\hat{\mathcal{C}}_\psi(\omega) \simeq 2\pi q\mathrm{R}'(1-q)\delta(\omega) + \epsilon\hat{c}_\psi(\omega) \tag{5.67}$$

where we have separated fluctuations into static and dynamical parts. We analyze the dynamical part next, but note, that also the static q will have contributions from ϵ. Thus for $\omega \neq 0$ we have

$$\hat{c}_\psi(\omega) = \hat{c}(\omega)\frac{\mathrm{A}(e^{-i\omega}\mathrm{R}(1-q), e^{i\omega}\mathrm{R}(1-q))}{(1-q)^2} \tag{5.68}$$

where now the value of q is computed for $\epsilon = 0$. We next express $\hat{c}(\omega)$ in terms of $\hat{c}_\psi(\omega)$ for small ϵ. The calculation in Appendix D.3 is based on the expansion

$$\mathcal{C}(t+1, t'+1) = \frac{1}{N}\sum_i \left\langle \tanh(u(t)+h_i)\tanh(u(t')+h_i)\right\rangle_u \tag{5.69}$$

up to first order in ϵ. The brackets denote expectations over the two dimensional Gaussian field $(u(t), u(t'))$ with $\langle u(t)u(t')\rangle \simeq s_0 + \epsilon(s(t-t') + \delta_{t,t'})$ for $\epsilon \to 0$, where $s_0 = q\mathrm{R}'(1-q)$ and $s(t-t') = c_\psi(t,t')$. For $t = t'$ the integral is over a single Gaussian only. The calculation shows that

$$\hat{c}(\omega) = \alpha(1 + \hat{c}_\psi(\omega)) \tag{5.70}$$

with α defined as in (5.49). Combining this relationship with (C.34) we have

$$\hat{c}(\omega) \simeq \alpha\left(1 - \frac{\alpha\mathrm{A}(e^{-i\omega}\mathrm{R}(1-q), e^{i\omega}\mathrm{R}(1-q))}{(1-q)^2}\right)^{-1}. \tag{5.71}$$

In fact, for the SK, Hopfield and random orthogonal models we have

$$\mathrm{Co}_{x^n y^k}[\mathrm{A}(x,y)] = 0, \quad \forall n \neq k. \tag{5.72}$$

Therefore (5.71) is actually independent of ω and from (5.59) we explicitly have

$$\hat{c}(\omega) = \frac{\alpha}{1 - \alpha\mathrm{R}'(1-q)}. \tag{5.73}$$

In general, the right-hand side of (5.71) must be non-negative to have a valid representation as a Fourier-transform of a time-dependent correlation function. While the term $\mathrm{A}(e^{-i\omega}\mathrm{R}(1-q), e^{i\omega}\mathrm{R}(1-q))$ is always positive, see (5.65), the second term is small and positive for sufficiently small β. But it changes sign and diverges. One expects that the divergence will occur first for the long-range fluctuations, i.e. for the limit of low frequencies. Taking the limit yields

$$\lim_{\omega\to 0} \hat{c}(\omega) = \frac{\alpha}{1-\alpha \mathrm{R}'(1-q)}. \tag{5.74}$$

The condition

$$\alpha \mathrm{R}'(1-q) = 1 \tag{5.75}$$

for the onset of instability agrees with the AT stability criterion.

6 Conclusions

We have presented a theoretical approach to the design of iterative algorithms for solving the TAP equations for the Ising model with random coupling matrix drawn from invariant ensembles. We were guided by the idea that one needs to subtract terms from the internal field which depend on the values of the magnetizations at previous times. Using dynamical functional theory we have shown that in such a way, memory terms can be canceled out and one arrives at a Gaussian distributed field, which eventually converges to the cavity field provided that a stability condition is fulfilled. We have presented a specific method which we have called the single-step memory construction. Our approach may be extended in several ways. For example, other subtraction methods are possible. One might design an alternative scheme, where the response function is required to be zero after one time step leading to a somewhat different algorithm and we will give details elsewhere. It would be interesting to see in which cases the explicit memory terms in the subtraction method can be simplified by introducing auxiliary variables, as is possible for the Hopfield model. Other extensions of our method can be to more general probabilistic models beyond the simple Ising case. This can include continuous random variables and other forms of interactions.

Chapter 6

Conclusions and Outlook

This chapter provides conclusions and an outlook of the thesis from a general perspective. We refer the reader to Section 6 of Chapters 3, 4 and 5 where conclusions related to the specific applications and problems considered in the thesis are presented.

We have addressed three new random matrix problems for information processing. While doing this, we have restricted the considered systems in such a way that their latent variables contribute equally to their Hamiltonian in a statistical sense. Furthermore, for mathematical convenience, we have limited our attention to invariant random matrices or random matrices that admit certain asymptotic freeness conditions when their dimensions grow to infinity. These restrictions have allowed us to understand and/or control the system via certain macroscopic quantities, i.e. quantities which do not make reference to specific variables in the systems. In a word, the many-body problems[1] have been reduced to one-body problems and thereby, the resulting characterizations have turned out to be simple and insightful, yet (apparently) sufficient.

The concept of asymptotic freeness has frequently been used in information theoretical analysis of wireless communication channels. In this contribution, we have shown that asymptotic freeness is a useful and fruitful concept for deriving/designing algorithms as well. We believe that the concept of asymptotic freeness will become a standard tool in the machine learning and signal processing communities for deriving and designing low-complexity algorithms for large systems.

The numerical validations of our framework have been carried out on the basis of simulated data. Therefore, it is an important task to test these results through real data. In particular, this is a significant issue when the random

[1]The many-body problem is a name for physical problems addressing certain properties of microscopic systems with a large number of interacting particles [93].

matrix ensemble models a physical entity. In this case, the real question, of course, is whether the random matrix ensemble accurately models the physical reality. Such a question can only be answered by means of a numerical validation based on real data. We did not address this issue in the thesis and leave it as future work.

From a purely mathematical point of view, the concept of asymptotic freeness may be limiting, since many derivations in which this concept is assumed also require that the involved matrices are invariant and have compactly supported LEDs and/or uniformly bounded empirical eigenvalue distributions. These may be fairly restrictive in practice. However, the ultimate goal in invoking assumptions that imply asymptotic freeness is to apply the additive and multiplicative free convolutions. We also expect that these free convolutions should typically provide accurate approximations for more general random matrices which have practical significance and are mathematically convenient. Therefore, we would like to stress the importance of gaining insight into the theoretical frameworks of additive and multiplicative free convolutions. For instance, we refer the reader to the elegant derivations presented in [94] and [95]. In particular, by using such clear derivations and invoking some advanced random matrix techniques, as in [94] and [95], we expect that techniques will be developed in a near future which will allow for quantifying the approximations provided by the free convolutions when they are applied to more general classes of random matrices of practical relevance.

Appendix A

Proofs – Chapter 2

Sections 2 and 3 of this appendix are based on parts of the materials of respectively

Manfred Opper, Burak Çakmak and Ole Winther, "A theory of solving TAP equations for Ising model with general invariant random matrices," Journal of Physics A: Mathematical and Theoretical, vol. 49, no. 11, February 2016, ©2016 IOP Publishing Ltd,

Burak Çakmak, Ralf Müller and Bernard H. Fleury, "Capacity scaling for MIMO systems with general unitarily invariant random matrices," arXiv preprint arXiv: 1306.2595, December 2015.

1 Proof of Theorem 2.1

From (2.16) we have

$$X_{ii} = \sum_{n=1}^{N} \lambda_n [(\boldsymbol{U}_n \boldsymbol{U}_n^\dagger)]_{ii} = \sum_{n=1}^{N} \lambda_n |U_{in}|^2 \tag{A.1}$$

where $\boldsymbol{U}_n$ is the nth column vector of Haar matrix $\boldsymbol{U}$ and $\lambda_n = \Lambda_{nn}$. By the law of total variance we have

$$\mathrm{Var}[X_{ii}] = \langle \mathrm{Var}[X_{ii}|\boldsymbol{\Lambda}] \rangle + \mathrm{Var}[\langle X_{ii}|\boldsymbol{\Lambda} \rangle]. \tag{A.2}$$

Here and in the following, for the random variables X and Y, $\mathrm{Var}[X]$ and $\mathrm{Cov}[X, Y]$ denote the variance X and the covariance of X and Y, respectively. We have

$$\langle X_{ii}|\boldsymbol{\Lambda} \rangle = \sum_{n=1}^{N} \lambda_n \left\langle |U_{in}|^2 \right\rangle = \mathrm{Tr}(\boldsymbol{X}) \tag{A.3}$$

$$\mathrm{Var}[X_{ii}|\boldsymbol{\Lambda}] = \sum_{n=1}^{N} \lambda_n^2 \mathrm{Var}[|U_{in}|^2] + 2 \sum_{n<k} \lambda_n \lambda_k \mathrm{Cov}[|U_{in}|^2, |U_{ik}|^2] \tag{A.4}$$

with nothing that $\left\langle |U_{ij}|^2 \right\rangle = 1/N$, $\forall i,j$. Since we assume that $\mathrm{Tr}(\boldsymbol{X})$ becomes self-averaging as $N \to \infty$, $\mathrm{Var}[\langle X_{ii}|\boldsymbol{\Lambda}\rangle]$ vanishes as $N \to \infty$. Thereby, for the proof we basically need to show that $\langle \mathrm{Var}[X_{ii}|\boldsymbol{\Lambda}]\rangle$ vanishes as $N \to \infty$. To do this we make use of Lemma 2.1:

$$\left\langle |U_{in}^2||U_{ik}^2| \right\rangle = \begin{cases} \frac{N+1}{N(N+\beta)(N+3-2\beta)} & n \neq k \\ \frac{1+\beta}{N(N+\beta)} & n = k \end{cases} \tag{A.5}$$

where $\beta = 2$ and $\beta = 1$ when $\boldsymbol{U}$ is real and complex, respectively. For simplicity, we consider the case $\beta = 2$; the proof for $\beta = 1$ follows similarly. Using this result, we obtain for the variance in (A.4)

$$\mathrm{Var}[X_{ii}|\boldsymbol{\Lambda}] = \frac{2(N-1)}{N^2(N+2)} \sum_{n=1}^{N} \lambda_n^2 + \frac{4}{N^2(N+2)(N-1)} \sum_{n<k} \lambda_n \lambda_k. \tag{A.6}$$

Note that we assume that $\langle \mathrm{Tr}(\boldsymbol{X}^2)\rangle$ and $\langle (\mathrm{Tr}(\boldsymbol{X}))^2\rangle$ converge to some finite limits as $N \to \infty$. This is sufficient for $\langle \mathrm{Var}[X_{ii}|\boldsymbol{\Lambda}]\rangle$ to vanish as $N \to \infty$. This completes the proof.

2 Proof of Theorem 2.6

For the proof, we use the so-called η-transform: $\eta(\gamma) \triangleq \int (1+\gamma x)^{-1} \mathrm{dF}(x)$, for $\gamma \in (0, \infty)$. In particular, we underline the following identity [36]

$$\int_0^{\gamma} \frac{1-\eta(t)}{t}\, \mathrm{d}t = \int \ln(1+\gamma x)\, \mathrm{dF}(x). \tag{A.7}$$

Moreover, we have the relationship [36]

$$\mathrm{R}(-\gamma\eta(\gamma)) = \frac{1-\eta(\gamma)}{\gamma\eta(\gamma)}. \tag{A.8}$$

Let $a = \gamma\eta(\gamma)$. Then, applying the substitution $\omega = t\eta(t)$ in the following integral we write

$$\int_0^a \mathrm{R}(-\omega)\, \mathrm{d}\omega = \int_0^{\gamma} \frac{\eta(t) + t\eta'(t)}{t\eta(t)} [1-\eta(t)]\, \mathrm{d}t \tag{A.9}$$

$$= \int_0^{\gamma} \frac{\eta'(t)}{\eta(t)} (1-\eta(t))\, \mathrm{d}t + \int_0^{\gamma} \frac{1-\eta(t)}{t}\, \mathrm{d}t \tag{A.10}$$

$$= \ln \eta(\gamma) + 1 - \eta(\gamma) + \int_0^{\gamma} \frac{1-\eta(t)}{t}\, \mathrm{d}t \tag{A.11}$$

$$= \ln \eta(\gamma) + 1 - \eta(\gamma) + \int \ln(1+\gamma x)\, \mathrm{dF}(x) \tag{A.12}$$

$$= \ln a + 1 - \eta(\gamma) + \int \ln(\gamma^{-1} + x)\, \mathrm{dF}(x). \tag{A.13}$$

In other words, by setting $\epsilon = 1/\gamma$ we have (2.50). Moreover, from (A.8) we have $\epsilon = a^{-1} - \mathrm{R}(-a)$. This completes the proof.

3 Proof of Theorem 2.7

For convenience let us define

$$\mathcal{I}(\epsilon; \mathrm{F}) = \int \ln(\epsilon + x)\, \mathrm{dF}(x). \tag{A.14}$$

By using identity [73, Eq. (5)] we can write

$$\mathcal{I}(\epsilon; \mathrm{F}) = -\epsilon \int_0^1 \ln(s) \partial\Psi(-\epsilon s)\, \mathrm{d}s \tag{A.15}$$

where $\partial\Psi(\omega) \triangleq \frac{\mathrm{d}\Psi(x)}{\mathrm{d}x}\Big|_{x=\omega}$ with Ψ defined as in (2.62). At this stage we point out that

$$\lim_{x \to 0^-} \Psi(\epsilon x) = 0. \tag{A.16}$$

Now we apply the variable substitution $z \triangleq \Psi(-\epsilon s) + 1$ in the integral in (A.15). Notice that with this substitution the upper and lower limits of this integral are $\Psi(-\epsilon) + 1$ and 1, respectively. As a result (A.15) is recast in the form

$$\mathcal{I}(\epsilon; \mathrm{F}) = \int_1^{\Psi+1} \ln\left(-\frac{1}{\epsilon}\Psi^{-1}(z-1)\right)\, \mathrm{d}z. \tag{A.17}$$

Then, by the definition of the S-transform, see (2.63), and Lemma A.1 below, we obtain

$$\mathcal{I}(\epsilon; \mathrm{F}) = \Psi \ln \epsilon + \int_1^{\Psi+1} \ln \frac{1-z}{z}\, \mathrm{d}z + \int_1^{\Psi+1} \ln \mathrm{S}(z-1)\, \mathrm{d}z \tag{A.18}$$

$$= \Psi \ln \epsilon + \tilde{H}(-\Psi) + \int_1^{\Psi+1} \ln \mathrm{S}(z-1)\, \mathrm{d}z \tag{A.19}$$

$$= \Psi \ln \epsilon + \tilde{H}(-\Psi) - \int_0^{-\Psi} \ln \mathrm{S}(-z)\, \mathrm{d}z \tag{A.20}$$

where $\Psi = \Psi(-\epsilon)$ and $\tilde{H}$ denotes the binary entropy function with the natural logarithm. Hence, we obtain (2.76), and thereby (2.74).

As regards to (2.75), let $\tilde{\mathrm{S}}$ denote the S-transform of $\tilde{\mathrm{F}}$. By using [36, Theorem 2.32] we write

$$\tilde{\mathrm{S}}(z) = \frac{z+1}{z+1/\alpha} \mathrm{S}(\alpha z), \quad -1 < z < 0. \tag{A.21}$$

Then, by invoking [73, Proposition 1] (i.e. (2.77)) and Lemma A.1 below we have

$$\alpha \int \ln(x)\, \mathrm{d}\tilde{\mathrm{F}}(x) = -\alpha \int_0^1 \ln \tilde{\mathrm{S}}(-x)\, \mathrm{d}x \tag{A.22}$$

$$= -\alpha \int_0^1 \ln \frac{1-x}{1/\alpha - x} \mathrm{S}(-\alpha x)\, \mathrm{d}x \tag{A.23}$$

$$= \tilde{H}(\alpha) - \alpha \int_0^1 \ln \mathrm{S}(-\alpha x)\, \mathrm{d}x \tag{A.24}$$

$$= \tilde{H}(\alpha) - \int_0^\alpha \ln \mathrm{S}(-x) \mathrm{d}x. \tag{A.25}$$

This completes the proof of the theorem.

Lemma A.1. *Let $p \in [0,1]$. Then we have*

$$\int_0^p \ln \frac{1-z}{p-z} \mathrm{d}z = \tilde{H}(p). \tag{A.26}$$

Proof. We first recast (A.26) into the equivalent identity

$$\lim_{x \to p} \int_0^x \ln \frac{1-z}{x-z} \mathrm{d}z = \tilde{H}(p). \tag{A.27}$$

To prove (A.27), we first apply a variable substitution

$$\int_0^x \ln \frac{1-t}{x-t} \mathrm{d}t = x \int_0^1 \log \frac{x^{-1}-z}{1-z} \mathrm{d}z \tag{A.28}$$

and decompose the right-hand side of (A.28) as

$$x \int_0^1 \ln(x^{-1}-z) \mathrm{d}z - x \int_0^1 \ln(1-z) \mathrm{d}z. \tag{A.29}$$

Define $u \triangleq \ln(x^{-1}-z)$ and $v = z$. Applying the integration by part rule, we obtain for the first integral:

$$\int_0^1 \ln\left(x^{-1}-z\right) \mathrm{d}z = uv|_0^1 - \int_0^1 v \mathrm{d}u \tag{A.30}$$

$$= x^{-1}\tilde{H}(x) - 1. \tag{A.31}$$

Using (A.31), we compute the second integral:

$$\int_0^1 \ln(1-z)\mathrm{d}z = \lim_{x\to 1}\int_0^1 \ln(x^{-1}-z)\mathrm{d}z = 1. \tag{A.32}$$

This completes the proof. □

Appendix B

Proofs – Chapter 3

This appendix is based directly on the appendix of

Burak Çakmak, Ralf Müller and Bernard H. Fleury, "Capacity scaling for MIMO systems with general unitarily invariant random matrices," arXiv preprint arXiv: 1306.2595, December 2015.

1 Convergence of Mutual information and Multiplexing Rate

In this section we provide some sufficient conditions that guarantee the convergence of the mutual information (3.5) and multiplexing rate (see (3.13)), in the large-system limit.

Proposition B.1. *As $R, T \to \infty$ with the ratio $\phi \triangleq T/R$ fixed let $\boldsymbol{J} = \boldsymbol{H}^\dagger \boldsymbol{H}$ have a LED function $\mathrm{F}_{\boldsymbol{J}}$. Furthermore, let*

$$\sup_T \int x \mathrm{d}\mathrm{F}_{\boldsymbol{J}}^T(x) < \infty \quad a.s. \quad . \tag{B.1}$$

Then, we have almost surely

$$\lim_{T\to\infty} \mathcal{I}(\gamma; \mathrm{F}_{\boldsymbol{J}}^T) = \mathcal{I}(\gamma; \mathrm{F}_{\boldsymbol{J}}). \tag{B.2}$$

Moreover, if in addition

$$\sup_T \int \frac{1}{x} \mathrm{d}\tilde{\mathrm{F}}_{\boldsymbol{J}}^T(x) < \infty \quad a.s. \tag{B.3}$$

we have almost surely

$$\lim_{T\to\infty} \mathcal{I}_0(\gamma; \mathrm{F}_{\boldsymbol{J}}^T) = \mathcal{I}_0(\gamma; \mathrm{F}_{\boldsymbol{J}}). \tag{B.4}$$

The proof is postponed after the discussion of this proposition.

Condition (B.1) is reasonable in practice. Otherwise the power amplification per dimension of the MIMO system explodes as its dimensions grow to infinity. One can show that for rectangular and unitarily invariant channel matrices, condition (B.3) is reasonable too, see (3.51) and the discussion therein. However, it might not hold when the channel matrix is square. As an example, consider a channel matrix $\boldsymbol{H}$ whose entries are iid with zero mean and variance σ^2/T. Then, condition (B.3) holds if $\phi \neq 1$, but is violated if $\phi = 1$. Indeed the latter case turns out critical for the convergence of the multiplexing rate, see e.g. [96], [36]. Nevertheless, both [97, Proposition 2.2] and numerical evidence lead us to conjecture that (B.4) holds when $\phi = 1$ as well. Thus, we conclude that the asymptotic convergence of the multiplexing rate, i.e. (B.4), is a mild assumption in practice.

Proof of Proposition B.1

We first provide a preliminary result that is required for the proof.

Theorem B.1. *For $n \in \mathbb{N}^+ \triangleq \{1, 2, ...\}$ let F^n be probability distribution functions on $[0, \infty)$. Furthermore let $1 - \mathrm{F}^n(0) = \alpha > 0$, $\forall n \in \mathbb{N}^+$. Moreover let S^n denote the S-transform of F^n. Then, if F^n converges weakly to a distribution function F as $n \to \infty$, we have*

$$\lim_{n\to\infty} \mathrm{S}^n(z) = \mathrm{S}(z), \quad -\alpha < z < 0 \tag{B.5}$$

where S is the S-transform of F.

Proof. Let us consider the function (see (2.62))

$$\Psi^n(z) \triangleq \int \frac{zx}{1-zx} \mathrm{dF}^n(x), \quad -\infty < z < 0. \tag{B.6}$$

The function $\frac{zx}{1-zx}$ is bounded and continuous with range $(0, 1)$. Thus the weak convergence of F^n implies that

$$\lim_{n\to\infty} \Psi^n(z) = \Psi(z), \quad -\infty < z < 0. \tag{B.7}$$

Since $\Psi^n(z)$ is a strictly increasing homeomorphism of $(-\infty, 0)$ onto $(-\alpha, 0)$ [73] we have (see e.g. [98, Proposition 0.1])

$$\lim_{n\to\infty} (\Psi^n)^{-1}(z) = \Psi^{-1}(z), \quad -\alpha < z < 0. \tag{B.8}$$

This completes the proof. □

For the sake of readability of the proof, whenever we consider a limit when the number of transmit antennas T tends to infinity, we implicitly assume that the ratio $\phi = T/R$ is fixed. For convenience, we define

$$\boldsymbol{Y} \triangleq \mathbf{I} + \gamma \boldsymbol{J}. \tag{B.9}$$

Obviously, $\mathrm{F}_{\boldsymbol{Y}}^{T}(0) = 0$ so that from (2.77) we have

$$\mathcal{I}(\gamma; \mathrm{F}_{\boldsymbol{J}}^{T}) = -\int_{-1}^{0} \log_2 \mathrm{S}_{\boldsymbol{Y}}^{T}(z)\mathrm{d}z. \tag{B.10}$$

The function $\mathrm{S}_{\boldsymbol{Y}}^{T}$ is strictly decreasing on $(-1, 0)$ if, and only if, $\mathrm{F}_{\boldsymbol{Y}}^{T}$ is not a Dirac distribution, see Lemma 2.4. If $\mathrm{F}_{\boldsymbol{Y}}^{T}$ is a Dirac distribution then $\mathrm{S}_{\boldsymbol{Y}}^{T}$ is a constant function. Without loss of generality, we assume that $\mathrm{F}_{\boldsymbol{Y}}^{T}$ is not a Dirac distribution function. Then, by invoking Lemma 2.4 we have

$$T/\mathrm{tr}(\boldsymbol{Y}) < \mathrm{S}_{\boldsymbol{Y}}^{T}(z) < \frac{1}{T}\mathrm{tr}(\boldsymbol{Y}^{-1}) \quad -1 < z < 0. \tag{B.11}$$

For convenience, we define the random variable

$$M \triangleq \sup_{T} \int x \mathrm{dF}_{\boldsymbol{J}}^{T}(x) \quad \text{s.t. } \phi = \frac{T}{R}. \tag{B.12}$$

Since the upper bound in (B.11) is smaller than one we have

$$\begin{aligned} |\log_2 \mathrm{S}_{\boldsymbol{Y}}^{T}(z)| &= -\log_2 \mathrm{S}_{\boldsymbol{Y}}^{T}(z) && \text{(B.13)} \\ &< \log_2 \frac{1}{T}\mathrm{tr}(\boldsymbol{Y}) && \text{(B.14)} \\ &\leq \log_2(1 + \gamma M). && \text{(B.15)} \end{aligned}$$

Because of (B.15), we can apply the Lebesgue's dominated convergence theorem [99, Theorem 10.21]:

$$\lim_{T\to\infty} \mathcal{I}(\gamma; \mathrm{F}_{\boldsymbol{J}}^{T}) = -\int_{-1}^{0} \lim_{T\to\infty} \log_2 \mathrm{S}_{\boldsymbol{Y}}^{T}(z)\, \mathrm{d}z. \tag{B.16}$$

Then, by invoking Theorem B.1 we complete the proof of (B.2):

$$\begin{aligned} \lim_{T\to\infty} \log_2 \mathrm{S}_{\boldsymbol{Y}}^{T}(z) &= \log_2 \lim_{T\to\infty} \mathrm{S}_{\boldsymbol{Y}}^{T}(z) && \text{(B.17)} \\ &= \log_2 \mathrm{S}_{\boldsymbol{Y}}(z). && \text{(B.18)} \end{aligned}$$

To proof (B.4), we apply the same argumentation as used above. In particular, by invoking Lemma 2.4 again we can write

$$\int x \, \mathrm{d}\tilde{\mathrm{F}}_{\boldsymbol{J}}^{T}(x) < \tilde{\mathrm{S}}_{\boldsymbol{J}}^{T}(z) < \int \frac{1}{x} \, \mathrm{d}\tilde{\mathrm{F}}_{\boldsymbol{J}}^{T}(x), \quad -1 < z < 0 \tag{B.19}$$

with $\tilde{\mathrm{S}}_{\boldsymbol{J}}^{T}$ denoting the S-transform of $\tilde{\mathrm{F}}_{\boldsymbol{J}}^{T}$. Unlike (B.11), the right-hand integral in (B.19) is not bounded in general, so we need the additional assumption (B.3). This completes the proof.

2 Proofs of Equations (3.23)–(3.25) and (3.27)–(3.29)

2.1 Proof of equations (3.23)–(3.25)

Consider the random matrix model defined in (3.22). With a convenient re-parameterization of [79, Eq. (19)] we write

$$\mathrm{S}_{\boldsymbol{J}}(z) = \prod_{n=1}^{N} \frac{\rho_n}{z+\rho_n}. \tag{B.20}$$

From Theorem 4.1 we have

$$\begin{aligned}\mathcal{I}(\gamma; \mathrm{F}_{\boldsymbol{J}}) = H(\eta_{\boldsymbol{J}}) + (1-\eta_{\boldsymbol{J}}) \log_2 \gamma \\ + \sum_{n=1}^{N} \int_0^{1-\eta_{\boldsymbol{J}}} \log_2(1 - \frac{z}{\rho_n})\, \mathrm{d}z.\end{aligned} \tag{B.21}$$

We can write the integrals in (B.21) as

$$\begin{aligned}&\int_0^{1-\eta_{\boldsymbol{J}}} \log_2(1 - \frac{z}{\rho_n})\, \mathrm{d}z = \\ &\log_2 \frac{1-\eta_{\boldsymbol{J}}}{\rho_n} + \int_0^1 \log_2(\frac{\rho_n}{1-\eta_{\boldsymbol{J}}} - z)\, \mathrm{d}z\end{aligned} \tag{B.22}$$

for $n \in \{1, \ldots, N\}$. By invoking the identity in (A.31) we obtain (3.23).

From the linearity property of the Lebesgue integral, it is easy to show that $\int_0^1 |\log_2 \tilde{\mathrm{S}}_{\boldsymbol{J}}(-z)\mathrm{d}z|$ is finite, which implies that $\int |\log(x)| \mathrm{d}\tilde{\mathrm{F}}_{\boldsymbol{J}}(x)$ is finite too and vice-versa [73]. Thus, the multiplexing rate is obtained by replacing the term $(1-\eta_{\boldsymbol{J}})$ in (3.23) with $\alpha_{\boldsymbol{J}}$ (due to Lemma 4.1). This leads to (3.25). Finally, we note that if $\alpha_{\boldsymbol{J}} < 1$ the S-transform $\mathrm{S}_{\boldsymbol{J}}(z)$ diverges as $z \to (-\alpha_{\boldsymbol{J}})$, see Lemma 2.4. Thus, from (B.20) the unique solution of $\alpha_{\boldsymbol{J}}$ is $\alpha_{\boldsymbol{J}} = \min(1, \rho_1, \rho_2, \ldots, \rho_N)$.

2.2 Proof of equations (3.27)–(3.29)

From (2.68) we have

$$\mathrm{S}_{\boldsymbol{J}}(z) = \frac{1+\beta_1 z}{\beta_2 + \beta_1 z}. \tag{B.23}$$

Moreover, notice that $\alpha_{\boldsymbol{J}} = 1 - \mathrm{F}_{\boldsymbol{J}}(0) = \min(1, \beta_2/\beta_1)$. For convenience, let $a \triangleq 1 - \eta_{\boldsymbol{J}}(\gamma) < \alpha_{\boldsymbol{J}}$. Then, we have

$$\int_0^a \log_2 \mathrm{S}_{\boldsymbol{J}}(-z)\, \mathrm{d}z = a \int_0^1 \log_2 \frac{1-\beta_1 a t}{\beta_2 - \beta_1 a t}\, \mathrm{d}t \tag{B.24}$$

$$= \frac{H(\beta_1 a)}{\beta_1} - \frac{\beta_2}{\beta_1} H\left(\frac{\beta_1}{\beta_2} a\right) \tag{B.25}$$

where (B.25) follows from (A.31). We obtain (3.27) from (3.20) with (B.25) inserted in (3.18). Moreover, by the definition of the S-transform we have

$$\beta_1(1-z)\Psi_{\boldsymbol{J}}^2(z) + (1-(\beta_1+\beta_2)z)\Psi_{\boldsymbol{J}}(z) - \beta_2 z = 0. \tag{B.26}$$

Note that $1+\Psi_{\boldsymbol{J}}(-\gamma) = \eta_{\boldsymbol{J}}(\gamma)$. Thus, (B.26) has two solutions for $\eta_{\boldsymbol{J}}(\gamma)$. Only one fulfills the properties of $\eta_{\boldsymbol{J}}(\gamma)$ stated in [36, pp. 41]. Specifically, from the property $\eta_{\boldsymbol{J}}(\gamma) \to 1$ as $\gamma \to 0$ we conclude that (3.28) is this solution. Finally it is also easy to show that $\int_0^1 |\log_2 \tilde{\mathrm{S}}_{\boldsymbol{J}}(-z)|\, \mathrm{d}z$ is finite in this case. This implies that $\int |\log(x)| \mathrm{d}\tilde{\mathrm{F}}_{\boldsymbol{J}}(x)$ is finite too. Thus, the multiplexing rate is obtained by replacing the term $(1-\eta_{\boldsymbol{J}})$ in (3.27) with $\alpha_{\boldsymbol{J}}$, which leads to (3.29).

3 Proof of Lemma 3.1, Theorem 3.2, Corollary 3.1 and Corollary 3.2

3.1 Proof of Lemma 3.1

Consider the singular value decomposition of the channel matrix

$$\boldsymbol{H} = \boldsymbol{U}[\boldsymbol{\Sigma}|\boldsymbol{0}]^\dagger \boldsymbol{V} \tag{B.27}$$

where $\boldsymbol{U}$ and $\boldsymbol{V}$ are respectively $R \times R$ and $T \times T$ unitary matrices, $\boldsymbol{\Sigma}$ is a $T \times T$ (almost surely) positive diagonal matrix and $\boldsymbol{0}$ is the $(R-T) \times T$ all zero matrix. Remark that (B.27) can be written as

$$\boldsymbol{H} = \boldsymbol{U}\boldsymbol{P}_\phi^\dagger \boldsymbol{\Sigma}\boldsymbol{V}. \tag{B.28}$$

For notational compactness, let us define $\boldsymbol{S} \triangleq \boldsymbol{\Sigma}\boldsymbol{V}$ and $\boldsymbol{Z}_\beta \triangleq \boldsymbol{P}_\phi \boldsymbol{U}^\dagger \boldsymbol{P}_\beta^\dagger \boldsymbol{P}_\beta \boldsymbol{U} \boldsymbol{P}_\phi^\dagger$. Then, we can write

$$\boldsymbol{J}_\beta = \boldsymbol{S}^\dagger \boldsymbol{Z}_\beta \boldsymbol{S}. \tag{B.29}$$

Note that $\boldsymbol{S}^\dagger \boldsymbol{Z}_\beta \boldsymbol{S}$ and $\boldsymbol{Z}_\beta \boldsymbol{S}\boldsymbol{S}^\dagger$ have the same eigenvalues. Thus we have

$$\log_2 |\boldsymbol{J}_\beta| = \log_2 |\boldsymbol{Z}_\beta| + \log_2 |\boldsymbol{\Sigma}^2|. \tag{B.30}$$

Since $\boldsymbol{J}_\beta$ for $\beta \geq \phi$ are assumed to have almost surely full rank, $\boldsymbol{\Sigma}$ and $T \times T$ matrix $\boldsymbol{Z}_\beta$ have also full rank. Hence, the rate loss reduces to (see (3.15))

$$\chi_{\boldsymbol{J}}^T(R, \beta R) = \frac{1}{T}\log_2 |\boldsymbol{Z}_1| - \frac{1}{T}\log_2 |\boldsymbol{Z}_\beta| \tag{B.31}$$

$$= -\frac{1}{T}\log_2 |\boldsymbol{Z}_\beta| \tag{B.32}$$

where we note that $\boldsymbol{Z}_1$ is the identity matrix. This completes the proof.

3.2 Theorem 3.2: Proof of equation (3.33)

Note that $\boldsymbol{J}$ is assumed to be unitarily invariant and have full rank. Therefore, the eigenbasis matrix of $\boldsymbol{J}$ is Haar (unitary). Moreover, one can show that $\boldsymbol{J}_\beta$ has full rank for $\beta \geq \phi$.

Now let us consider an auxiliary random matrix $\boldsymbol{X} \in \mathbb{C}^{R\times T}$ whose entries are iid zero-mean circularly-symmetric complex Gaussian and $\phi = T/R \leq 1$. Then, from Lemma 3.1 we have that

$$\chi^T_{\boldsymbol{X}^\dagger\boldsymbol{X}}(R,\beta R) = \frac{1}{T}\left(\log_2|\boldsymbol{X}^\dagger\boldsymbol{X}| - \log_2|\boldsymbol{X}^\dagger\boldsymbol{P}_\beta^\dagger\boldsymbol{P}_\beta\boldsymbol{X}|\right) \tag{B.33}$$

$$= -\frac{1}{T}\log_2|\boldsymbol{P}_\phi\tilde{\boldsymbol{U}}^\dagger\boldsymbol{P}_\beta^\dagger\boldsymbol{P}_\beta\tilde{\boldsymbol{U}}\boldsymbol{P}_\phi^\dagger| \tag{B.34}$$

where $\tilde{\boldsymbol{U}}$ is the eigenbasis matrix of $\boldsymbol{X}^\dagger\boldsymbol{X}$ which is also a Haar matrix. In other words, $\chi^T_{\boldsymbol{X}^\dagger\boldsymbol{X}}$ and $\chi^T_{\boldsymbol{J}}$ obey the same probability distribution. Thus, we have

$$\left\langle \chi^T_{\boldsymbol{J}}(R,\beta R)\right\rangle_{\boldsymbol{J}} = \left\langle \chi^T_{\boldsymbol{X}^\dagger\boldsymbol{X}}(R,\beta R)\right\rangle_{\boldsymbol{X}}. \tag{B.35}$$

Without loss of generality we can assume that the entries of $\boldsymbol{H}$ are iid complex Gaussian with zero mean and variance $1/R$. In this way, we can use the explicit expression for the ergodic "log det" of the Gaussian ensemble [36, Eq.(2.12)]. Doing so leads directly to (3.33).

3.3 Theorem 3.2: Proof of equation (3.34)

We first show that

$$\lim_{R\to\infty}\chi^T_{\boldsymbol{J}}(R,\beta R) = -\int \log_2(x)\ \mathrm{dF}_{\boldsymbol{Z}_\beta}(x) \tag{B.36}$$

almost surely. The random matrix $\boldsymbol{Z}_\beta = \boldsymbol{P}_\phi\boldsymbol{U}^\dagger\boldsymbol{P}_\beta^\dagger\boldsymbol{P}_\beta\boldsymbol{U}\boldsymbol{P}_\phi^\dagger$ is a Jacobi matrix, Definition 2.6. Following the notations of [46], $\boldsymbol{Z}_\beta$ is distributed according to $\mathcal{J}_{\phi R}(\beta R,(1-\beta)R,\mathbb{C})$. For $\beta \geq \phi$, [46, Eq. (4.23)] is equivalent to (B.36) (with the minus scaling). Then, from (3.29) it is immediate that

$$-\int \log_2(x)\ \mathrm{dF}_{\boldsymbol{Z}_\beta}(x) = \frac{1}{\phi}H(\phi) - \frac{\beta}{\phi}H\left(\frac{\phi}{\beta}\right). \tag{B.37}$$

This completes the proof.

3.4 Proof of Corollary 3.1

For the proof we first recall the following well-known result.

Lemma B.1. *[100] Let $\boldsymbol{A}$ and $\boldsymbol{A}+\boldsymbol{B}$ be invertible and $\boldsymbol{B}$ have rank 1. Furthermore let $g \triangleq \mathrm{tr}(\boldsymbol{B}\boldsymbol{A}^{-1}) \neq -1$. Then, we have*

$$(\boldsymbol{A}+\boldsymbol{B})^{-1} = \boldsymbol{A}^{-1} - \frac{1}{g+1}\boldsymbol{A}^{-1}\boldsymbol{B}\boldsymbol{A}^{-1}. \tag{B.38}$$

We point out the relationship [36]

$$\frac{\mathrm{d}\{\mathcal{I}(\gamma;\mathrm{F}_{\boldsymbol{J}}^{T})-\mathcal{I}(\gamma;\mathrm{F}_{\boldsymbol{J}_\beta}^{T})\}}{\mathrm{d}\gamma}=\frac{\eta_{\boldsymbol{J}_\beta}^{T}(\gamma)-\eta_{\boldsymbol{J}}^{T}(\gamma)}{\gamma\log 2}. \tag{B.39}$$

Thus, to proof Corollary 3.1 we simply need to show that

$$\mathrm{tr}\left\{(\mathbf{I}+\gamma\boldsymbol{J}_\beta)^{-1}-(\mathbf{I}+\gamma\boldsymbol{J})^{-1}\right\}\geq 0 \tag{B.40}$$

where the equality holds when $\beta = 1$. To prove (B.40) it is sufficient to consider the removal of a single receive antenna, i.e. $\beta = (R-1)/R$. It is immediate that

$$\boldsymbol{J}=\boldsymbol{J}_\beta+\boldsymbol{h}_R^{\dagger}\boldsymbol{h}_R \tag{B.41}$$

with $\boldsymbol{h}_R \in \mathbb{C}^{1\times T}$ representing the Rth row of $\boldsymbol{H}$. Then, (B.40) follows directly from Lemma B.1.

To show the convergence in mean of $\chi_{\boldsymbol{J}}^{T}$ we make use of identity (B.35). Without loss of generality we can assume that the entries of $\boldsymbol{H}$ are iid Gaussian with zero mean and variance $1/R$. Then, the "log det" convergence in mean for the iid Gaussian ensemble [17, Proposition 2] implies that

$$\lim_{R\to\infty}\left\langle\chi_{\boldsymbol{J}}^{T}(R,\beta R)\right\rangle_{\boldsymbol{J}}=-\int\log_2(x)\;\mathrm{dF}_{\boldsymbol{Z}_\beta}(x) \tag{B.42}$$

where $\boldsymbol{Z}_\beta=\boldsymbol{P}_\phi\boldsymbol{U}^{\dagger}\boldsymbol{P}_\beta^{\dagger}\boldsymbol{P}_\beta\boldsymbol{U}\boldsymbol{P}_\phi^{\dagger}$. Hence, (3.37) converges to (3.34) in the large-system limit. This completes the proof.

3.5 Proof of Corollary 3.2

Note that $\boldsymbol{J}_\beta$ is almost surely non-singular. Hence, we can write

$$\left\langle\mathcal{I}_0(\gamma;\mathrm{F}_{\boldsymbol{Q}\boldsymbol{J}_\beta}^{T})\right\rangle_{\boldsymbol{J}} \tag{B.43}$$

$$=\log_2\gamma+\frac{1}{T}\left\langle\log_2|\boldsymbol{Q}\boldsymbol{J}_\beta|\right\rangle_{\boldsymbol{J}} \tag{B.44}$$

$$=\log_2\gamma+\frac{1}{T}\left\langle\log_2|\boldsymbol{J}_\beta|\right\rangle_{\boldsymbol{J}}+\frac{1}{T}\log_2|\boldsymbol{Q}|. \tag{B.45}$$

Due to the constraint $\mathrm{tr}(\boldsymbol{Q}) = T$, $\boldsymbol{Q} = \mathbf{I}$ maximizes (B.45). So far we have shown that

$$\mathcal{C}_0(\gamma;\mathrm{F}_{\boldsymbol{J}_\beta}^{T})\triangleq\max_{\boldsymbol{Q}:\mathrm{tr}(\boldsymbol{Q})=\mathrm{T}}\left\langle\mathcal{I}_0(\gamma;\mathrm{F}_{\boldsymbol{Q}\boldsymbol{J}_\beta}^{T})\right\rangle_{\boldsymbol{J}} \tag{B.46}$$

$$=\left\langle\mathcal{I}_0(\gamma;\mathrm{F}_{\boldsymbol{J}_\beta}^{T})\right\rangle_{\boldsymbol{J}}. \tag{B.47}$$

It follows from the definitions in (3.36) and (B.46) that

$$\lim_{\gamma\to\infty} \mathcal{C}_0(\gamma; \mathrm{F}^T_{\boldsymbol{J}_\beta}) - \mathcal{C}(\gamma; \mathrm{F}^T_{\boldsymbol{J}_\beta}) \geq 0. \tag{B.48}$$

On the other hand we have

$$\mathcal{C}_0(\gamma; \mathrm{F}^T_{\boldsymbol{J}_\beta}) = \left\langle \mathcal{I}_0(\gamma; \mathrm{F}^T_{\boldsymbol{J}_\beta}) \right\rangle_{\boldsymbol{J}} < \left\langle \mathcal{I}(\gamma; \mathrm{F}^T_{\boldsymbol{J}_\beta}) \right\rangle_{\boldsymbol{J}} \leq \mathcal{C}(\gamma; \mathrm{F}^T_{\boldsymbol{J}_\beta}). \tag{B.49}$$

Hence, the limit in (B.48) must be zero.

4 Proof of Equation (3.44)

It is sufficient to proof the result for $1/2 < \phi < 1$. From (3.33), $T\chi(R, \phi R)$ can be written as

$$\begin{aligned} &\sum_{l=0}^{(1-\phi)R-1} \psi(R-l) + \sum_{l=(1-\phi)R}^{\phi R-1} \psi(R-l) \\ &- \sum_{l=0}^{R(2\phi-1)+1} \psi(\phi R-l) - \sum_{l=R(2\phi-1)}^{\phi R-1} \psi(\phi R-l) \end{aligned} \tag{B.50}$$

by noting that $\phi R \geq (1-\phi)R + 1$, since ϕR is integer and $\phi R > (1-\phi)R$. Note that we can write

$$\sum_{l=(1-\phi)R}^{\phi R-1} \psi(R-l) = \sum_{l=0}^{R(2\phi-1)+1} \psi(\phi R-l) \tag{B.51}$$

$$\sum_{l=R(2\phi-1)}^{\phi R-1} \psi(\phi R-l) = \sum_{l=0}^{(1-\phi)R-1} \psi((1-\phi)R-l). \tag{B.52}$$

Thus, $\chi(R, \phi R) = \chi(R, (1-\phi)R)$. This completes the proof.

5 Solution of Example 3.4

Note that we do not assume that $\boldsymbol{H}$ has Gaussian entries. However it is well known that for any distribution of the entries of $\boldsymbol{H}$, the distribution function $\mathrm{F}^N_{\boldsymbol{J}_\beta}$ converges weakly and almost surely to the Marčenko-Pastur distribution. In other words, we get the same asymtotic results regardless of whether we restrict the entries of $\boldsymbol{H}$ to be Gaussian or not. Thus, without loss of generality we can assume that the entries of $\boldsymbol{H}$ are Gaussian, so that $\boldsymbol{J}$ is unitarily invariant. We have $\mathrm{S}_{\boldsymbol{J}}(z) = (1+z)^{-1}$ [36]. Then, we immediately obtain (3.52) from Lemma 3.2.

6 Proof of Lemma 3.2

Note that $\alpha_{J_\beta} = \beta$. Since $\tilde{\mathrm{F}}_{J_\beta} = \mathrm{F}_{P_\beta J P_\beta^\dagger}$,

$$\mathcal{I}_0(\gamma; \mathrm{F}_{J_\beta}) = \beta \mathcal{I}_0(\gamma; \tilde{\mathrm{F}}_{J_\beta}) = \beta \mathcal{I}_0(\gamma; \mathrm{F}_{P_\beta J P_\beta^\dagger}). \tag{B.53}$$

Furthermore, from identity (2.71) we have

$$\tilde{\mathrm{S}}_{J_\beta}(z) = \mathrm{S}_J(\beta z) \tag{B.54}$$

where $\tilde{\mathrm{S}}_{J_\beta}$ is the S-transform of $\tilde{\mathrm{F}}_{J_\beta}$. In the sequel we first show that

$$\int_0^1 \left|\log_2 \tilde{\mathrm{S}}_{J_\beta}(-z)\right| \, \mathrm{d}z = \int_0^1 \left|\log_2 \mathrm{S}_J(-\beta z)\right| \, \mathrm{d}z < \infty. \tag{B.55}$$

To do so, it is sufficient to show that $\int_0^1 \left|\log_2 \mathrm{S}_J(-z)\right| \, \mathrm{d}z < \infty$. Since F_H has a compact support, $\mathcal{I}(\gamma; \mathrm{F}_J)$ is finite. Now we show that $\log x$ is absolutely integrable over F_J if, and only if, $\mathcal{I}(1; \mathrm{F}_J)$ and $\Delta\mathcal{I}(1; \mathrm{F}_J)$ are finite [73]:

$$\begin{aligned}\int_0^\infty |\log_2(x)| \, \mathrm{dF}_J(x) = &\int_0^1 \log_2\left(\frac{1}{x}\right) \, \mathrm{dF}_J(x) \\ &+ \int_1^\infty \log_2(x) \, \mathrm{dF}_J(x).\end{aligned} \tag{B.56}$$

Thus, we have

$$\int_0^1 \log_2\left(\frac{1}{x}\right) \, \mathrm{dF}_J(x) < \infty \iff \Delta\mathcal{I}(1; \mathrm{F}_J) < \infty, \tag{B.57}$$

$$\int_1^\infty \log_2(x) \, \mathrm{dF}_J(x) < \infty \iff \mathcal{I}(1; \mathrm{F}_J) < \infty. \tag{B.58}$$

with $\iff$ denoting the logical equivalence. Hence, (B.56) is finite. This implies that $\int_0^1 \left|\log_2 \mathrm{S}_J(-z)\right| \, \mathrm{d}z$ is finite too. Then, by invoking (2.77), (B.53) and (B.54) we have

$$\mathcal{I}_0(\gamma; \mathrm{F}_{J_\beta}) = \beta \log_2 \gamma - \beta \int_0^1 \log_2 \mathrm{S}_J(-\beta z) \, \mathrm{d}z. \tag{B.59}$$

Due to (B.55), it follows from the linearity property of the Lebesgue integral that

$$\Delta\mathcal{L}(\beta;\mathrm{F}_{\boldsymbol{J}}) = \mathcal{I}_0(\gamma;\mathrm{F}_{\boldsymbol{J}_\beta}) - \beta\mathcal{I}_0(\gamma;\mathrm{F}_{\boldsymbol{J}}) \tag{B.60}$$

$$= -\beta\int_0^1 \log_2\frac{\mathrm{S}_{\boldsymbol{J}}(-\beta z)}{\mathrm{S}_{\boldsymbol{J}}(-z)}\,\mathrm{d}z. \tag{B.61}$$

This completes the proof.

7 Proof of Remark 3.2

For the sake of notational simplicity we introduce

$$\boldsymbol{Y}_\beta \triangleq \mathbf{I} + \gamma\boldsymbol{P}_\beta\boldsymbol{H}\boldsymbol{H}^\dagger\boldsymbol{P}_\beta^\dagger \tag{B.62}$$

$$= \boldsymbol{P}_\beta(\mathbf{I} + \gamma\boldsymbol{H}\boldsymbol{H}^\dagger)\boldsymbol{P}_\beta^\dagger \tag{B.63}$$

$$= \boldsymbol{P}_\beta\boldsymbol{Y}_1\boldsymbol{P}_\beta^\dagger \tag{B.64}$$

where $\mathbf{I}$ denotes the identity matrix. The matrix $\boldsymbol{Y}_1$ is unitarily invariant since $\boldsymbol{H}\boldsymbol{H}^\dagger$ is. Furthermore, since $\boldsymbol{H}\boldsymbol{H}^\dagger$ has a compactly support LED so does $\boldsymbol{Y}_1$. Thus, $\boldsymbol{Y}_1$ is asymptotically free of $\boldsymbol{P}_\beta^\dagger\boldsymbol{P}_\beta$ [12]. Then, with the identity (2.71) we have in the limit $N \to \infty$

$$\mathrm{S}_{\boldsymbol{Y}_\beta}(z) = \mathrm{S}_{\boldsymbol{Y}_1}(\beta z). \tag{B.65}$$

Here, we note that $\mathrm{S}_{\boldsymbol{Y}_\beta}(z)$ is strictly decreasing on $(-1,0)$ if, and only if, $\mathrm{F}_{\boldsymbol{Y}_\beta}$ is not a Dirac distribution function, see Lemma 2.4, or equivalently due to (B.65) $\mathrm{F}_{\boldsymbol{J}}$ is not a Dirac distribution function.

We recall the following property of $\eta_{\boldsymbol{J}}(\gamma)$ (see (3.17)) first [36]:

$$\frac{\mathrm{d}\{\mathcal{I}(\gamma;\mathrm{F}_{\boldsymbol{J}_\beta}) - \beta\mathcal{I}(\gamma;\mathrm{F}_{\boldsymbol{J}})\}}{\mathrm{d}\gamma} = \frac{1-\eta_{\boldsymbol{J}_\beta} - \beta(1-\eta_{\boldsymbol{J}})}{\gamma\log 2}, \tag{B.66}$$

where for convenience we write $\eta_{\boldsymbol{J}}$ as short for $\eta_{\boldsymbol{J}}(\gamma)$. Hence, in order to prove the remark it is sufficient to show that

$$(1-\beta) + \beta\eta_{\boldsymbol{J}} - \eta_{\boldsymbol{J}_\beta} \geq 0 \tag{B.67}$$

where the equality holds when $\beta = 1$. Furthermore, by using [36, Lemma 2.26] we have

$$\eta_{\boldsymbol{J}_\beta} = (1-\beta) + \beta\eta_{\boldsymbol{P}_\beta\boldsymbol{J}\boldsymbol{P}_\beta^\dagger}. \tag{B.68}$$

Thus, the right-hand side of (B.67) is equal to $\beta(\eta_{\boldsymbol{J}} - \eta_{\boldsymbol{P}_\beta\boldsymbol{J}\boldsymbol{P}_\beta^\dagger})$. Therefore, we are left with proving $\eta_{\boldsymbol{J}} \geq \eta_{\boldsymbol{P}_\beta\boldsymbol{J}\boldsymbol{P}_\beta^\dagger}$. Firstly, remark that

$$\eta_{\boldsymbol{P}_\beta\boldsymbol{J}\boldsymbol{P}_\beta^\dagger} = \int\frac{1}{x}\,\mathrm{dF}_{\boldsymbol{Y}_\beta}(x). \tag{B.69}$$

Then, by using (2.4) and (B.65) we obtain

$$\eta_{\boldsymbol{P}_\beta \boldsymbol{J} \boldsymbol{P}_\beta^\dagger} = \lim_{z \to -1^+} \mathrm{S}_{\boldsymbol{Y}_\beta}(z) \tag{B.70}$$

$$= \lim_{z \to -1^+} \mathrm{S}_{\sqrt{\boldsymbol{Y}_1}}(\beta z) \tag{B.71}$$

$$= \mathrm{S}_{\boldsymbol{Y}_1}(-\beta)\,, \quad 0 < \beta < 1 \tag{B.72}$$

which is strictly increasing with β, see Lemma 2.4. This completes the proof.

8 Proof of Remark 3.3

The matrices $\boldsymbol{X}$, $\boldsymbol{Y}$ and $\boldsymbol{P}_\beta^\dagger \boldsymbol{P}_\beta$ are asymptotically free [12]. Then, from Lemma 3.2 and the linearity property of the Lebesgue integral we have

$$\Delta\mathcal{L}(\beta; \mathrm{F}_{\boldsymbol{XY}}) = -\beta \int_0^1 \log_2 \frac{\mathrm{S}_{\boldsymbol{X}}(-\beta z)\mathrm{S}_{\boldsymbol{Y}}(-\beta z)}{\mathrm{S}_{\boldsymbol{X}}(-z)\mathrm{S}_{\boldsymbol{Y}}(-z)}\, \mathrm{d}z \tag{B.73}$$

$$= \Delta\mathcal{L}(\beta; \mathrm{F}_{\boldsymbol{X}}) + \Delta\mathcal{L}(\beta; \mathrm{F}_{\boldsymbol{Y}}). \tag{B.74}$$

Appendix C

Proofs – Chapter 4

This appendix is based directly on the appendix of
Burak Çakmak, Manfred Opper, Bernard H. Fleury and Ole Winther, "Self-averaging expectation propagation," arXiv preprint arXiv: 1608.06602, August 2016.

1 Proof of Theorem 4.1

From the assumptions of the theorem we have $\phi(\boldsymbol{X}) < \infty$ and $\phi(\boldsymbol{X}^{-1}) < \infty$ for $\boldsymbol{X} = \boldsymbol{\Lambda}_{\mathrm{x}} + \boldsymbol{H}^{\dagger}\boldsymbol{\Lambda}_{\mathrm{z}}\boldsymbol{H}$. Thus, from Proposition B.1 we have

$$\lim_{K\to\infty} \frac{1}{K} \ln|\boldsymbol{\Lambda}_{\mathrm{x}} + \boldsymbol{H}^{\dagger}\boldsymbol{\Lambda}_{\mathrm{z}}\boldsymbol{H}| = \int \ln(x)\, \mathrm{dF}_{\boldsymbol{\Lambda}_{\mathrm{x}}+\boldsymbol{H}^{\dagger}\boldsymbol{\Lambda}_{\mathrm{z}}\boldsymbol{H}}(x) \tag{C.1}$$

where the ratio $\alpha = N/K$ is fixed. Then, invoking successively Corollary 2.1 and the additive free convolution (4.33) we have

$$\int \ln(x)\, \mathrm{dF}_{\boldsymbol{\Lambda}_{\mathrm{x}}+\boldsymbol{H}^{\dagger}\boldsymbol{\Lambda}_{\mathrm{z}}\boldsymbol{H}}(x) = \int_0^{\chi_{\mathrm{x}}} \mathrm{R}_{\boldsymbol{\Lambda}_{\mathrm{x}}+\boldsymbol{H}^{\dagger}\boldsymbol{\Lambda}_{\mathrm{z}}\boldsymbol{H}}(-\omega)\, \mathrm{d}\omega - \ln\chi_{\mathrm{x}} - 1 \tag{C.2}$$

$$= \int_0^{\chi_{\mathrm{x}}} \mathrm{R}_{\boldsymbol{\Lambda}_{\mathrm{x}}}(-\omega)\, \mathrm{d}\omega + \int_0^{\chi_{\mathrm{x}}} \mathrm{R}_{\boldsymbol{H}^{\dagger}\boldsymbol{\Lambda}_{\mathrm{z}}\boldsymbol{H}}(-\omega)\, \mathrm{d}\omega - \ln\chi_{\mathrm{x}} - 1 \tag{C.3}$$

where $\chi_{\mathrm{x}} = \phi(\boldsymbol{\Lambda}_{\mathrm{x}} + \boldsymbol{H}^{\dagger}\boldsymbol{\Lambda}_{\mathrm{z}}\boldsymbol{H})^{-1}$. Here for convenience, we introduce

$$v_{\mathrm{x}} \triangleq \mathrm{R}_{\boldsymbol{H}^{\dagger}\boldsymbol{\Lambda}_{\mathrm{z}}\boldsymbol{H}}(-\chi_{\mathrm{x}}) \tag{C.4}$$

$$\lambda_{\mathrm{x}} \triangleq \mathrm{R}_{\boldsymbol{\Lambda}_{\mathrm{x}}}(-\chi_{\mathrm{x}}). \tag{C.5}$$

Then, by invoking Lemma 2.2 we can write $\chi_{\mathrm{x}} = 1/(\lambda_{\mathrm{x}} + v_{\mathrm{x}})$. Moreover, with the conditions stated in Assumption 4.1 that $\chi_{\mathrm{x}} < \phi(\boldsymbol{A}^{\dagger}\boldsymbol{\Lambda}_{\mathrm{z}}\boldsymbol{A})^{-1}$ and $\mathrm{F}_{\boldsymbol{H}^{\dagger}\boldsymbol{\Lambda}_{\mathrm{z}}\boldsymbol{H}}$ is supported on $[0, \infty)$, it turns out that both quantities λ_{x} and v_{x} are positive. At this stage we also note that λ_{x} can be interpreted via the "scalarization"

$$\phi(\boldsymbol{\Lambda}_{\mathrm{x}} + \boldsymbol{H}^{\dagger}\boldsymbol{\Lambda}_{\mathrm{z}}\boldsymbol{H})^{-1} = \phi(\lambda_{\mathrm{x}}\mathbf{I} + \boldsymbol{H}^{\dagger}\boldsymbol{\Lambda}_{\mathrm{z}}\boldsymbol{H})^{-1}. \tag{C.6}$$

Note that the support of $\mathrm{F}_{\boldsymbol{\Lambda}_\mathrm{x}}$ is not necessarily in $[0,\infty)$ but it is assumed to be compact. Hence, we can define an auxiliary positive definite matrix $\boldsymbol{\Lambda}_\epsilon \triangleq \boldsymbol{\Lambda}_\mathrm{x} + \epsilon\mathbf{I}$, such that there exists a positive $\epsilon < \infty$ with $\phi(\boldsymbol{\Lambda}_\epsilon^{-1}) < \chi_\mathrm{x}$. Doing so we can write

$$\int_0^{\chi_\mathrm{x}} \mathrm{R}_{\boldsymbol{\Lambda}_\mathrm{x}}(-\omega)\,\mathrm{d}\omega = -\chi_\mathrm{x}\epsilon + \int_0^{\chi_\mathrm{x}} \mathrm{R}_{\boldsymbol{\Lambda}_\epsilon}(-\omega)\,\mathrm{d}\omega. \tag{C.7}$$

In this way both integrals in (C.3) are recast in a form suitable for applying Lemma 2.6 from which we easily obtain

$$\int \ln(x)\,\mathrm{dF}_{\boldsymbol{\Lambda}_\mathrm{x}+\boldsymbol{H}^\dagger\boldsymbol{\Lambda}_\mathrm{z}\boldsymbol{H}}(x) = \int \ln(x+v_\mathrm{x})\,\mathrm{dF}_{\boldsymbol{\Lambda}_\mathrm{x}}(x) + \int \ln(x+\lambda_\mathrm{x})\,\mathrm{dF}_{\boldsymbol{H}^\dagger\boldsymbol{\Lambda}_\mathrm{z}\boldsymbol{H}}(x). \tag{C.8}$$

This result still involves difficult terms via the product $\boldsymbol{H}^\dagger\boldsymbol{\Lambda}_\mathrm{z}\boldsymbol{H}$. We will resolve these difficulties by means of multiplicative free convolution. We first perform a convenient transformation

$$\int \ln(x+\lambda_\mathrm{x})\,\mathrm{dF}_{\boldsymbol{H}^\dagger\boldsymbol{\Lambda}_\mathrm{z}\boldsymbol{H}}(x) = (1-\alpha)\ln\lambda_\mathrm{x} + \alpha\int \ln(x+\lambda_\mathrm{x})\,\mathrm{dF}_{\boldsymbol{H}\boldsymbol{H}^\dagger\boldsymbol{\Lambda}_\mathrm{z}}(x). \tag{C.9}$$

We simplify the integral in the right-hand side of (C.9) by invoking successively (2.76), the multiplicative free convolution (4.34) and (2.74):

$$\begin{aligned}
&\int \ln(x+\lambda_\mathrm{x})\,\mathrm{dF}_{\boldsymbol{H}\boldsymbol{H}^\dagger\boldsymbol{\Lambda}_\mathrm{z}}(x) = \int_0^{\chi} \ln \mathrm{S}_{\boldsymbol{H}\boldsymbol{H}^\dagger\boldsymbol{\Lambda}_\mathrm{z}}(-z)\,\mathrm{d}z + H(\chi) + (1-\chi)\ln\lambda_\mathrm{x} \\
&= -\int_0^{\chi} \ln \mathrm{S}_{\boldsymbol{H}\boldsymbol{H}^\dagger}(-z)\,\mathrm{d}z - \int_0^{\chi} \ln \mathrm{S}_{\boldsymbol{\Lambda}_\mathrm{z}}(-z)\,\mathrm{d}z + H(\chi) + (1-\chi)\ln\lambda_\mathrm{x} \\
&= \int \ln(x+v_\mathrm{a})\,\mathrm{dF}_{\boldsymbol{H}\boldsymbol{H}^\dagger}(x) + \int \ln(x+v_\mathrm{z})\,\mathrm{dF}_{\boldsymbol{\Lambda}_\mathrm{z}}(x) + (1-\chi)\ln\frac{\lambda_\mathrm{x}}{v_\mathrm{a}v_\mathrm{z}} - H(\chi).
\end{aligned} \tag{C.10}$$

Here, we define

$$\chi \triangleq \phi\left\{\mathbf{I} - \left(\mathbf{I} + \frac{1}{\lambda_\mathrm{x}}\boldsymbol{H}\boldsymbol{H}^\dagger\boldsymbol{\Lambda}_\mathrm{z}\right)^{-1}\right\}. \tag{C.11}$$

Moreover, from (2.73) we write

$$\lambda_\mathrm{x} = \frac{1-\chi}{\chi \mathrm{S}_{\boldsymbol{H}\boldsymbol{H}^\dagger\boldsymbol{\Lambda}_\mathrm{z}}(-\chi)} \tag{C.12}$$

$$= \frac{1-\chi}{\chi \mathrm{S}_{\boldsymbol{H}\boldsymbol{H}^\dagger}(-\chi)\mathrm{S}_{\boldsymbol{\Lambda}_\mathrm{z}}(-\chi)} \tag{C.13}$$

$$v_\mathrm{a} = \frac{1-\chi}{\chi \mathrm{S}_{\boldsymbol{H}\boldsymbol{H}^\dagger}(-\chi)} \tag{C.14}$$

$$v_\mathrm{z} = \frac{1-\chi}{\chi \mathrm{S}_{\boldsymbol{\Lambda}_\mathrm{z}}(-\chi)}. \tag{C.15}$$

Thus, we get the identity

$$\lambda_{\mathrm{x}} = \frac{\chi}{1-\chi} v_{\mathrm{a}} v_{\mathrm{z}} \tag{C.16}$$

and thereby $(1-\chi)\ln\frac{\lambda_{\mathrm{x}}}{v_{\mathrm{a}} v_{\mathrm{z}}} - H(\chi) = \ln\chi$. Combining this with (C.10) and (C.9) yields

$$\begin{aligned}&\int \ln(x+\lambda_{\mathrm{x}})\,\mathrm{dF}_{\boldsymbol{H}^\dagger \boldsymbol{\Lambda}_{\mathrm{z}} \boldsymbol{H}}(x) \\ &= \int \ln(x+v_{\mathrm{a}})\,\mathrm{dF}_{\boldsymbol{A}^\dagger \boldsymbol{A}}(x) + \int \ln(x+v_{\mathrm{z}})\,\mathrm{dF}_{\boldsymbol{\Lambda}_{\mathrm{z}}}(x) + \ln\chi + (\alpha^{-1}-1)\ln\frac{\lambda_{\mathrm{x}}}{v_{\mathrm{s}}}\end{aligned} \tag{C.17}$$

where we use the transformation

$$\int \ln(x+v_{\mathrm{a}})\,\mathrm{dF}_{\boldsymbol{H}\boldsymbol{H}^\dagger}(x) = (1-\alpha^{-1})\ln v_{\mathrm{a}} + \int \ln(x+v_{\mathrm{a}})\,\mathrm{dF}_{\boldsymbol{H}^\dagger \boldsymbol{H}}(x). \tag{C.18}$$

We highlight the following facts:

- From (C.14) and (C.16) we have

$$v_{\mathrm{z}} = \lambda_{\mathrm{x}} \mathrm{S}_{\boldsymbol{H}\boldsymbol{H}^\dagger}(-\chi). \tag{C.19}$$

- From (C.6) and (C.11) we have

$$\begin{aligned}\chi &= \alpha^{-1}\phi\left\{\mathbf{I} - \left(\mathbf{I} + \frac{1}{\lambda_{\mathrm{x}}}\boldsymbol{H}^\dagger \boldsymbol{\Lambda}_{\mathrm{z}} \boldsymbol{H}\right)^{-1}\right\} && \text{(C.20)}\\ &= \alpha^{-1}\phi\left\{\mathbf{I} - \lambda_{\mathrm{x}}\left(\lambda_{\mathrm{x}}\mathbf{I} + \boldsymbol{H}^\dagger \boldsymbol{\Lambda}_{\mathrm{z}} \boldsymbol{H}\right)^{-1}\right\} && \text{(C.21)}\\ &= \alpha^{-1} v_{\mathrm{x}} \chi_{\mathrm{x}}. && \text{(C.22)}\end{aligned}$$

- By the scaling property of the R-transform we have

$$v_{\mathrm{x}} = \mathrm{R}_{\boldsymbol{H}^\dagger \boldsymbol{\Lambda}_{\mathrm{z}} \boldsymbol{H}}(-\chi_{\mathrm{x}}) \iff 1 = \mathrm{R}_{\frac{1}{v_{\mathrm{x}}} \boldsymbol{H}^\dagger \boldsymbol{\Lambda}_{\mathrm{z}} \boldsymbol{H}}(-v_{\mathrm{x}}\chi_{\mathrm{x}}). \tag{C.23}$$

  We express this identity in terms of the S-transform via (2.65). Doing so yields

$$\begin{aligned}1 &= \mathrm{S}_{\frac{1}{v_{\mathrm{x}}} \boldsymbol{H}^\dagger \boldsymbol{\Lambda}_{\mathrm{z}} \boldsymbol{H}}(-v_{\mathrm{x}}\chi_{\mathrm{x}}) && \text{(C.24)}\\ &= \mathrm{S}_{\frac{1}{v_{\mathrm{x}}} \boldsymbol{H}^\dagger \boldsymbol{H}}(-v_{\mathrm{x}}\chi_{\mathrm{x}}) \mathrm{S}_{\boldsymbol{\Lambda}_{\mathrm{z}}}(-v_{\mathrm{x}}\chi_{\mathrm{x}}/\alpha) && \text{(C.25)}\\ &= \frac{1}{\lambda_{\mathrm{z}}} \mathrm{S}_{\frac{1}{v_{\mathrm{x}}} \boldsymbol{H}^\dagger \boldsymbol{H}}(-v_{\mathrm{x}}\chi_{\mathrm{x}}) && \text{(C.26)}\\ &= \mathrm{S}_{\frac{\lambda_{\mathrm{z}}}{v_{\mathrm{x}}} \boldsymbol{H}^\dagger \boldsymbol{H}}(-v_{\mathrm{x}}\chi_{\mathrm{x}}) && \text{(C.27)}\end{aligned}$$

where we define $\lambda_z \triangleq 1/\mathrm{S}_{\mathbf{\Lambda}_z}(-v_x\chi_x/\alpha)$ and (C.27) follows from the scaling property of the S-transform. We now obtain the scaling factor λ_z and express the result in terms of the R-transform. Solving for v_x yields

$$v_x = \mathrm{R}_{\lambda_z \boldsymbol{H}^\dagger \boldsymbol{H}}(-\chi_x). \tag{C.28}$$

Moreover, note that $\chi = v_x\chi_x/\alpha$. Thus, from (C.15) we have

$$\lambda_z = 1/\mathrm{S}_{\mathbf{\Lambda}_z}(-\chi) = \frac{v_z\chi}{1-\chi}. \tag{C.29}$$

- From (D.4) we have $v_a = \lambda_x/\lambda_z$.
- Now, we introduce the auxiliary variable $\chi_z = \phi(\mathbf{\Lambda}_z + v_z\mathbf{I})$. Then, it follows from the definition of the S-transform and (C.15) that $\chi = \lambda_z\chi_z$ by noting that $\lambda_z \triangleq 1/\mathrm{S}_{\mathbf{\Lambda}_z}(-\chi)$.

By invoking the facts above and (C.17), we finally obtain

$$\begin{aligned}\lim_{K\to\infty} \frac{1}{K} \ln|\mathbf{\Lambda}_x + \boldsymbol{H}^\dagger \mathbf{\Lambda}_z \boldsymbol{H}| = \int \ln(x+v_x)\, \mathrm{dF}_{\mathbf{\Lambda}_x}(x) + \alpha \int \ln(x+v_z)\, \mathrm{dF}_{\mathbf{\Lambda}_z}(x) + \\ + \int \ln(\lambda_x + \lambda_z x)\, \mathrm{dF}_{\boldsymbol{H}^\dagger\boldsymbol{H}}(x) + \ln\chi_x + \alpha \ln\chi_z\end{aligned} \tag{C.30}$$

where $\chi_z = \phi(\mathbf{\Lambda}_z + v_z\mathbf{I})^{-1}$, $\lambda_z = \chi_z^{-1} - v_z$, $v_x = \lambda_z \mathrm{R}_{\boldsymbol{H}^\dagger\boldsymbol{H}}(-\lambda_z\chi_x)$ and $v_z = \lambda_x \mathrm{S}_{\boldsymbol{H}\boldsymbol{H}^\dagger}(-\lambda_z\chi_z)$. Recall that $\phi(\mathbf{\Lambda}_x) < \infty$ and $\phi(\mathbf{\Lambda}_z) < \infty$ are assumptions in the theorem. Furthermore, χ_x and χ_z are finite as well. Moreover, because we assume that $\boldsymbol{H}$ has uniformly bounded spectral norm, we have $\mathrm{R}^K_{\boldsymbol{H}^\dagger\boldsymbol{H}}(\omega) \to \mathrm{R}_{\boldsymbol{H}^\dagger\boldsymbol{H}}(\omega)$ as $K \to \infty$, see [12, Lemma 3.3.4]. This property turns out to be sufficient for representing the quantity v_z in terms of a finite size representation of the S-transform. In summary, from Proposition B.1 for sufficiently large N, K we can consider a finite size representation of (C.30) by three convenient log det terms in a way that each term converges to one of the integrals in (C.30). In this way we obtain Theorem 4.1.

2 The AT Line of Stability

The AT line of stability [28] is a fundamental concept in spin glass theory. It determines a region where the TAP approach or the so-called "replica ansatz" can provide valid (physical) results [101]. For example, it is known that below the AT line of stability, the "replica ansatz" predicts the entropy as a negative quantity for the standard Ising model [102], [26]. In this section we extend the concept of AT line of stability to our TAP approach. Basically, we

introduce the AT line of stability conditions that dictate that the two matrices $(\boldsymbol{\Lambda}_{\mathrm{x}} + \boldsymbol{H}^{\mathsf{T}}\boldsymbol{\Lambda}_{\mathrm{z}}\boldsymbol{H})$ and $\boldsymbol{\Lambda}_{\mathrm{z}}$ are positive definite.

In order to derive the AT line of stability we follow the conventional approach [103] [27] which consist in investigating the divergence of the so-called total susceptibility

$$\chi_{\mathrm{x}}^{(2)} \triangleq \lim_{K\to\infty} \frac{1}{K}\sum_{n,k}(\boldsymbol{\Lambda}_{\mathrm{x}} + \boldsymbol{H}^{\mathsf{T}}\boldsymbol{\Lambda}_{\mathrm{z}}\boldsymbol{H})^{-1}_{n,k} \tag{C.31}$$

$$= \lim_{K\to\infty} \frac{1}{K}\sum_{k}(\boldsymbol{\Lambda}_{\mathrm{x}} + \boldsymbol{H}^{\mathsf{T}}\boldsymbol{\Lambda}_{\mathrm{z}}\boldsymbol{H})^{-2}_{k}. \tag{C.32}$$

Under Assumption 4.1 we show in Appendix C.3 that

$$\chi_{\mathrm{x}}^{(2)} = \frac{\alpha_{\mathrm{x}}}{1 - \alpha_{\mathrm{x}}\mathrm{R}'_{\lambda_{\mathrm{z}}\boldsymbol{H}^{\mathsf{T}}\boldsymbol{H}}(-\chi_{\mathrm{x}})}. \tag{C.33}$$

Here we have the self-averaging EP quantities in their asymptotic form, i.e. $\chi_{\mathrm{a}} = \phi\left(\boldsymbol{\Lambda}_{\mathrm{a}} + v_{\mathrm{a}}\mathbf{I}\right)^{-1}$, $\lambda_{\mathrm{a}} = 1/\chi_{\mathrm{a}} - v_{\mathrm{a}}$ for $\mathrm{a} \in \{\mathrm{x}, \mathrm{z}\}$ where v_{a} is given in the form (4.49d) and (4.49e) with the replacement $\langle\boldsymbol{\chi}_{\mathrm{a}}\rangle \to \chi_{\mathrm{a}}$. Moreover, $\alpha_{\mathrm{x}} = \phi\left(\boldsymbol{\Lambda}_{\mathrm{a}} + v_{\mathrm{a}}\mathbf{I}\right)^{-2}$. Here we point out that from the analysis of self-averaging EP in Section 4 of Chapter 4 we can consider the approximation $\alpha_{\mathrm{x}} \simeq \boldsymbol{\chi}_{\mathrm{x}}^{\dagger}\boldsymbol{\chi}_{\mathrm{x}}/K$ where $\boldsymbol{\chi}_{\mathrm{x}}$ is the variance of the pdf $\tilde{q}_{\mathrm{x}}$ in (4.47). The total susceptibility $\chi_{\mathrm{x}}^{(2)}$ diverges at

$$1 - \alpha_{\mathrm{x}}\mathrm{R}'_{\lambda_{\mathrm{z}}\boldsymbol{H}^{\mathsf{T}}\boldsymbol{H}}(-\chi_{\mathrm{x}}) = 0. \tag{C.34}$$

This is the AT line of stability which dictates that the matrix $(\boldsymbol{\Lambda}_{\mathrm{x}} + \boldsymbol{H}^{\mathsf{T}}\boldsymbol{\Lambda}_{\mathrm{z}}\boldsymbol{H})$ is positive definite. It extends the previous AT line of stability results, e.g. [81], to the general model (4.3).

The positive definiteness of the matrix $(\boldsymbol{\Lambda}_{\mathrm{x}} + \boldsymbol{H}^{\mathsf{T}}\boldsymbol{\Lambda}_{\mathrm{z}}\boldsymbol{H})$ implies in our derivation that the matrix $(\boldsymbol{\Lambda}_{\mathrm{z}}^{-1} + \frac{1}{\lambda_{\mathrm{x}}}\boldsymbol{H}\boldsymbol{H}^{\mathsf{T}})\boldsymbol{\Lambda}_{\mathrm{z}}$ is positive definite too (asymptotically). Therefore, $\boldsymbol{\Lambda}_{\mathrm{z}}$ is positive definite if $(\boldsymbol{\Lambda}_{\mathrm{z}}^{-1} + \frac{1}{\lambda_{\mathrm{x}}}\boldsymbol{H}\boldsymbol{H}^{\mathsf{T}})$ is positive definite. Hence, we now introduce the total susceptibility as

$$\chi_{\mathrm{z}}^{(2)} \triangleq \lim_{N\to\infty} \frac{1}{N}\sum_{n,k}(\boldsymbol{\Lambda}_{\mathrm{z}}^{-1} + \frac{1}{\lambda_{\mathrm{x}}}\boldsymbol{H}\boldsymbol{H}^{\mathsf{T}})^{-1}_{n,k}. \tag{C.35}$$

To calculate $\chi_{\mathrm{z}}^{(2)}$ in addition to Assumption 4.1 we assume that $\boldsymbol{\Lambda}_{\mathrm{z}}^{-1}$ and $\boldsymbol{H}\boldsymbol{H}^{\mathsf{T}}$ are asymptotically free. This is indeed a mild assumption due to (4.34). Following the derivation of (C.33) in Appendix C.3 one can show that

$$\chi_{\mathrm{z}}^{(2)} = \frac{\alpha_{\mathrm{m}}}{1 - \alpha_{\mathrm{m}}\mathrm{R}'_{\frac{1}{\lambda_{\mathrm{x}}}\boldsymbol{H}\boldsymbol{H}^{\mathsf{T}}}(-\chi_{\mathrm{m}})}. \tag{C.36}$$

Here we define $\chi_{\mathrm{m}} \triangleq v_{\mathrm{z}}(1 - v_{\mathrm{z}}\chi_{\mathrm{z}})$ and $\alpha_{\mathrm{m}} \triangleq \phi \left(\boldsymbol{\Lambda}_{\mathrm{z}}^{-1} + v_{\mathrm{z}}^{-1}\mathbf{I}\right)^{-2}$. Moreover, from the analysis of self-averaging EP in Section 4 of Chapter 4 we can consider the approximation

$$\alpha_{\mathrm{m}} \simeq \frac{1}{N}\sum_{i}(v_{\mathrm{z}}(1 - v_{\mathrm{z}}[\boldsymbol{\chi}_{\mathrm{z}}]_i))^2 \tag{C.37}$$

where $\boldsymbol{\chi}_{\mathrm{z}}$ is the variance of the pdf $\tilde{q}_{\mathrm{z}}$ in (4.48). The total susceptibility $\chi_{\mathrm{z}}^{(2)}$ diverges at

$$1 - \alpha_{\mathrm{m}}\mathrm{R}'_{\frac{1}{\lambda_{\mathrm{x}}}\boldsymbol{H}\boldsymbol{H}^{\dagger}}(-\chi_{\mathrm{m}}) = 0. \tag{C.38}$$

We thereby complete the AT line of analysis for the positive definiteness of $(\boldsymbol{\Lambda}_{\mathrm{x}} + \boldsymbol{H}^{\dagger}\boldsymbol{\Lambda}_{\mathrm{z}}\boldsymbol{H})$ which is (C.33), and the positive definiteness of $\boldsymbol{\Lambda}_{\mathrm{z}}$ which is (C.33) and (C.38).

3 Proof of Equation (C.33)

In order to calculate the susceptibility $\chi_{\mathrm{x}}^{(2)}$ we introduce

$$\chi_{\mathrm{x}}(\omega) \triangleq \phi(\boldsymbol{\Lambda}_{\mathrm{x}} + \boldsymbol{H}^{\dagger}\boldsymbol{\Lambda}_{\mathrm{z}}\boldsymbol{H} - \omega\mathbf{I})^{-1}, \quad \omega \in (-\infty, 0).$$

Then, we have

$$\chi_{\mathrm{x}}^{(2)} = \lim_{\omega\to 0}\frac{\partial}{\partial\omega}\chi_{\mathrm{x}}(\omega) \tag{C.39}$$

$$= \lim_{\omega\to 0}\frac{\partial}{\partial\omega}\phi(\boldsymbol{\Lambda}_{\mathrm{x}} + \{\mathrm{R}_{\boldsymbol{H}^{\dagger}\boldsymbol{\Lambda}_{\mathrm{z}}\boldsymbol{H}}(-\chi_{\mathrm{x}}(\omega)) - \omega\}\mathbf{I})^{-1} \tag{C.40}$$

$$= \phi\left(\boldsymbol{\Lambda}_{\mathrm{x}} + \mathrm{R}_{\boldsymbol{H}^{\dagger}\boldsymbol{\Lambda}_{\mathrm{z}}\boldsymbol{H}}(-\chi_{\mathrm{x}})\mathbf{I}\right)^{-2}\left[1 + \chi'_{\mathrm{x}}(0)\mathrm{R}'_{\boldsymbol{H}^{\dagger}\boldsymbol{\Lambda}_{\mathrm{z}}\boldsymbol{H}}(-\chi_{\mathrm{x}})\right] \tag{C.41}$$

$$= \phi\left(\boldsymbol{\Lambda}_{\mathrm{x}} + \mathrm{R}_{\lambda_{\mathrm{z}}\boldsymbol{H}^{\dagger}\boldsymbol{H}}(-\chi_{\mathrm{x}})\mathbf{I}\right)^{-2}\left[1 + \chi'_{\mathrm{x}}(0)\mathrm{R}'_{\lambda_{\mathrm{z}}\boldsymbol{H}^{\dagger}\boldsymbol{H}}(-\chi_{\mathrm{x}})\right] \tag{C.42}$$

where for short we wrote $\chi_{\mathrm{x}} = \chi_{\mathrm{x}}(0)$ and $\chi'_{\mathrm{x}}(\omega) = \partial\chi_{\mathrm{x}}(\omega)/\partial\omega$. The results (C.40) and (C.42) are the consequence of (4.33) and (4.34), respectively. With a convenient reformulation of the right-hand side of (C.42) we obtain (C.33).

4 Updating the EP Cavity Variances

The update equations (4.23)–(4.25) are common to EP and self-averaging EP. The update equations for the cavity variances $\mathbf{v}_{\mathrm{x}}(t)$ and $\mathbf{v}_{\mathrm{z}}(t)$ in EP are ob-

tained from (4.31) as

$$[\boldsymbol{\Lambda}_{\mathrm{z}}(t)]_{ii} = 1/[\boldsymbol{\chi}_{\mathrm{z}}(t-1)]_i - [\mathbf{V}_{\mathrm{z}}(t-1)]_{ii} \tag{C.43}$$

$$\boldsymbol{\Sigma}_{\mathrm{x}}(t) = (\boldsymbol{\Lambda}_{\mathrm{x}}(t-1) + \boldsymbol{H}^{\mathsf{T}}\boldsymbol{\Lambda}_{\mathrm{z}}(t)\boldsymbol{H})^{-1} \tag{C.44}$$

$$[\mathbf{V}_{\mathrm{z}}(t)]_{ii} = 1/[(\boldsymbol{H}\boldsymbol{\Sigma}_{\mathrm{x}}(t)\boldsymbol{H}^{\mathsf{T}})]_{ii} - [\boldsymbol{\Lambda}_{\mathrm{z}}(t)]_{ii} \tag{C.45}$$

$$[\boldsymbol{\Lambda}_{\mathrm{x}}(t)]_{ii} = 1/[\boldsymbol{\chi}_{\mathrm{x}}(t)]_i - [\mathbf{V}_{\mathrm{x}}(t-1)]_{ii} \tag{C.46}$$

$$[\mathbf{V}_{\mathrm{x}}(t)]_{ii} = 1/[(\boldsymbol{\Sigma}_{\mathrm{x}}(t))]_{ii} - [\boldsymbol{\Lambda}_{\mathrm{x}}(t)]_{ii}. \tag{C.47}$$

The provided EP algorithm is naive and it has a poor convergence, in particular for large $\alpha = N/K$. One may need to adaptively select the initialization of the algorithm to the given parameter values.

Appendix D

Proofs – Chapter 5

This appendix is based directly on the appendix of

Manfred Opper, Burak Çakmak and Ole Winther, "A theory of solving TAP equations for Ising model with general invariant random matrices," Journal of Physics A: Mathematical and Theoretical, vol. 49, no. 11, February 2016, ©2016 IOP Publishing Ltd.

1 Derivation of Results from Dynamical Functional Theory

For the sake of notational compactness, let us define

$$\mathrm{g}(\{\boldsymbol{m}(\tau),\boldsymbol{\gamma}(\tau)\}_{\tau=0}^{t}) \triangleq \delta(\boldsymbol{m}(t)-f\left(\{\boldsymbol{\gamma}(\tau),\boldsymbol{m}(\tau)\}_{\tau=0}^{t-1}\right)). \tag{D.1}$$

By using the Fourier representation of the Dirac delta function we write

$$Z(\{\boldsymbol{l}(t)\}) = \int \prod_{t=0}^{T-1} \mathrm{d}\boldsymbol{m}(t)\mathrm{d}\boldsymbol{\gamma}(t)\mathrm{d}\hat{\boldsymbol{\gamma}}(t)\ \mathrm{g}(\{\boldsymbol{m}(\tau),\boldsymbol{\gamma}(\tau)\}_{\tau=0}^{t})\times \\ \times\, e^{\mathrm{i}\hat{\boldsymbol{\gamma}}(t)^{\intercal}(\boldsymbol{\gamma}(t)-\boldsymbol{h}-\boldsymbol{J}\boldsymbol{m}(t))}e^{\mathrm{i}\boldsymbol{\gamma}(t)^{\intercal}\boldsymbol{l}(t)}. \tag{D.2}$$

The derivation is split into two parts: i) computing the disorder average; ii) applying the saddle-point method.

1.1 Computation of the disorder average

For convenience, let us introduce $N\times T$ matrices $\boldsymbol{X}$ and $\hat{\boldsymbol{X}}$ with $X_{nt}=\frac{m_n(t+1)}{\sqrt{N}}$ and $\hat{X}_{nt}=\frac{\hat{\gamma}_n(t+1)}{\mathrm{i}\sqrt{N}}$. We need to evaluate

$$\left\langle e^{-\frac{\mathrm{i}}{2}\sum_t\left\{\hat{\boldsymbol{\gamma}}(t)^{\intercal}\boldsymbol{J}\boldsymbol{m}(t)+\boldsymbol{m}(t)^{\intercal}\boldsymbol{J}\hat{\boldsymbol{\gamma}}(t)\right\}}\right\rangle_{\boldsymbol{J}} = e^{O(1)+\frac{N}{2}\sum_{n\geq 1}\frac{c_n}{n}\mathrm{tr}(\boldsymbol{Q}^n)} \tag{D.3}$$

with $\boldsymbol{Q} = \hat{\boldsymbol{X}}\boldsymbol{X}^\dagger + \boldsymbol{X}\hat{\boldsymbol{X}}^\dagger$. Here (D.3) follows from (5.3). We next evaluate

$$\mathrm{tr}(\boldsymbol{Q}^n) = \mathrm{tr}\left((\hat{\boldsymbol{X}}\boldsymbol{X}^\dagger + \boldsymbol{X}\hat{\boldsymbol{X}}^\dagger)^n\right) \tag{D.4}$$

in terms of the matrices (D.4)

$$\mathcal{G} \triangleq \boldsymbol{X}^\dagger\hat{\boldsymbol{X}} \tag{D.5}$$

$$\mathcal{C} \triangleq \boldsymbol{X}^\dagger\boldsymbol{X} \tag{D.6}$$

$$\tilde{\mathcal{C}} \triangleq \hat{\boldsymbol{X}}^\dagger\hat{\boldsymbol{X}}. \tag{D.7}$$

Then, by using cyclic invariance of the trace we obtain the expression

$$\mathrm{tr}(\boldsymbol{Q}^n) = 2\mathrm{tr}(\mathcal{G}^n) + n\mathrm{tr}\sum_{k=0}^{n-2}\left\{\mathcal{G}^k\mathcal{C}(\mathcal{G}^\dagger)^{n-2-k}\tilde{\mathcal{C}}\right\} + \mathrm{I}(\mathcal{G},\mathcal{C},\tilde{\mathcal{C}}) \tag{D.8}$$

where the function I satisfies

$$\left.\frac{\partial \mathrm{I}(\mathcal{G},\mathcal{C},\tilde{\mathcal{C}})}{\partial\tilde{\mathcal{C}}}\right|_{\tilde{\mathcal{C}}=\mathbf{0}} = \mathbf{0}. \tag{D.9}$$

This means that I contains more than one factor $\tilde{\mathcal{C}}$ and thus – at the saddle–point value – $\tilde{\mathcal{C}} = \mathbf{0}$ does not contribute to the saddle-point equations.

1.2 The saddle-point calculation

We write as

$$\begin{aligned}\langle Z(\{\boldsymbol{l}(t)\})\rangle_{\boldsymbol{J}} \simeq \int \mathrm{d}\mathcal{G}\mathrm{d}\mathcal{C}\mathrm{d}\tilde{\mathcal{C}}\; e^{O(1)+\frac{N}{2}\sum_{n\geq 1}\frac{c_n}{n}\left(2\mathrm{tr}(\mathcal{G}^n)+n\mathrm{tr}\sum_{k=0}^{n-2}\left\{\mathcal{G}^k\mathcal{C}(\mathcal{G}^\dagger)^{n-2-k}\tilde{\mathcal{C}}\right\}+\mathrm{I}(\mathcal{G},\mathcal{C},\tilde{\mathcal{C}})\right)}\\ \int\prod_{t=0}^{T-1}\left\{\mathrm{d}\boldsymbol{m}(t)\mathrm{d}\boldsymbol{\gamma}(t)\mathrm{d}\hat{\boldsymbol{\gamma}}(t)\;\mathrm{g}(\{\boldsymbol{m}(\tau),\boldsymbol{\gamma}(\tau)\}_{\tau\leq t})e^{\mathrm{i}\hat{\boldsymbol{\gamma}}(t)^\dagger(\boldsymbol{\gamma}(t)-\boldsymbol{h})}e^{i\boldsymbol{\gamma}(t)^\dagger\boldsymbol{I}(t)}\right\}\\ \prod_{t,s}\delta\left(\mathrm{i}N\mathcal{G}(t,s)-\boldsymbol{m}(t)^\dagger\hat{\boldsymbol{\gamma}}(s)\right)\delta\left(N\mathcal{C}(t,s)-\boldsymbol{m}(t)^\dagger\boldsymbol{m}(s)\right)\delta\left(N\tilde{\mathcal{C}}(t,s)+\hat{\boldsymbol{\gamma}}(t)^\dagger\hat{\boldsymbol{\gamma}}(s)\right).\end{aligned} \tag{D.10}$$

By the Fourier representation of the Dirac delta function we write the last line of (D.10) as

$$\begin{aligned}c\int\mathrm{d}\hat{\mathcal{G}}\mathrm{d}\hat{\mathcal{C}}\mathrm{d}\hat{\tilde{\mathcal{C}}}\;\exp\Bigg(\sum_{(t,s)}\mathrm{i}\hat{\mathcal{G}}(t,s)\left(\mathrm{i}N\mathcal{G}(t,s)-\boldsymbol{m}(t)^\dagger\hat{\boldsymbol{\gamma}}(s)\right)+\\ +\mathrm{i}\hat{\mathcal{C}}(t,s)\left(N\mathcal{C}(t,s)-\boldsymbol{m}(t)^\dagger\boldsymbol{m}(s)\right)-\hat{\tilde{\mathcal{C}}}(t,s)\left(N\tilde{\mathcal{C}}(t,s)+\hat{\boldsymbol{\gamma}}(t)^\dagger\hat{\boldsymbol{\gamma}}(s)\right)\Bigg).\end{aligned} \tag{D.11}$$

Here c is a constant irrelevant for the saddle-point calculation. We define the auxiliary "single-site" partition function

$$\begin{aligned}\tilde{Z}_n(l_n,\hat{\mathcal{G}},\hat{\mathcal{C}},\hat{\tilde{\mathcal{C}}}) \triangleq \int \prod_{t=0}^{T-1} \{ & \mathrm{d}m_n(t)\mathrm{d}\gamma_n(t)\mathrm{d}\hat{\gamma}_n(t)\ \mathrm{g}(\{m_n(\tau),\gamma_n(\tau)\}_{\tau\le t}) \\ & e^{\mathrm{i}\hat{\gamma}_n(t)(\gamma_n(t)-h_n)} e^{\mathrm{i}\gamma_n(t)l_n(t)}\Big\} \\ & e^{-\sum_{(t,s)}[\mathrm{i}\hat{\mathcal{G}}(t,s)m_n(t)\hat{\gamma}_n(s)+\mathrm{i}\hat{\mathcal{C}}(t,s)m_n(t)m_n(s)+\hat{\tilde{\mathcal{C}}}(t,s)\hat{\gamma}_n(t)\hat{\gamma}_n(s)]}.\end{aligned} \tag{D.12}$$

In this way we can write (D.10) as

$$\begin{aligned}\langle Z(\{\boldsymbol{I}(t)\})\rangle_{\boldsymbol{J}} = \int \mathrm{d}\mathcal{G}\mathrm{d}\hat{\mathcal{G}}\mathrm{d}\mathcal{C}\mathrm{d}\hat{\mathcal{C}}\mathrm{d}\tilde{\mathcal{C}}\mathrm{d}\hat{\tilde{\mathcal{C}}} & \\ e^{O(1)+\frac{N}{2}\sum_{n\ge1}\frac{c_n}{n}\left(2\mathrm{tr}(\mathcal{G}^n)+n\mathrm{tr}\sum_{k=0}^{n-2}\left\{\mathcal{G}^k\mathcal{C}(\mathcal{G}^\intercal)^{n-2-k}\tilde{\mathcal{C}}\right\}+\mathrm{I}(\mathcal{G},\mathcal{C},\tilde{\mathcal{C}})\right)} & \\ e^{N\sum_{(t,s)}[-\hat{\mathcal{G}}(t,s)\mathcal{G}_{t,s}+i\hat{\mathcal{C}}(t,s)\mathcal{C}(t,s)-\hat{\tilde{\mathcal{C}}}(t,s)\tilde{\mathcal{C}}(t,s)]+\sum_n \log\tilde{Z}_n(l_n,\hat{\mathcal{G}},\hat{\mathcal{C}},\hat{\tilde{\mathcal{C}}})}.\end{aligned} \tag{D.13}$$

In the large-system limit we can perform the integrations over $\mathcal{G},\hat{\mathcal{G}},\mathcal{C},\hat{\mathcal{C}},\tilde{\mathcal{C}},\hat{\tilde{\mathcal{C}}}$ with the saddle-point methods. Doing so yields

$$\mathcal{G}(t,s) = -\frac{\mathrm{i}}{N}\sum_n \langle m_n(t)\hat{\gamma}_n(s)\rangle_{\tilde{Z}_n} \tag{D.14}$$

$$\mathcal{C}(t,s) = \frac{1}{N}\sum_n \langle m_n(t)m_n(s)\rangle_{\tilde{Z}_n} \tag{D.15}$$

$$\tilde{\mathcal{C}}(t,s) = -\frac{1}{N}\sum_n \langle \hat{\gamma}_n(t)\hat{\gamma}_n(s)\rangle_{\tilde{Z}_n} \tag{D.16}$$

with $\langle\ \rangle_{\tilde{Z}_n}$ denoting the average with respect to the single-site partition function. Here the quantity (D.16) has only the trivial solution $\tilde{\mathcal{C}}_{t,s}=0$. Other solutions may violate the normalization $Z(\{\boldsymbol{I}(t)=0\})=1$. Furthermore, this solution leads to $\hat{\mathcal{C}}=\mathbf{0}$. By invoking (D.8) we have

$$\hat{\mathcal{G}} = \mathrm{R}(\mathcal{G}) \tag{D.17}$$

$$\hat{\tilde{\mathcal{C}}} = \frac{1}{2}\sum_{n=1}^{\infty} c_n \sum_{k=0}^{n-2} \mathcal{G}^k\mathcal{C}(\mathcal{G}^\intercal)^{n-2-k}. \tag{D.18}$$

Thus, we get the factorization of the generating function

$$\begin{aligned}\langle Z(\{\boldsymbol{I}(t)\})\rangle_{\boldsymbol{J}} = \prod_{n=1}^{N}\int\prod_{t=0}^{T-1}\Big\{ & \mathrm{d}m_n(t)\mathrm{d}\gamma_n(t)\ \mathrm{g}(\{m_n(\tau),\gamma_n(\tau)\}_{\tau\le t})e^{\mathrm{i}\gamma_n(t)l_n(t)+O(N^{-1})} \\ & e^{\mathrm{i}\hat{\gamma}_n(t)(\gamma_n(t)-h_n-\sum_s\hat{\mathcal{G}}(t,s)m_n(s))}e^{-\sum_s\hat{\tilde{\mathcal{C}}}(t,s)\hat{\gamma}_n(t)\hat{\gamma}_n(s)}\Big\}.\end{aligned} \tag{D.19}$$

We linearize the quadratic terms in $\hat{\gamma}_n(t)$ by introducing auxiliary Gaussian random fields $\phi_n(t)$ which are iid with zero mean and covariance $\mathcal{C}_\phi(t,s) \triangleq 2\hat{\tilde{\mathcal{C}}}(t,s) \triangleq \langle \phi_n(t)\phi_n(s)\rangle$. In this way, we can write

$$e^{-\sum_{t,s}\hat{\tilde{\mathcal{C}}}(t,s)\hat{\gamma}_n(t)\hat{\gamma}_n(s)} = \left\langle e^{-\mathrm{i}\sum_t \phi_n(t)\hat{\gamma}_n(t)} \right\rangle_{\phi_n} . \tag{D.20}$$

Doing so (D.19) is recast as follows:

$$\langle Z(\{\boldsymbol{\imath}(t)\})\rangle_{\boldsymbol{J}} = \prod_{n=1}^{N} \int \mathrm{d}\mathcal{N}(\{\phi_n(t)\};0,\mathcal{C}_\phi) \prod_{t=0}^{T-1} \Big\{ \delta(m_n(t) - f_t\left\{m_n(\tau),\gamma_n(\tau)\right\}_{\tau=0}^{t-1}) \\ \delta\left(\gamma_n(t) - h_n - \sum_{s<t}\hat{\mathcal{G}}(t,s)m_n(s) - \phi_n(t)\right) e^{\mathrm{i}\gamma_n(t)l_n(t)+O(N^{-1})}\, \mathrm{d}m_n(t)\mathrm{d}\gamma_n(t) \Big\}. \tag{D.21}$$

Finally, notice that $-i\langle m_n(t)\hat{\gamma}_n(s)\rangle_{\phi_n} = \langle \frac{\partial m_n(t)}{\partial \phi_n(s)}\rangle_{\phi_n}$. Thus, $\mathcal{G}$ equals the response function (5.15). This completes the derivation.

2 Proof of Equation (5.54)

First note that from (5.21) and (5.24) we have

$$\mathcal{C}_\psi(t-1,t'-1) = \frac{(\mathcal{G}\mathcal{C}_\phi\mathcal{G}^\dagger)(t,t')}{(1-q(t))(1-q(t'))} \tag{D.22}$$

where $\mathcal{C}_\phi$ is defined as in (5.14). For the sake of compactness, let $f(x) = \mathrm{R}^{-1}(x)$. By elementary combinatorics and using $\mathcal{G} = f(\hat{\mathcal{G}})$ we show that any power of the matrix $\mathcal{G}$ can be written as

$$\mathcal{G}^k = \sum_{n=1}^{\infty} \mathrm{Co}_{x^n}(f(x)^k)\hat{\mathcal{G}}^n \tag{D.23}$$

where for any power series $f(x) = \sum_n a_n x^n$ we write $a_k \triangleq \mathrm{Co}_{x^k}(f(x))$. This means that we have

$$\mathcal{G}^k(t,\tau) = \mathrm{Co}_{x^{t-\tau}}(f(x)^k) \prod_{s=\tau}^{t-1} \hat{\mathcal{G}}(s+1,s). \tag{D.24}$$

Hence we also get

$$(\mathcal{G}^{k+1}\mathcal{C}(\mathcal{G}^\dagger)^{n-1-k})(t-1,t'-1) = \sum_{l<t,m<t'} \left(\prod_{s=l}^{t-1}\hat{\mathcal{G}}(s+1,s)\right)\left(\prod_{s=m}^{t'-1}\hat{\mathcal{G}}(s+1,s)\right) \\ \times \mathcal{C}(l,m)\mathrm{Co}_{x^{t-l}y^{t'-m}}(f(x)^{k+1}f(y)^{n-1-k}) \tag{D.25}$$

where we write $\mathrm{Co}_{x^n y^k}[f(x,y)] \triangleq a_n b_k$ for double power series

$$f(x,y) = \sum_{n,k\geq 0} a_n b_k x^n y^k. \tag{D.26}$$

Summing up the geometric series, we have

$$\sum_{k=0}^{n-2} \mathrm{Co}_{x^{t-l}y^{t'-m}}(f(x)^{k+1} f(y)^{n-1-k}) = \mathrm{Co}_{x^{t-l}y^{t'-m}}\left(\frac{f(y)^{n-1} - f(x)^{n-1}}{[f(y)-f(x)]/[f(x)f(y)]}\right) \tag{D.27}$$

and

$$\sum_{n=1}^{\infty} c_n \mathrm{Co}_{x^{t-l}y^{t'-m}}\left(\frac{f(y)^{n-1} - f(x)^{n-1}}{[f(y)-f(x)]/[f(x)f(y)]}\right) \tag{D.28}$$

$$= \mathrm{Co}_{x^{t-l}y^{t'-m}}\left(\frac{y-x}{[f(y)-f(x)]/[f(x)f(y)]}\right). \tag{D.29}$$

Putting everything together completes the proof.

3 Proof of Equation (5.70)

For the sake of compactness, without loss of generality, we may set $h_i = h$. Using the representation of the Gaussian density in terms of the characteristic function we have the expansion for $t \neq t'$

$$\begin{aligned}
&\left\langle \tanh(u(t)+h)\tanh(u(t')+h)\right\rangle_u \simeq \int \mathrm{d}u_1\mathrm{d}u_2\mathrm{d}k_1\mathrm{d}k_2 \\
&\times \exp\left[i(k_1u_1+k_2u_2) - \frac{1}{2}\{s_0+\epsilon(s(t,t)+1)\}(k_1^2+k_2^2) - \{s_0+\epsilon s(t,t')\}k_1k_2\right] \times \\
&\times \tanh(u_1+h)\tanh(u_2+h) \\
&\simeq\ q - \frac{\epsilon}{2}\int \mathrm{d}u_1\mathrm{d}u_2\mathrm{d}k_1\mathrm{d}k_2\ \exp\left[i(k_1u_1+k_2u_2) - \frac{s_0}{2}(k_1^2+k_2^2+2k_1k_2)\right] \times \\
&\times \tanh(u_1+h)\tanh(u_2+h)\left\{(s(t,t)+1)(k_1^2+k_2^2) + 2s(t,t')k_1k_2\right\} \\
&=\ q + \epsilon(s(t,t)+1)\left\langle \tanh(u+h)\frac{\partial^2\tanh(u+h)}{\partial u^2}\right\rangle + \epsilon s(t_1,t_2)\left\langle\left(\frac{\partial\tanh(u+h)}{\partial u}\right)^2\right\rangle .
\end{aligned} \tag{D.30}$$

The last line is obtained by representing $k_1, k_2, \ldots$ by means of derivatives with respect to u_1 and u_2. Repeating the same procedure leading to the above

expansion we get

$$\left\langle \tanh^2(u(t)+h) \right\rangle_u = q + \frac{\epsilon}{2}(s(t,t)+1)\left\langle \frac{\partial^2 \tanh^2(u+h)}{\partial u^2} \right\rangle = \\ = q + \epsilon(s(t,t)+1)\left\langle \tanh(u+h)\frac{\partial^2 \tanh(u+h)}{\partial u^2} + \left(\frac{\partial \tanh(u+h)}{\partial u}\right)^2 \right\rangle. \tag{D.31}$$

Both expansions can be represented in the single equation

$$\frac{\mathrm{d}\left\langle \tanh(u(t)+h)\tanh(u(t')+h)\right\rangle_u}{\mathrm{d}\epsilon} = (s(t,t)+1)\left\langle \tanh(u+h)\frac{\partial^2 \tanh(u+h)}{\partial u^2} \right\rangle \\ + (s(t,t')+\delta_{t,t'})\left\langle \left(\frac{\partial \tanh(u+h)}{\partial u}\right)^2 \right\rangle. \tag{D.32}$$

Note that only the second term contributes to the dynamic part of the fluctuations. Hence, by taking the Fourier transform and noting that $\frac{\partial \tanh(u+h)}{\partial u} = 1 - \tanh^2(u+h)$ we obtain (5.70).

Bibliography

[1] J. Sethna, *Statistical Mechanics: Entropy, Order Parameters, and Complexity*. Oxford University Press, 2006, vol. 14.

[2] H. Gould and J. Tobochnik. (2007) From microscopic to macroscopic behavior. [Online]. Available: http://psi.phys.wits.ac.za/stat_phys/on_line_text/chapter_1.pdf

[3] A. D. Jackson. (2002) A brief introduction to random matrices. [Online]. Available: http://www.nbi.dk/~jackson/

[4] V. Barone and M. Cossi, "Quantum calculation of molecular energies and energy gradients in solution by a conductor solvent model," *The Journal of Physical Chemistry A*, vol. 102, no. 11, pp. 1995–2001, 1998.

[5] M. L. Mehta, *Random Matrices*. Elsevier Academic press, 2004.

[6] G. Parisi and M. Potters, "Mean-field equations for spin models with orthogonal interaction matrices," *Journal of Physics A: Mathematical and General*, vol. 28.18, p. 5267, October 1995.

[7] K. Takeda, S. Uda, and Y. Kabashima, "Analysis of CDMA systems that are characterized by eigenvalue spectrum," *EPL (Europhysics Letters)*, vol. 76, pp. 1193–1199, 2006.

[8] B. Zaidel, R. Muller, A. Moustakas, and R. de Miguel, "Vector precoding for Gaussian MIMO broadcast channels: Impact of replica symmetry breaking," *IEEE Transactions on Information Theory*, vol. 58, no. 3, pp. 1413–1440, March 2012.

[9] A. M. Tulino, G. Caire, S. Shamai, and S. Verdú, "Support recovery with sparsely sampled free random matrices," *IEEE Transactions on Information Theory*, vol. 59, pp. 4243–4271, 2013.

[10] M. Vehkapera, Y. Kabashima, and S. Chatterjee, "Analysis of regularized LS reconstruction and random matrix ensembles in compressed sensing," *IEEE Transactions on Information Theory*, vol. 62, no. 4, pp. 2100–2124, 2016.

[11] F. Mezzadri, "How to generate random matrices from the classical compact groups," *arXiv preprint arXiv:math-ph/0609050*, September 2006.

[12] F. Hiai and D. Petz, *The Semicirle Law, Free Random Variables and Entropy*. American Mathematical Society, 2006.

[13] G. W. Anderson and B. Farrell, "Asymptotically liberating sequences of random unitary matrices," *Advances in Mathematics*, vol. 255, pp. 381 – 413, 2014.

[14] C. E. Shannon, "A mathematical theory of communication," *The Bell System Technical Journal*, vol. 27, no. 55, p. 623–666, October 1944.

[15] T. M. Cover and J. A. Thomas, *Elements of Information Theory*. John Wiley & Sons, New York, 1991.

[16] S. Shamai (Shitz) and S. Verdú, "The effect of frequency-flat fading on the spectral efficiency of CDMA," *IEEE Transactions on Information Theory*, vol. 47, no. 4, pp. 1302–1327, May 2001.

[17] A. Lozano, A. M. Tulino, and S. Verdú, "High-SNR power offset in multiantenna communication," *IEEE Transactions on Information Theory*, vol. 51, no. 12, pp. 4134–4151, December 2005.

[18] D. Tse and P. Viswanath, *Fundamentals of Wireless Communication*. Cambridge University Press, 2005.

[19] M. K. Simon and M.-S. Alouini, *Digital Communication over Fading Channels*. John Wiley & Sons, 2005, vol. 95.

[20] M. Opper and O. Winther, "Gaussian processes for classification: Mean-field algorithms," *Neural Computation*, pp. 2655–2684, 2000.

[21] T. P. Minka, "Expectation propagation for approximate Bayesian inference," in *Proceedings of the 17th Conference in Uncertainty in Artificial Intelligence*, ser. UAI '01, 2001, pp. 362–369.

[22] Y. Kabashima, "A CDMA multiuser detection algorithm on the basis of belief propagation," *Journal of Physics A: Mathematical and General*, vol. 36.43, p. 11111, October 2003.

[23] D. L. Donoho, A. Maleki, and A. Montanari, "Message-passing algorithms for compressed sensing," *Proceedings of the National Academy of Sciences*, vol. 106, pp. 18 914–18 919, September 2009.

[24] F. Krzakala, M. Mézard, F. Sausset, Y. Sun, and L. Zdeborová, "Probabilistic reconstruction in compressed sensing: algorithms, phase diagrams, and threshold achieving matrices," *Journal of Statistical Mechanics: Theory and Experiment*, vol. 2012, no. P08009, 2012.

[25] S. Rangan, "Generalized approximate message passing for estimation with random linear mixing," in *Proc. IEEE International Symposium on Information Theory (ISIT)*, Saint-Petersburg, Russia, July 2011.

[26] M. Mézard, G. Parisi, and M. Virasoro, *Spin Glass Theory and Beyond*. World Scientific, 1987, vol. 9.

[27] K. H. Fisher and J. A. Hertz, Eds., *Spin Glasses*. Cambridge University Press, 1993, vol. 1.

[28] J. R. L. De Almeida and D. J. Thouless, "Stability of the Sherrington-Kirkpatrick solution of a spin glass model," *Journal of Physics A: Mathematical and General*, vol. 11, no. 5, p. 983, 1978.

[29] L. Zdeborová and F. Krzakala, "Statistical physics of inference: Thresholds and algorithms," *arXiv preprint arXiv:1511.02476*, 2015.

[30] P. C. Martin, E. D. Siggia, and H. A. Rose, "Statistical dynamics of classical systems," *Physical Review A*, vol. 8.1, p. 423, 1973.

[31] H. Eisfeller and M. Opper, "New method for studying the dynamics of disordered spin systems without finite-size effects," *Physical Review Letters*, vol. 68, p. 2094, 1992.

[32] R. D. Henkel and M. Opper, "Parallel dynamics of the neural network with the pseudoinverse coupling matrix." *Journal of Physics A: Mathematical and General*, vol. 24.9, p. 2201, 1991.

[33] E. Bolthausen, "An iterative construction of solutions of the TAP equations for the Sherrington–Kirkpatrick model," *Communications in Mathematical Physics*, vol. 325.1, pp. 333–366., October 2014.

[34] J. Wishart, "The generalised product moment distribution in samples from a normal multivariate population," *Biometrika*, vol. 20A, no. 1/2, pp. 32–52, 1928.

[35] E. P. Wigner, "Characteristic vectors of bordered matrices with infinite dimensions," *Annals of Mathematics*, vol. 62, no. 3, pp. 548–564, 1955.

[36] A. M. Tulino and S. Verdú, *Random Matrix Theory and Wireless Communications*. Now Publishers Inc., June 2004, vol. 1, no. 1.

[37] H. Orland and A. Zee, "RNA folding and large N matrix theory," *Nuclear Physics B*, vol. 620, no. 3, pp. 456 – 476, 2002.

[38] R. R. Müller, "Applications of large random matrices in communications engineering," in *International Conference on Advances in the Internet, Processing, Systems, and Interdisciplinary Research (IPSI)*, Sveti Stefan, Montegro, October 2003.

[39] C. R. Rao, *Linear Statistical Inference and Its Applications*. John Wiley & Sons, 2009, vol. 22.

[40] A. Edelman and N. R. Rao, "Random matrix theory," *Acta Numerica*, vol. 14, pp. 233–297, 5 2005.

[41] B. Collins and P. Sniady, "Integration with respect to the Haar measure on unitary, orthogonal and symplectic group," *Communications in Mathematical Physics*, vol. 264.3, pp. 773–795, 2006.

[42] B. Collins and S. Matsumoto, "On some properties of orthogonal Weingarten functions," *Journal of Mathematical Physics*, vol. 50 (11), p. 113516, 2009.

[43] A. Edelman and B. D. Sutton, "The beta-Jacobi matrix model, the CS decomposition, and generalized singular value problems," *Foundations of Computational Mathematics*, vol. 8.2, pp. 259–285, July 2008.

[44] R. Dar, M. Feder, and M. Shtaif, "The Jacobi MIMO channel," *IEEE Transactions on Information Theory*, vol. 59, pp. 2426–2441, 2013.

[45] A. Karadimitrakis, A. Moustakas, and P. Vivo, "Outage capacity for the optical MIMO channel," *IEEE Transactions on Information Theory*, vol. 60, no. 7, pp. 4370–4382, July 2014.

[46] A. Rouault, "Asymptotic behavior of random determinants in the Laguerre, Gram and Jacobi ensembles," *Latin American Journal of Probability and Mathematical Statistics (ALEA), 3*, pp. 181–230, 2007.

[47] S. M. Collins, Benoit and N. Saad, "Integration of invariant matrices and moments of inverses of Ginibre and Wishart matrices," *Journal of Multivariate Analysis*, vol. 126, no. 11, pp. 1–13, 2014.

[48] B. Farrell, "Limiting empirical singular value distribution of restrictions of discrete Fourier transform matrices," *Journal of Fourier Analysis and Applications*, vol. 17, no. 4, pp. 733–753, 2011.

[49] F. J. Dyson, "Statistical theory of the energy levels of complex systems. i," *Journal of mathematical physics*, vol. 3, no. 3, pp. 140 – 146, 1962.

[50] G. W. Anderson, A. Guionnet, and O. Zeitouni, Eds., *An Introduction to Random Matrices*. Cambridge University Press, 2010, no. 118.

[51] K. L. Chung, *A Course in Probability Theory*. Academic press, 2001.

[52] T. Tao, "Intuitive understanding of the stieltjes transform," MathOverflow, uRL:http://mathoverflow.net/q/79129 (version: 2011-10-25). [Online]. Available: http://mathoverflow.net/q/79129

[53] Z. Bai and J. W. Silverstein, Eds., *Spectral Analysis of Large Dimensional Random Matrices*. New York: Springer, 2010, vol. 118.

[54] J. N. Walid Hachem, Philippe Loubaton, "Deterministic equivalents for certain functionals of large random matrices," *The Annals of Applied Probability*, vol. 17, no. 3, pp. 875–930, 2007.

[55] R. Couillet and M. Debbah, *Random Matrix Methods for Wireless Communications*. Cambridge University Press, 2011.

[56] A. Nica and R. Speicher, "Lectures on the combinatorics of free probability," *London Mathematical Society Lecture Note Series*, vol. 365, 2006.

[57] O. Ryan and M. Debbah, "Channel capacity estimation using free-probability theory," *IEEE Transactions on Signal Processing*, vol. 56, no. 11, pp. 5654–5667, Nov 2008.

[58] V. A. Marčenko and L. A. Pastur, "Distribution of eigenvalues for some sets of random matrices," *Matematicheskii Sbornik*, vol. 114.4, no. 1/2, pp. 507–536, 1967.

[59] D. Voiculescu, "Addition of certain noncommuting random variables," *J. Funct. Anal.*, vol. 66, pp. 323–346, 1986.

[60] D. V. Voiculescu, K. J. Dykema, and A. Nica, *Free Random Variables*. American Mathematical Society, 1992, vol. 1.

[61] A. Guionnet and M. Maïda, "A Fourier view on the R-transform and related asymptotics of spherical integrals," *Journal of Functional Analysis*, vol. 222, no. 2, pp. 435 – 490, 2005.

[62] I. W. Mottelson. (2012, July) Introduction to non–commutative probability. [Online]. Available: "http://www.math.ku.dk/

[63] J. Pielaszkiewicz, D. von Rosen, and M. Singull, "Cumulant-moment relation in free probability theory," *Acta et Commentationes Universitatis Tartuensis de Mathematica*, vol. 18.2, pp. 265–278, 2014.

[64] G. Akemann, J. Baik, and P. Di Francesco, Eds., *The Oxford Handbook of Random Matrix Theory*. Oxford University Press, 2011.

[65] C. Itzykson and J.-B. Zuber, "The planar approximation. ii," *Journal of Mathematical Physics*, vol. 21, no. 3, pp. 411–421, 1980.

[66] E. Marinari, G. Parisi, and F. Ritort, "Replica field theory for deterministic models. ii. a non-random spin glass with glassy behaviour," *Journal of Physics A: Mathematical and General*, vol. 27.23, p. 7647, October 1994.

[67] B. Collins and P. Śniady, "New scaling of Itzykson–Zuber integrals," *Annales de l'Institut Henri Poincare (B) Probability and Statistics*, vol. 43, no. 2, pp. 139 – 146, 2007.

[68] L. V. Ahlfors, *Complex Analysis: An Introduction to the Theory of Analytic Functions of One Complex Variable*, 2nd ed. McGraw-Hill Education, 1953.

[69] A. Nica and R. Speicher, "On the multiplication of free N-tuples of noncommutative random variables," *American Journal of Mathematics*, pp. 799–837, 1996.

[70] D. Voiculescu, "Multiplication of certain noncommuting random variables." *J. Operator Theory*, vol. 18, p. 223–235, 1987.

[71] U. Haagerup and F. Larsen, "Brown's spectral distribution measure for R-diagonal elements in finite von Neumann algebras," *Neumann Algebras, Journ. Functional Analysis*, vol. 176, pp. 331–367, 1999.

[72] R. R. Müller, "A random matrix model for communication via antenna arrays," *IEEE Transactions on Information Theory*, vol. 48, no. 9, pp. 2495–2506, September 2002.

[73] U. Haagerup and S. Möller, "The law of large numbers for the free multiplicative convolution," *Operator Algebra and Dynamics. Springer Proceedings in Mathematics & Statistics*, vol. 58, pp. 157–186, 2013.

[74] E. J. Candes and T. Tao, "Near-optimal signal recovery from random projections: Universal encoding strategies?" *IEEE Transactions on Information Theory*, vol. 52, no. 12, pp. 5406–5425, Dec 2006.

[75] S. Verdú and S. Shamai (Shitz), "Spectral efficiency of CDMA with random spreading," *IEEE Transactions on Information Theory*, vol. 45, no. 2, pp. 622–640, March 1999.

[76] A. M. Tulino, A. Lozano, and S. Verdú, "Impact of antenna correlation on the capacity of multiantenna channels," *IEEE Transactions on Information Theory*, vol. 51, no. 7, pp. 2491– 2509, July 2005.

[77] J. Lee and N. Jindal, "High SNR analysis for MIMO broadcast channels: Dirty paper coding versus linear precoding," *IEEE Transactions on Information Theory*, vol. 53, no. 12, pp. 4787–4792, Dec 2007.

[78] Y. Chen, A. Goldsmith, and Y. Eldar, "Backing off from infinity: Performance bounds via concentration of spectral measure for random MIMO channels," *IEEE Transactions on Information Theory*, vol. 61, no. 1, pp. 366–387, Jan 2015.

[79] R. R. Müller, "On the asymptotic eigenvalue distribution of concatenated vector-valued fading channels," *IEEE Transactions on Information Theory*, vol. 48, no. 7, pp. 2086–2091, July 2002.

[80] M. Opper, U. Paquet, and O. Winther, "Perturbative corrections for approximate inference in Gaussian latent variable models," *J. Mach. Learn. Res.*, vol. 14, no. 1, pp. 2857–2898, jan 2013.

[81] M. Opper and O. Winther, "Adaptive and self-averaging Thouless-Anderson-Palmer mean field theory for probabilistic modeling," *Physical Review E*, vol. 64, pp. 056 131–(1–14), October 2001.

[82] Y. Kabashima, "Inference from correlated patterns: a unified theory for perceptron learning and linear vector channels," *Journal of Physics: Conference Series*, vol. 95, no. 1, 2008.

[83] M. Opper and O. Winther, "Expectation consistent approximate inference," *Journal of Machine Learning Research*, 6 (2005): 2177-2204.

[84] K. B. Petersen and M. S. Pedersen, *The Matrix Cookbook*. Copenhagen, Denmark: Technical University of Denmark, 2008.

[85] C. TEMPLATES. (2012) 1bit compressive sensing. [Online]. Available: http://dsp.rice.edu/1bitCS/

[86] B. Çakmak, O. Winther, and B. H. Fleury, "S-AMP: Approximate message passing for general matrix ensembles," in *Proc. IEEE Information Theory Workshop (ITW)*, Hobart, Tasmanina, Australia, November 2014.

[87] M. Bayati and A. Montanari, "The dynamics of message passing on dense graphs, with applications to compressed sensing," *IEEE Transactions on Information Theory*, vol. 57, pp. 764–785, February 2011.

[88] M. Bayati, M. Lelarge, and A. Montanari, "Universality in polytope phase transitions and message passing algorithms," *The Annals of Applied Probability*, vol. 25, no. 2, pp. 753–822, 04 2015.

[89] K. Mimuura and M. Okada, "Generating functional analysis for iterative CDMA multiuser detectors," *IEEE Transactions on Information Theory*, vol. 60, pp. 3645–3670, June 2014.

[90] N. Merhav, "Statistical physics and information theory," *Foundations and Trends in Communications and Information Theory*, vol. 6, no. 1–2, pp. 1–212, 2010. [Online]. Available: http://dx.doi.org/10.1561/0100000052

[91] L. F. Cugliandolo and J. Kurchan, "On the out-of-equilibrium relaxation of the Sherrington-Kirkpatrick model," *Journal of Physics A: Mathematical and General*, vol. 27.17, p. 5749, 1994.

[92] T. Tanaka, "Asymptotics of Harish-Chandra-Itzykson-Zuber integrals and free probability theory," *Journal of Physics: Conference Series*, vol. 95, no. 1, p. 012002, 2008.

[93] Wikipedia, "Many-body problem — wikipedia, the free encyclopedia," 2016, [Online; accessed 27-September-2016]. [Online]. Available: https://en.wikipedia.org/w/index.php?title=Many-body_problem&oldid=741370593

[94] T. Tao, Ed., *Topics in Random Matrix Theory*. American Mathematical Society, 2012, vol. 132.

[95] A. Guionnet. (2012, November) Free probability and random matrices. [Online]. Available: http://jointmathematicsmeetings.org/meetings/national/jmm2013/amssc-Guionnet.pdf

[96] D. Jonsson, "Some limit theorems for the eigenvalues of a sample covariance matrix," *Journal of Multivariate Analyis*, vol. 12, pp. 1–38, 1982.

[97] T. Tao, V. Vu, and M. Krishnapur, "Random matrices: universality of ESDs and the circular law," *The Annals of Probability*, vol. 38, pp. 2023–2065, 2010.

[98] S. I. Resnick, *Extreme Values, Regular Variation, and Point Processes*. Springer, 2007.

[99] A. Browder, *Mathematical Analysis: An Introduction*. New York: Springer-Verlag, 1996.

[100] K. S. Miller, "On the inverse of the sum of matrices," *Mathematics Magazine*, pp. 67–72, 1981.

[101] T. Tanaka, "A statistical-mechanics approach to large-system analysis of CDMA multiuser detectors," *IEEE Transactions on Information Theory*, vol. 48, no. 11, pp. 2888–2910, Nov 2002.

[102] D. Sherrington and S. Kirkpatrick, "Solvable model of a spin-glass," *Physical Review Letters*, vol. 35.26, p. 1792, 1975.

[103] A. J. Bray and M. A. Moore, "Metastable states, internal field distributions and magnetic excitations in spin glasses," *Journal of Physics C: Solid State Physics*, vol. 14, p. 2629, 1981.

SUMMARY

The thesis studies three important applications of random matrices to information processing. Our main contribution is that we consider probabilistic systems involving more general random matrix ensembles than the classical ensembles with iid entries, i.e. models that account for statistical dependence between the entries. Specifically, the involved matrices are invariant or fulfill a certain asymptotic freeness condition as their dimensions grow to infinity. Informally speaking, all latent variables contribute to the system model in a democratic fashion – there are no preferred latent variables in the system.

ISSN (online): 2246-1248
ISBN (online): 978-87-7112-828-4

AALBORG **UNIVERSITETSFORLAG**